Differences in methane production, storage and transport among plant community types during a wet summer at Mer Bleue bog, Ottawa

by

Elizabeth Cowan

A thesis submitted to the Faculty of Graduate and Postdoctoral Affairs in partial fulfillment of the requirements for the degree of

Master of Science

in

Geography

Carleton University

Ottawa, Ontario

ABSTRACT

This study assessed indicators of methane (CH_4) production, storage and transport among plant community types to investigate the spatial and temporal variability in CH_4 dynamics during a wet summer at the Mer Bleue bog. Community type was largely differentiated by sedge (*Eriophorum vaginatum*) presence, which increased as the average water table depth approached the surface. Stable isotope analysis identified CO_2 reduction as the dominant methanogenic pathway in all plots, but with more depleted source signatures as percent *Eriophorum* increased, possibly due to CH_4 transport via aerenchymatous tissues. Increasing peat temperature contributed to increasing CH_4 concentrations at 50 cm, near the long-term average water table, and dissolved organic carbon and total dissolved nitrogen at all depths, and a seasonal increase in chamber CH_4 emissions. Plant community did not relate to spatial differences in pore water characteristics, but increasing percent *Eriophorum* was associated with greater CH_4 emissions.

ACKNOWLEDGEMENTS

I would like to thank everyone who contributed to this research. In particular, I express my deepest appreciation for the continual guidance and insight provided by my supervisor, Dr. Elyn Humphreys. She demonstrated endless patience and provided constant support as I navigated through my graduate studies at Carleton University. Her steadfast optimism and persistent encouragement opened numerous doors and pushed my work to the highest possible standard. In addition, I thank my committee member, Dr. Murray Richardson and mentors Dr. Tim Moore, Dr. Ruth Varner and Dr. Carmody McCalley. Your research served as a model for my own work and your collective input was invaluable throughout the development of this thesis. Furthermore, the support, reflections and interest expressed by participants of the Mer Bleue Working Group and Peatland Workshop meetings were greatly appreciated.

A sincere thank you to my field assistant, Rachel Canham, who was always eager and willing to help and provided intellectual, physical and moral support throughout our field season at Mer Bleue. I am also very appreciative of the assistance that Claire Elliott provided in the field during the fall months for Mer Bleue maintenance. A special thank you to Dr. Mike Treberg for his help with building our sampling devices and maintaining the site. Thank you to Mike Dalva and Michael Templeton from McGill University, who provided vital assistance in the field and in the lab for DOC, TDN and SUVA analysis. I am appreciative of the isotope gas analysis provided by Annalisa Sarno (PhD Candidate) and Dr. Hinsby Cadillo-Quiroz at Arizona State University. I am also indebted to Alice Wilson, who graciously supplied her ArcMap skills on short notice.

This research was made possible through the funding support of the National Sciences and Engineering Research Council (NSERC), Ontario Ministry of Environment and Climate Change, Ontario Graduate Scholarship (OGS) program, and Carleton University. In addition, thank you to Ottawa's National Capital Commission (NCC) for providing site access and support.

Finally, I would like to acknowledge the support provided by my friends and family throughout each stage of this thesis. Your motivational words and attentiveness inspired me to enhance my critical thinking while maintaining a healthy lifestyle, and I would not have completed this research without you. Special thanks to Dad's garage, which was ready and willing to tackle all our crazy projects! A simple "thank you" could never suffice, but know that I am infinitely grateful for each and every one of you.

TABLE OF CONTENTS

LIST OF TABLES

LIST OF FIGURES

LIST OF SYMBOLS AND ABBREVIATIONS

Symbol	Units	Definition
A	m^2	chamber surface area
Abs_{254}	m^{-1}	absorbance at 254 nm
c_a	μmol mol^{-1}	ecosystem atmospheric CH_4 concentration
c_b	μmol mol^{-1}	background CH_4 concentration
c_s	μmol mol^{-1}	source CH_4 concentration
C		carbon
C-A		*Chamaedaphne* automatic chamber
CH_4		methane
CO_2		carbon dioxide
C/N		carbon to nitrogen ratio
CRDS		cavity ring-down spectroscopy
$\delta^{13}C_a$	‰	isotopic composition of the sampled CH_4
$\delta^{13}C_b$	‰	isotopic composition of the background CH_4
$\delta^{13}C_s$	‰	isotopic composition of the CH_4 source component
$\delta^{13}C\text{-}CH_4$	‰	ratio of $^{13}CH_4$ to $^{12}CH_4$ relative to V-PDB marine carbonate standard
dC/dt	μmol mol^{-1} dry air s^{-1}	rate of change in CH_4 mixing ratio
DOC	mg L^{-1}	dissolved organic carbon
DOY		day of year
E-M		*Eriophorum* manual chamber
ES		early summer (DOY 155-189)
EV		*Eriophorum vaginatum*

EV%	%	% LAI attributed to *Eriophorum vaginatum*
F_{CH4}	mg m^{-2} h^{-1}	CH_4 flux
H_2		hydrogen
L-A		*Ledum* automatic chamber
LAI	m^2 m^{-2}	leaf area index
LAI-2000	m^2 m^{-2}	total biomass LAI as measured with LAI-2000
LS		late summer (DOY 222-255)
LSp		late spring (DOY 132-154)
MS		mid-summer (DOY 190-221)
N		nitrogen
NEE	μmol m^{-2} s^{-1}	net ecosystem exchange of CO_2
O_2		oxygen
OM		organic matter
ρ	Pa	air pressure
PVC		polyvinyl chloride
PW_{CH4}	μmol L^{-1}	pore water CH_4 concentration
*R**	8.314 J K^{-1} mol^{-1}	ideal gas constant
sccm	sccm	standard cubic centimeter per minute
S_{CH4}	mg m^{-2} h^{-1}	storage change of pore water CH_4
$SUVA_{254}$	L m^{-1} mg^{-1} DOC	UV absorbance at 254 nm standardized to DOC
T_{air}	°C	air temperature measured at tower site
T_{tower}	°C	peat temperature measured at tower site
T_{10cm}	°C	peat temperature at 10 cm depth (chamber-specific)
T_{50cm}	°C	peat temperature at 50 cm depth at tower location
TDN	mg L^{-1}	total dissolved nitrogen

Tg	10^{12} g	teragram
V	m^3	chamber volume
WT	cm	water table

LIST OF APPENDICES

1.0 INTRODUCTION

Wetlands have been identified as particularly important ecosystems for global carbon (C) dynamics (Bridgham *et al.* 2006). In particular, northern peatland ecosystems have sequestered 76-96 Tg C a^{-1} through the uptake of carbon dioxide (CO_2) over the long term (Gorham 1991, Gorham 1995). However, they also emit approximately 38 Tg methane (CH_4) a^{-1}, which has a higher potential for climate forcing over the short term in comparison to CO_2 (Bartlett & Harriss 1993). Considering the variable atmospheric growth rate over the past 3 decades, including a recent increase in the growth rate of CH_4 concentrations since 2007 (Kirschke *et al.* 2013), there is a current need to examine the potential feedbacks and responses of peatland CH_4 emissions to climate change. Atmospheric CH_4 depends on a number of sources and sinks, with wetland emissions of CH_4 representing the largest natural emitter. Increased understanding of the processes that lead to CH_4 loss in wetlands such as peatlands is crucial for the development of a global CH_4 budget that accurately captures CH_4 source and sink estimates (Mikaloff Fletcher *et al.* 2004a, Chanton *et al.* 2005, Kirschke *et al.* 2013).

Climate change projections indicate a multitude of possible responses by northern peatlands (Bridgham *et al.* 2013). For example, vascular plants (especially deciduous shrubs and graminoids) are expected to dominate over mosses and lichens as temperatures and growing season length increases (Walker *et al.* 2006, IPCC 2007, Gallego-Sala & Prentice 2013). The composition of the peatland plant community, which reflects environmental variables such as nutrient availability and long-term water table (WT) depths, is often used as an indicator of the potential magnitude of CH_4 emissions among and within peatlands. The dominant vegetative communities of northern peatlands

also directly impact CH_4 exchange by influencing substrate availability for methane-producing microorganisms and gas transport above and below the WT via aerenchymatous tissues (Couwenberg *et al.* 2011, Bridgham *et al*. 2013, Ward *et al.* 2013).

While vegetative community has been identified as an important ecosystem response indicator, there remains a need for increased understanding of the complex relation between plant community composition and CH_4 emission. This study seeks to couple the use of autochamber CH_4 flux measurements with pore water and stable carbon isotope analyses to achieve a better understanding of CH_4 production, storage and transport pathways for different vegetative communities along depth profiles at a temperate ombrotrophic bog. This will aid in determining the relative importance of dominant environmental controls, including vegetation type, on CH_4 emission dynamics.

Three key research hypotheses follow from this central research aim:

1. Spatial and temporal variability in CH_4 emissions will vary with plant community characteristics, where sedge-dominated plots are expected to have greater emissions than plots dominated by hummock species. This hypothesis follows findings by Lai *et al.* (2014a) and is based on the notion that CH_4 production, storage and transport will all be impacted by the abiotic and biotic variables that are associated with the different plant community types. These include, for example, the average WT depth and the presence of vegetation with aerenchymatous tissues.

2. As the growing season progresses, increasing peat temperature and plant growth will be associated with changes in belowground pore water characteristics that suggest increased substrate availability and increased CH_4 production rates, especially with reducing conditions in the saturated zone at a depth close to the long-term average WT. This hypothesis is based on previous laboratory studies that have identified these environmental factors as important controls on methanogenic metabolism (Dunfield *et al.* 1993, Moore & Dalva 1993, Yavitt & Seidman-Zager 2006).
3. The seasonal increase in CH_4 storage will be lowest at chamber plots that are associated with the highest seasonal CH_4 emissions, as these emissions represent a loss of stored CH_4 from peat. This follows previous evidence of a decoupling between CH_4 production and emission to the atmosphere due to transport limitations (i.e. diffusive transport of CH_4 dominates over plant-mediated transport) (Moore & Dalva 1993, Blodau 2002, Brown *et al.* 2014).

2.0 BACKGROUND

2.1 Northern peatlands and climate

According to a digital, high-resolution database of wetland sites developed by Matthews & Fung (1987), wetlands were historically estimated to cover a global area of approximately 5.3×10^{12} m^2 or roughly 3.6% of the global terrestrial surface. More recent wetland inventory analyses suggest this estimate may be up to 2 times greater (Bridgham *et al.* 2013). The total northern wetland area used in global CH_4 emission studies varies widely from 2.6×10^{12} to 9.0×10^{12} m^2 (Petrescu *et al.* 2010) and is a major source of uncertainty when assessing the global CH_4 budget (Kirschke *et al.* 2013). While the distribution of these wetlands tends to be scattered and the areas small, they represent an important component in the global C cycle (Matthews & Fung 1987, Bridgham *et al.* 2013). Among these wetlands are northern peatlands where organic matter (OM) has accumulated as peat to a depth of 40 cm or more (Gorham 1995). These northern peatland ecosystems cover an area of approximately 3.5×10^{12} m^2 and have a mean peat depth of ~2.3 m (Gorham 1991). They are estimated to contain between 273 and 455 $\times$ 10^{15} g of C, 98.5% of which is in the form of peat (Gorham 1991, Turunen *et al.* 2002). This large range in C storage estimation is attributed to uncertainty surrounding global peat depths and area (Gorham 1991).

Northern peatlands are currently or have been net sinks for C because net primary production (i.e. photosynthetic uptake of carbon dioxide, CO_2) occurs at a greater rate than the decomposition of OM, resulting in the accumulation of peat (Gorham 1991, Gorham 1995, Moore *et al.* 1998). However, the persistent oxygen (O_2)-depleted

conditions in wetlands are also favourable for the production of CH_4, with natural wetlands representing the largest natural CH_4 source and contributing ~30% of global CH_4 emissions (Bridgham *et al.* 2013, Kirschke *et al.* 2013). Bartlett & Harriss (1993) estimated that wetlands north of 45°N release up to 38 Tg CH_4 a^{-1} while globally, wetlands may emit 55 to 231 Tg CH_4 a^{-1} (Houweling *et al.* 2000, Wuebbles & Hayhoe 2002, Neef *et al.* 2010). For northern peatlands, the global long-term rate of net atmospheric CO_2 sequestration ranges from 76-96 Tg C a^{-1} over the past 4600 years (Gorham 1991, Gorham 1995). At individual site level, the mean 6-year CO_2 exchange at the Mer Bleue temperate ombrotrophic bog was -40.2 ± 40.5 g C-CO_2 m^{-2} a^{-1} (where negative values indicate a net uptake by the peatland), while CH_4 exchange and dissolved organic C (DOC) export were 3.7 ± 0.5 g C-CH_4 m^{-2} a^{-1} and 14.9 ± 3.1 g C-DOC m^{-2} a^{-1} respectively. While the CH_4 exchange component at Mer Bleue is small in comparison to DOC export, many peatlands have a seasonal CH_4 flux value in the same range as DOC loss (Roulet *et al.* 2007). However, while characterized by significant spatial and temporal variability, CO_2 uptake usually offsets CH_4 emissions in the long-term (i.e. several centuries) in wetlands (Petrescu *et al.* 2015). For example, at the Stordalen palsa mire complex in subarctic Sweden, average annual CH_4 emissions were 18-22 g C-CH_4 m^{-2} while annual CO_2 uptake was 46 g C-CO_2 m^{-2} over 8 years (2001-2008) of micrometeorological monitoring (Christensen *et al.* 2012). At the Degerö Stormyr boreal minerogenic oligotrophic mire complex in northern Sweden, annual CH_4 emissions and CO_2 uptake were 9 g C-CH_4 m^{-2} and 55 g C-CO_2 m^{-2}, respectively, during 2004 (Nilsson *et al.* 2008). Methane emissions from the western peatland flux station northeast of Athabasca, Alberta (2.4 g C-CH_4 m^{-2}; Long *et al.* 2010) are much less than the average

annual uptake of CO_2 of 144 g C-CO_2 m^{-2} (Syed *et al.* 2006). At a fen area with continuous permafrost in northeastern Greenland, CH_4 emissions were also less than CO_2 uptake (2.8 g C-CH_4 m^{-2} vs. 48.7 g C-CO_2 m^{-2}, over 87 and 62 days respectively; Friborg *et al.* 2000, Soegaard *et al.* 2000). Although CH_4 emissions may be much less than CO_2 sequestration and CH_4 is short-lived in the atmosphere, it is more effective at absorbing incoming infrared radiation and is thus a more potent greenhouse gas than CO_2 (Bartlett & Harriss 1993). According to the Intergovernmental Panel on Climate Change (2013), CH_4 has 86 times the relative cumulative forcing index as CO_2 on a mass basis over a 20-year period. Although characterized by large inter-annual variability, growth of CH_4 concentrations in the atmosphere slowed and stabilized during the mid-1990's, remaining relatively constant until 2006 (Bridgham *et al*. 2013). Since 2007, however, atmospheric CH_4 concentrations have been on the rise with an average atmospheric concentration of 1.80 ppm in 2010 (Kirschke *et al.* 2013). The variable atmospheric growth rate of CH_4 over recent decades signals a need for increased understanding of the factors influencing natural peatland CH_4 emissions. Yet, the controls over CH_4 production, consumption and transport are poorly represented in current CH_4 biogeochemistry models, largely due to a limited number of CH_4 flux datasets with which these models may be improved and validated (Bridgham *et al*. 2013, Kirschke *et al.* 2013).

Peatlands are often neglected in global climate change models despite their importance for global C cycling, as there exist large uncertainties surrounding wetland controls on C fluxes, such as wetland specific plant functional types (Moore *et al.* 1998, IPCC 2013). Dissolved organic carbon (DOC) export, CO_2 exchange, CH_4 exchange, and C storage constitute the major components of peatland C cycles and are primarily

controlled by air and substrate temperature, pH, plant community structure, substrate availability/quality and reduction/oxidation (i.e. redox) boundaries associated with WT position (Moore *et al.* 1998, Blodau 2001).

2.1.1 CH_4 production

According to Klass (1984), biogenic CH_4 production requires modest temperatures, ambient pressures, fully saturated conditions and the absence of other free-energy electron acceptors (e.g. O_2, nitrate, sulphate). The production of CH_4 is directly dependent on microbial activity, thus an organic C substrate and mixed population of CH_4-producing microorganisms (i.e. methanogens) is also necessary (Klass 1984, Clark & Fritz 1997). This organic C substrate serves as a food source to support methanogens, which require small, simple dissolved organic molecules with molecular weights < 600 g mol^{-1} (Fenchel *et al.* 1998, Blodau 2001). These molecules are produced when fermentive bacteria reduce complex organic molecules in the peat to simpler molecules like fatty acids, which are then transformed by acetogenic bacteria to acetate with CO_2 and hydrogen (H_2) as byproducts (Equation 1). Organic-rich environments thus facilitate reactant supply (i.e. acetate, H_2 and CO_2) for methanogenic pathways (Clark & Fritz 1997).

(1) $$CH_3CH_2COOH+2H_2O \rightarrow CH_3COOH+CO_2+3H_2$$

Recent ^{14}C-labelling studies suggest that root exudates (i.e. plant photosynthate) serve as organic C substrate for CH_4 production in the rhizosphere. These root exudates also indirectly increase CH_4 production through priming effects, where they trigger the

decomposition of less labile soil OM (Bridgham *et al.* 2013). Additionally, methanogens require mineral nutrients, a reducing agent and a source of nitrogen (i.e. NH_4^+). As obligate anaerobes, methanogens cannot tolerate O_2 and are most active under strongly reducing conditions of less than -200 mV as demonstrated in Table 2-1 (Zhi-Guang 1985, Mansfeldt 2003, Vorenhout *et al.* 2004).

Table 2-1: Redox pairs and redox values (Eh) at transformation at reference pH of 7.0 (Adapted from Vorenhout *et al.* 2004)

	Oxidized form	*Reduced form*	*Eh at transformation (mV)*
Oxygen	O_2	H_2O	+600 to +400
Nitrogen	NO_3^-	N_2O, N_2, NH_4^+	250
Manganese	Mn^{4+}	Mn^{2+}	225
Iron	Fe^{3+}	Fe^{2+}	+100 to -100
Sulfur	SO_4^{2-}	S^{2-}	-100 to -200
Carbon	CO_2	CH_4	< -200

An understanding of the CH_4 production pathways remains limited (Galand *et al.* 2010). It has been established that the decomposition of OM by a form of anaerobic respiration in methanogenic *Archea* produces CH_4 as an ultimate end product (Conrad 2005). Methane is primarily produced in the upper portion of saturated peat and/or sedimentary environments, where O_2 is absent, yet methanogens still have access to sufficient organic substrate (Chanton *et al.* 2005). The two main CH_4 production pathways in terrestrial freshwater systems include acetoclastic methanogenesis (Equation 2) and hydrogenotrophic methanogenesis (Equation 3) (Chanton *et al.* 2005).

(2) $$CH_3COOH \rightarrow CH_4 + CO_2$$

(3) $$CO_2 + 4H_2 \rightarrow CH_4 + 2H_2O$$

The fermentation of acetate (acetoclastic methanogenesis, Equation 2) occurs when acetic acid (CH_3COOH) acts as the terminal electron acceptor (i.e. food source) resulting in the production of CH_4 and CO_2 gas (Clark & Fritz 1997). While acetoclastic methanogenesis can play an important role in both ombrotrophic and minerotrophic peatlands, only a few species of methanogens can use acetate as a substrate (Avery *et al.* 1999, Kotsyurbenko *et al.* 2004, Kotsyurbenko *et al.* 2007, Galand *et al.* 2010). Thus, CO_2 reduction with H_2 gas to form CH_4 (hydrogenotrophic methanogenesis, Equation 3) is typically viewed as the dominant pathway of peatland CH_4 production. The methanogens required for this process are thought to be present in differing levels of diversity in all peatlands (Kotsyurbenko *et al.* 2007). While these two mechanisms have been identified as the main drivers of methanogenesis in most environments, identifying their relative contributions and how each pathway is controlled by environmental factors remains a challenge (Conrad 2005, Kotsyurbenko *et al.* 2007,Galand *et al.* 2010). For example, freshwater wetlands seem to be heavily influenced by vegetation: *Sphagnum*-moss-vegetated bogs produce CH_4 mainly by CO_2 reduction while fens dominated by *Carex* sedges rely on acetate fermentation (Chanton *et al.* 2005). Additionally, stable isotope measurements from pore water depth profiles obtained at two temperate wetlands show that the upper peat layers (rich in labile organic C) are favourable for acetoclastic methanogenesis, while CO_2 reduction is increasingly important as peat becomes more recalcitrant with depth (Hornibrook *et al.* 1997).

2.1.2 CH_4 consumption

As the CH_4 produced in the anaerobic saturated zone diffuses up through the aerobic peat layer along a concentration gradient, CH_4-consuming microbes (i.e. methanotrophs) reoxidize CH_4 to methanol (CH_3OH), formaldehyde (CH_2O), formate ($CHOO^-$) then CO_2 (Whalen 2005). The main CH_4 consumption types include low and high affinity oxidation, which occur at high (>40 ppm) and close to atmospheric (<12 ppm) CH_4 concentrations respectively (Segers 1998, Le Mer & Roger 2001). In northern peatlands, low affinity oxidation occurring at high CH_4 concentrations is the dominant CH_4 consumption process (Bender & Conrad 1995). The CH_4 is used as a C and energy source by methanotrophs (Le Mer & Roger 2001). For CH_4 oxidation to proceed, the presence of O_2 is key as it acts as an electron acceptor for the formation of CO_2. Oxidizing conditions >400 mV indicate the predominance of O_2 in a substrate, and are thus associated with maximum methanotrophic activity (Zhi-Guang 1985, Mansfeldt 2003).

As sufficient O_2 is present in the aerobic zone (i.e. above WT) and maximum CH_4 substrate occurs in the anaerobic zone (i.e. below WT), there is some evidence that CH_4 consumption peaks within ~25 cm of the aerobic/anaerobic interface or average WT position before CH_4 concentrations are too low to support methanotrophs (Segers 1998). Methanotrophs could potentially form hotspots of CH_4 oxidation below the average WT position if sufficient O_2 reaches these depths through plant transport. For example, C deprivation experiments have demonstrated that methanotrophic bacteria persist under anaerobic conditions, suggesting that methanotrophs can enter an anaerobic dormant state and significantly attenuate internal metabolism (Roslev & King 1994, Roslev & King

1995). Thus, when aerenchymatous tissues transport sufficient O_2 below the WT, methanotrophic activity can proceed through the oxidation of these high CH_4 concentrations in the saturated zone.

2.1.3 CH_4 transport

Molecular diffusion and ebullition (i.e. sudden release of CH_4 bubbles) through the peat and diffusion through plant aerenchyma (i.e. soft plant tissue containing air spaces) comprise the three main pathways of CH_4 emission to the atmosphere (Figure 2-1). The diffusion pathway is driven by a CH_4 concentration gradient where CH_4 concentrations decrease traveling up the peat profile from the zone of CH_4 production (i.e. deeper anaerobic peat layers) to the atmosphere (Blodau *et al.* 2007, Dorodnikov *et al*. 2013). While diffusive transport is the slowest of the three pathways (especially in the saturated anaerobic peat layers), it serves the important role of transporting CH_4 through the aerobic upper peat layer where microbial CH_4 consumption through oxidative processes can occur (Whalen 2005).

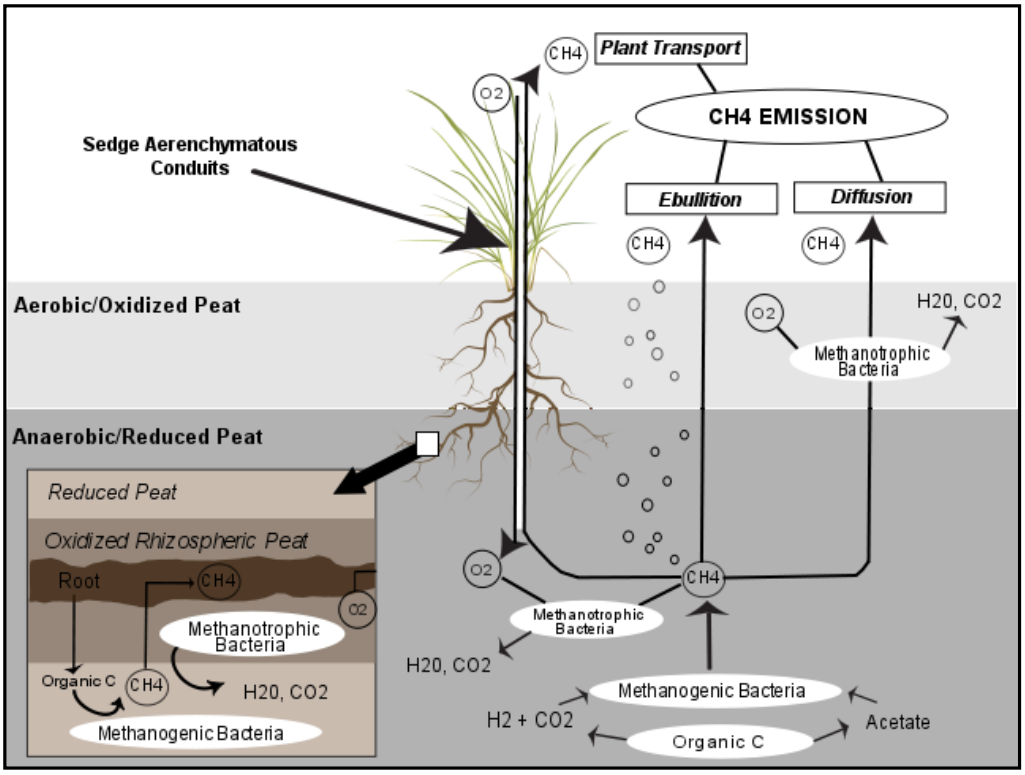

Figure 2-1: Methane production, consumption and transport pathways in peat layers (Adapted from Le Mer & Roger 2001).

The atmospheric release of free-phase CH_4 in gas bubbles, known as ebullition, can be episodic in nature where it is initiated by pore water CH_4 supersaturation at depth (i.e. in anaerobic zone of CH_4 production). Bubbles form when the hydrostatic pressure in peat is exceeded by the partial pressure of all dissolved gases in solution (Chanton & Whiting 1995). These CH_4 bubbles are not immediately released to the atmosphere; rather, the gas bubbles accumulate in peat pores until overpressure zones develop in peat and the bubbles move towards the peat surface (Kellner *et al.* 2004). Slow ebullition, where bubbles are released at a steady rate, typically results in a large proportion of bubble CH_4 being consumed through oxidation in the peat column above the WT (Rosenberry *et al.* 2006). Episodic ebullition events, however, involve much higher rates of degassing. These sudden bubbling events can overwhelm CH_4 oxidation potential by

methanotrophs in the aerobic peat layer and release much greater volumes of CH_4 than slow ebullition (Rosenberry *et al.* 2006). The rupture of a peat fabric/layer may create a preferential flow path thereby enabling such large volumes of gas release through episodic ebullition. For example, ebullition has been shown to release 40-53 g CH_4 m^{-2} per event at the Red Lake peatland, northern Minnesota (Glaser *et al.* 2004). Falling atmospheric pressure has also been associated with episodic ebullition events, with results by Tokida *et al.* (2007) indicating an increase in CH_4 flux by 2 orders of magnitude over short time scales (<2 hours). These large releases of CH_4 significantly contribute to total CH_4 flux in some northern peatlands (Tokida *et al.* 2007).

The third transport pathway is facilitated by the aerenchymatous tissues of some vascular peatland plants such as sedges, which function as conduits for CH_4 gas transport from the roots to the atmosphere. Methane travels up through the aerenchyma as a result of molecular diffusion along the concentration gradient and bulk flow due to pressure differences between internal plant air spaces and the atmosphere (Lai 2009). While transport capabilities are species specific, this relatively fast pathway reduces the residence time of CH_4 in the aerobic zone and thus limits CH_4 oxidation potential in upper peat layers (Blodau 2001, Strack *et al.* 2006). Sedges in particular often have roots that reach below the WT depth, with sedge root biomass peaking close to 50 cm below peat surface and extending as deep as 1 m in a temperate bog where the average WT is ~42 cm below the surface (Moore *et al.* 2002, Murphy & Moore 2010). These roots add labile C and other substrates to the anaerobic zone (Strack *et al.* 2006). In the opposite direction, aerenchyma provide a conduit for the diffusion of atmospheric O_2 to the rhizosphere below the aerobic/anaerobic boundary (i.e. radial oxygen loss), creating

aerated volumes or oxic "pockets" where CH_4 oxidation could occur at depth (Vasander & Kettunen 2006). Thus, a larger sedge root biomass may cause increased CH_4 consumption by enabling O_2 transport and associated reoxidation of CH_4 in the rhizosphere below the WT (Blodau 2001, Strack *et al.* 2006). However, there is some evidence suggesting that not all aerenchymatous plant species provide the opportunity for CH_4 oxidation at depth. For example, Frenzel and Rudolph (1998) could not determine any significant CH_4 oxidation at depth for *Eriophorum* species. They concluded that this species was associated with low CH_4 oxidation rates and did not reduce CH_4 emissions. This could result from plant influence on biogeochemistry at depth, where different species produce root exudates of varying type and quality (Frenzel & Rudolph 1998).

2.2 Environmental controls on peatland CH_4 emissions

2.2.1 Redox boundary associated with WT position

Methane emissions can vary spatially and temporally at fine scales as numerous interactive environmental factors affect biologically mediated CH_4 emissions from soils (Bartlett & Harriss 1993, Blodau 2001, Chanton *et al.* 2005). The microtopography of peatlands is typically divided into horizontal microstructure levels that have characteristic WT positions and vegetative communities (Strack *et al.* 2008, Rydin & Jeglum 2013). For example, hummock-hollow microtopography is common in ombrotrophic bogs. Hummocks are characterized by dwarf shrubs and tend to be 20-50 cm above the lowest surface level (Rydin & Jeglum 2013). Hollows refer to the depressions between hummocks, which can be a combination of lawns, carpets and mud-bottoms where graminoids and/or mosses dominate and the WT is closer to the peat surface (Rydin &

Jeglum 2013). The microtopographic differences in vegetative community and associated depth to WT influence CH_4 dynamics and contribute to its spatial variability. These processes are also governed by the vertical structuring of peatlands, which is intricately linked with WT position. Aerobic conditions (presence of O_2) occur above the WT in the *acrotelm* or unsaturated upper peat layer (top ~5-40 cm). Beneath this layer, the *catotelm* is characterized by saturated, anaerobic conditions (depletion of O_2) (Rydin & Jeglum 2013).

The boundary between aerobic and anaerobic conditions shifts according to the position of the WT, inducing both biotic and abiotic changes (Limpens *et al.* 2008, Rydin & Jeglum 2013). Such changes could include alterations in dominant vegetation types. For example, Bubier *et al.* (2006) found that WT, in conjunction with water chemistry, was an important control on vegetation distribution at Mer Bleue, a temperate bog. Their results showed that most dominant ericaceous shrubs, including *Vaccinium myrtilloides, Ledum groenlandicum* and *Chamaedaphne calyculata*, favoured drier microtopographic positions while *Kalmia angustifolia* and *Eriophorum vaginatum* had higher biomass with WT closer to the peat surface (Bubier *et al.* 2006). Shifts in WT position could also induce variations in decomposition rates and processes (Rydin & Jeglum 2013). This hydrological control (i.e. WT position) defines the boundary between reduction and oxidation zones in the soil profile and is thus identified as a critical factor for CH_4 production in many CH_4 flux studies within peatlands (e.g. Turetsky *et al.* 2008, Lai *et al*. 2014a, Lai *et al.* 2014b) and among peatlands (e.g. Turetsky *et al.* 2014). Theoretically, a WT closer to the peat surface would result in larger CH_4 emissions as the saturated CH_4 production zone increases while the unsaturated CH_4 consumption zone shrinks. For

example, Turetsky *et al.* (2008) manipulated WT position at an ecosystem-scale in an Alaskan peatland and found that a raised WT resulted in the largest CH_4 fluxes. However, a study at a poor fen site demonstrated that a lowered WT led to increased biomass in hollows and CH_4 fluxes remained relatively high despite the thicker aerobic peat layer (Strack *et al.* 2008). This suggests that increased biomass could offset lowered WT effects through substrate addition and enhanced plant-mediated CH_4 transport at peatland hollows over a time scale of 2-5 years, highlighting the importance of climate change feedbacks in relation to vegetation and WT position (Strack *et al.* 2008).

At short time scales (i.e. weeks to months), the interaction between CH_4 production, consumption and transport processes may not be at equilibrium with varying environmental controls, such as WT position (Blodau 2002). It has been suggested that rates of CH_4 production in peat are decoupled from atmospheric fluxes to some extent (Blodau 2002). Changes in storage of CH_4 within the peat pore water would result. For example, Moore *et al.* (1990) observed large negative changes in stored CH_4 in peat pore water (260 to <90 μmol L^{-1}) corresponding with increased CH_4 fluxes in subarctic/northern boreal fens. The largest mean daily CH_4 flux (262 ± 205 mg m^{-2} d^{-1}) on August 12, 1989, released 3-4 g CH_4 m^{-2} from storage (Moore *et al.* 1990). Also, CH_4 production itself may not respond immediately to driving variables. Results from peat incubations have provided evidence for a time lag between the onset of saturated conditions and the initiation of CH_4 production processes (Öquist & Sundh 1998). Kettunen *et al.* (1999) found that a 1-week period of aerobic conditions followed by re-saturation of the peat profile produced low CH_4 fluxes due to a time lag between rising WT (i.e. re-saturation) and reactivation of CH_4 production processes. Similar results were

previously demonstrated through laboratory peat column experiments, where CH_4 emission rates did not reach significant levels until up to 10 days after the WT was raised to the surface of the column (Moore & Dalva 1993). Knorr *et al.* (2008) observed that draining (i.e. experimental drought) followed by rewetting delayed CH_4 production in temperate peat by weeks to months. Recent results indicate that dropping WT levels can reoxidize terminal electron acceptors in peat, thus suppressing CH_4 production processes after WT is raised until more favourable terminal electron acceptors have been consumed (Deppe *et al*. 2010b). The result is hysteresis in the relationship between CH_4 emissions and WT (Blodau & Moore 2003). The zone of WT fluctuation in particular exhibits a memory for CH_4 production rates based on past conditions. The history at a particular depth location thus affects CH_4 production rates when saturated anaerobic conditions commence (Blodau 2002).

2.2.2 Organic substrate supply

Once the peat is saturated, CH_4 production becomes limited by the availability of organic substrate (Segers 1998). The compounds that comprise DOC (e.g. acetate, cell residues, humic/fulvic macromolecules) have a variety of sources and functions in peatlands (Blodau 2001). As previously detailed, annual DOC export can be in the same range as annual CH_4 emissions (Roulet *et al.* 2007). The production and supply of this DOC impacts the activity of methanogens. Simple compounds such as acetate, ethanol and glucose have been identified as the dominant substrates used by methanogens for CH_4 production, with ethanol being preferentially consumed in the first 12 hours after laboratory incubation of rice paddy sediment (Chawanakul *et al.* 2009, Kirstine & Galbally 2012). For fen peat samples, Coles and Yavitt (2002) demonstrated that

available substrates influence methanogenic activity. After adding acetate, ethanol or glucose, their results showed that net methanogenesis increased immediately following acetate addition, and within 24 hours after addition of ethanol and glucose, which must be degraded by fermentation into smaller compounds for uptake by methanogens (Coles & Yavitt 2002). As measurements were made immediately following substrate addition, the increase in CH_4 production cannot be attributed to population growth response, which requires more time, and thus provides evidence for substrate limitation of methanogenesis. The quantity of organic substrate was also highlighted as a limitation on CH_4 production through in vitro assays, where CH_4 production was enhanced by the addition of substrates to saturated peat originating from bog hollows (Yavitt & Seidman-Zager 2006).

The quality of the DOC supply can also influence CH_4 production rates. The quality of DOC is influenced by major environmental controls including WT position, peat temperature and surface vegetation (Lai 2009). Recent studies found that DOC for peatlands with a raised WT was more labile and less humified in comparison to lowered WT conditions. WT drawdown resulted in increased pore water DOC concentrations with higher aromaticity, possibly resulting from DOC leaching from increased plant production under lowered WT conditions (Moore *et al.* 1998, Hribljan 2012, Hribljan *et al*. 2014). A peat warming experiment in a poor fen in Michigan showed that pore water DOC increased in both lability and concentration for warmed plots (Kane *et al.* 2014). This is expected as the rate of temperature-dependent decomposition processes increase with warming (Kane *et al.* 2014). Furthermore, the quality of peatland DOC can be influenced by surface vegetation characteristics, as acid-insoluble OM is typical of shrub-

dominated sites and has been shown to be negatively correlated with CH_4 production in peat from Appalachian wetland sites (Yavitt & Lang 1990). Similarly, in a substrate manipulation experiment with incubated peat samples collected from five different sites at Storåmyren, Sweden, (minerotrophic lawn, ombrotrophic lawn, ombrotrophic wet carpet, mud-bottom, ombrotrophic hummock), Bergman *et al.* (2000) suggested that easily degradable substrate availability, as well as temperature, influenced CH_4 production rates within sites. Chanton *et al.* (2008) examined peat from a variety of northern peatland sites (Minnesota, Northern Alberta, and Alaska) and their results suggest that DOC from sedge-dominated peatlands is more labile than DOC from peatlands dominated by *Sphagnum* or other woody plants. DOC was relatively young in comparison to bulk peat for these peatlands regardless of surface vegetation, indicating that fresh and more recent plant C is important for DOC dynamics (Chanton *et al.* 2008). As DOC fuels CH_4 producing microbes in saturated peat layers, the quantity and quality of DOC substrate supply represent important environmental controls on peatland CH_4 emissions.

2.2.3 Peat temperature and acidity

Northern peatland CH_4 production and emission rates increase with increasing peat temperature. Moore and Dalva (1993) demonstrated this through a laboratory column study of subarctic and temperate peat in which averaged CH_4 emissions at 23°C were 6.6 times greater than at 10°C. Temperature relations are commonly expressed using Q_{10} values, which represent the change in reaction rate per 10°C change in temperature. For example, CH_4 emissions from peat monoliths (originating from Scottish Ellergower moss hollows) suggested methanogenesis Q_{10} values ranging from 2.1-4.0

(Thomas *et al.* 1996). In an incubation analysis of peat slurries from temperate and subarctic peatlands, CH_4 production also demonstrated strong temperature dependence with Q_{10} values ranging from 5.3 to 16 (Dunfield *et al.* 1993). Both CH_4 production and consumption processes were optimized at about 25°C in this study. However, consumptive CH_4 oxidation processes were not as sensitive to temperature, as indicated by lower Q_{10} values of 1.4 to 2.1 (Dunfield *et al.* 1993).

Methane transport mechanisms can also be influenced by temperature. Ebullition CH_4 flux in particular can be moderated by temperature, where peat cooling events cause the contraction of ebullition bubbles and dissolution of CH_4 which limit ebullition over the short-term (Fechner-Levy & Hemond 1996). Increases in peat temperature could potentially increase CH_4 transport through ebullition as bubble volumes increase and CH_4 gas accumulates (Fechner-Levy & Hemond 1996). Plant CH_4 transport can also be enhanced with warmer temperatures as pressurized ventilation in the aerenchyma increases and subsequently allows for greater flow of CH_4 to the atmosphere (Groβe 1996). As such, numerous studies have reported the importance of peat temperature near the average position of the WT as an important control on CH_4 emissions (Bubier *et al.* 1995b, Moore *et al.* 2011, Lai *et al*. 2014a, Brown *et al.* 2014, Turetsky *et al.* 2014).

Peat acidity is also a control on CH_4 processes as the activities of methanogenic and methanotrophic organisms peak under specific optimum conditions. Methanogens have been shown to grow optimally at pH ranging from 6 to 8 (Garcia *et al.* 2000). Methanotrophs favour more acidic peat ranging from pH 4.3 to 5.9 (Kamal & Varma 2008). After incubating peat slurries, Dunfield *et al.* (1993) found that native peat pH was about 2 pH units lower than optimum pH ranges for CH_4 production and consumption in

temperate and subarctic peat (5.5-7.0 and 5.0-6.5 respectively). As *Sphagnum*-dominated ombrotrophic bogs such as Mer Bleue are rain-fed peatlands, they do not receive significant quantities of mineral bases derived from groundwater. Consequently, the acidic decomposition products remain unneutralized and the surface waters of bogs are characterized by an acidic pH of about 4 (Shotyk 1988). As the pH of ombrotrophic bogs lies outside the optimum ranges for CH_4 production and consumption, the acidity of these peatlands may limit the activity of both methanogens and methanotrophs.

2.2.4 Vegetation community structure

As northern latitude peatlands are expected to experience higher temperatures and longer growing seasons, predictions suggest vascular plants will out-compete bryophytes and lichens (Walker *et al.* 2006, IPCC 2007, Gallego-Sala & Prentice 2013). Warming experiments have demonstrated the potential for deciduous shrubs and graminoids to increase in height and cover, while mosses and lichens decrease in cover due to shade intolerance (Walker *et al.* 2006).

Previous studies have demonstrated that vegetative community composition is a good indicator of CH_4 exchange within and among peatlands (Bubier 1995, Bubier *et al.* 1995a, Dias *et al.* 2010, Couwenberg *et al.* 2011, Levy *et al.* 2012, Gallego-Sala & Prentice 2013, Ward *et al.* 2013). The composition of the plant community not only reflects environmental variables such as nutrient availability and long-term WT depths, but also directly impacts CH_4 exchange by supplying root exudates, increasing available substrates to methanogens, regulating peat moisture and influencing transport through the CH_4 consumption zone (Couwenberg *et al.* 2011, Bridgham *et al*. 2013, Ward *et al.*

2013). For instance, Ward *et al.* (2013) found that vegetative community composition, particularly graminoid presence, was more important than a 1°C increase in air temperature for regulating CH_4 flux within an ombrotrophic blanket bog in northern England. Similarly, a CH_4 flux model for data from 21 sites in the United Kingdom showed that the highest explanatory power stemmed from plant composition data (Levy *et al.* 2012). As previously detailed, plant communities dominated by sedges are associated with enhanced CH_4 emission presumably because sedges allow CH_4 produced at depth to bypass the consumption zone through aerenchymatous tissues (Couwenberg *et al.* 2011, Ward *et al.* 2013). Sedges also provide methanogens with an increased supply of acetate and other organic substrates (Ward *et al.* 2013). However, Strack *et al.* (2008) suggest that at sites with dense sedge cover (i.e. drained lawns), O_2 transported below the WT may enhance oxidation in the catotelm over the short term (2-5 years) and could reduce net CH_4 emissions.

2.3 Measurement techniques and approaches

2.3.1 Autochamber CH_4 flux measurements

Methane gas exchange between the surface and the atmosphere may be measured using a number of techniques including chambers and eddy covariance. The manual static non-steady state chamber method uses the increase in CH_4 concentration in the chamber headspace over time to calculate the CH_4 flux at the surface (Pihlatie *et al.* 2013). This method is 'static' in that there is no air flow circulating between the chamber and an analyzer. Instead, discrete air samples are collected over time manually. While chambers are portable and inexpensive, the CH_4 flux data from these chambers are limited both

spatially and temporally (e.g. fewer plots sampled at weekly to monthly intervals) due to practical constraints of manual sample collection (Lai *et al.* 2014a). In the eddy covariance technique, CH_4 fluxes are measured as the covariance of high frequency vertical wind velocity fluctuations and CH_4 mixing ratio fluctuations over a period of time such as 30 min with the appropriate air density and water vapour corrections applied (e.g. Brown *et al.* 2014). Eddy covariance CH_4 flux measurements represent the flux from an integrated area of roughly 1 ha and are thus difficult to interpret in relation to dominant vegetation types and common environmental variables that vary spatially (Lai *et al.* 2014a). These limitations highlight the value of automated chamber measurements, which achieve a higher temporal resolution than manual chamber measurements (e.g. one measured flux for each chamber every half hour) and increase the likelihood of observing elevated but transient CH_4 emission phenomena in specific plots representing the plant communities.

2.3.2 Stable isotope analysis

In conjunction with autochamber CH_4 flux measurements, stable C isotope analysis has the potential to reveal more detail into peatland CH_4 emission processes. Carbon exists as two stable isotopes in natural environments, ^{12}C and ^{13}C, with relative abundances of 98.9% and 1.1% respectively (Farquhar *et al.* 1989). Stable isotope fractionation occurs because heavier isotopes (i.e. ^{13}C) are cycled and transformed differently than lighter isotopes (i.e. ^{12}C) through biogeochemical processes including photosynthesis, respiration, and physical processes such as diffusion (Dawson & Siegwolf 2007). These processes alter the $^{13}C/^{12}C$ composition of C-containing matter

and gases in the soil, biosphere and atmosphere, creating isotopic signatures that can be used to trace C transformation processes (Farquhar *et al.* 1989, Werner *et al.* 2012).

Stable C isotope analysis adopted the use of delta notation to express any sample's abundance of ^{13}C in relation to ^{12}C (Werner *et al.* 2012). According to Quay *et al.* (1991), $\delta^{13}C$ is the ratio of ^{13}C to ^{12}C in parts per thousand, per mil (‰), relative to a marine carbonate standard, PeeDee Belemnite:

$$\delta^{13}C = \left(\frac{{}^{13}C/{}^{12}C_{SAM}}{{}^{13}C/{}^{12}C_{V-PDB}} - 1 \right) \times 1000 \quad (4)$$

The PeeDee Belemnite international standard was based on a marine fossil found in South Carolina's Pee Dee formation, which had an unusually high ratio of ^{13}C relative to ^{12}C (Werner *et al.* 2012). PeeDee Belemnite was established as $\delta^{13}C$=0 ‰, thus most natural samples have a negative $\delta^{13}C$ value because they are more depleted in ^{13}C than the standard. With increasing isotope studies and greater demand for use of the standard, the original PeeDee Belemnite had to be replaced with Vienna PeeDee Belemnite (V-PDB) (Werner *et al.* 2012).

The three main CH_4 source categories have distinct isotopic signatures, with microbially produced CH_4 having more depleted average values ($\delta^{13}C$-CH_4 = -60 ‰) than fossil fuel CH_4 ($\delta^{13}C$-CH_4 = -40 ‰) or biomass burning CH_4 ($\delta^{13}C$-CH_4 = -25 ‰) (Quay *et al.*1991, Miller 2005). The measured steady state atmospheric $\delta^{13}C$-CH_4 value of -47‰ is offset by 6‰ from the signature of atmospheric CH_4 sources ($\delta^{13}C$-CH_4 = -53‰) due to isotopic fractionation associated with global CH_4 sinks (i.e. tropospheric OH, soils, and stratosphere) (Whiticar 2000, Miller 2005). Peatland CH_4 emissions are dominated by

microbially produced CH_4 with $\delta^{13}C$-CH_4 values ranging from -85 to -40‰ due to the influence of production, consumption, and transport processes (Hornibrook *et al.* 2000a). Peatland isotopic signatures also vary depending on the time of year. For example, Avery *et al.* (1999) found that $\delta^{13}C$-CH_4 of pore water could shift by up to 11‰ annually at a Michigan peatland. This temporal variation was attributed to the shift of dominant CH_4 production pathway from CO_2 reduction (~-71‰) in the winter to acetate fermentation (-44‰) in the spring. The CH_4 production pathways can be distinguished by their $\delta^{13}C$-CH_4 values as acetate fermentation yields a relatively ^{13}C-enriched signature (-65 to -50 ‰) compared to the more depleted CO_2 reduction signature (-110 to -60 ‰) (Whiticar *et al.* 1986). This is due to stronger methanogenic discrimination against ^{13}C during CO_2 reduction relative to acetate fermentation (Dorodnikov *et al.* 2013). Parent OM (i.e. C_3 vs. C_4 vegetation) will also influence $\delta^{13}C$-CH_4 values (Chanton *et al.* 2005). An increased understanding of these CH_4 production pathways reveals information about decomposition patterns (i.e. fresh vs. old C) and the fate of C pools (i.e. pools with rapid turnover time vs. pools with longer turnover time) (Dorodnikov *et al.* 2013).

Methane consumption processes driven by methanotrophs cause shifts in ^{13}C isotopic signatures as well. Coleman *et al.* (1981) found that residual CH_4 from bacterial CH_4 oxidation became enriched in ^{13}C. Thus, the microbes preferentially consume lighter ^{12}C-CH_4, leaving residual CH_4 enriched with the heavier ^{13}C isotope in the upper peat layer (Dorodnikov *et al.* 2013). This C isotope fractionation factor was found to range from 5 to 30 ‰ in various culture experiments (Whiticar 1999).

Transport processes also affect CH_4 isotopic signatures. The CH_4 diffusion distance through the aerated zone influences the $\delta^{13}C$-CH_4 value since methanotrophs

fractionate C as discussed above while at the same time, diffusion and plant-mediated transport processes preferentially remove lighter ^{12}C-CH_4. Methane fractionation may then be dependent on WT position (i.e. thickness of aerobic zone), transport mechanism and day of year/time of day (Dorodnikov *et al.* 2013). As increased sedge cover would allow for increased plant-mediated CH_4 transport, the vegetation community structure may influence the dominant CH_4 transport pathway and $\delta^{13}C$-CH_4 values accordingly.

2.3.3 Keeling Plot Approach

The $\delta^{13}C$-CH_4 signatures of CH_4 sources can be determined using the Keeling Plot approach. First proposed by Charles Keeling (1958, 1960), the "Keeling Plot" two end-member mixing model analyzes the relationship between the concentration and isotopic abundance of trace gases, such as CH_4, in the atmosphere (Miller & Tans 2003, Pataki *et al.* 2003). This approach relies on the conservation of mass, where the sampled ecosystem atmospheric CH_4 concentration (c_a) is a combination of the background CH_4 concentration (c_b) and source CH_4 concentration (c_s) (Pataki *et al.* 2003):

(5) $$c_a = c_b + c_s$$

This method assumes that the only two gas components mixing are the source and background CH_4 and that their isotopic ratio stays constant over the observation period (Pataki *et al.* 2003). As such, each CH_4 component's C isotope ratio ($\delta^{13}C$) follows the equation:

(6) $$\delta^{13}C_a c_a = \delta^{13}C_b c_b + \delta^{13}C_s c_s$$

By substituting equation (5) into equation (6),

(7) $$\delta^{13}C_a c_a = \delta^{13}C_b c_b + \delta^{13}C_s (c_a - c_b)$$

(8) $$\delta^{13}C_a c_a = \delta^{13}C_b c_b + \delta^{13}C_s c_a - \delta^{13}C_s c_b$$

(9) $$\delta^{13}C_a c_a = c_b(\delta^{13}C_b - \delta^{13}C_s) + \delta^{13}C_s c_a$$

(10) $$\delta^{13}C_a = (c_b / c_a)(\delta^{13}C_b - \delta^{13}C_s) + \delta^{13}C_s$$

where $\delta^{13}C_a$ is the isotopic composition of the sampled CH_4, $\delta^{13}C_b$ is the isotopic composition of the background CH_4, and $\delta^{13}C_s$ is the isotopic composition of the CH_4 source component. As Equation 10 is in *y=(m/x)+b* linear form, the source $\delta^{13}C_s$ value is the y-intercept *b* in this linear regression approach (Miller & Tans 2003). Figure 2-2 demonstrates a sample Keeling Plot, where the inverse CH_4 concentration is plotted against $\delta^{13}C$-CH_4 to obtain a y-intercept that represents the isotopic signature of the CH_4 source (Miller & Tans 2003, Pataki *et al.* 2003). In this example, the relatively depleted source $\delta^{13}C$-CH_4 value of -71.7 ‰ indicates the dominance of the CO_2 reduction pathway for CH_4 production.

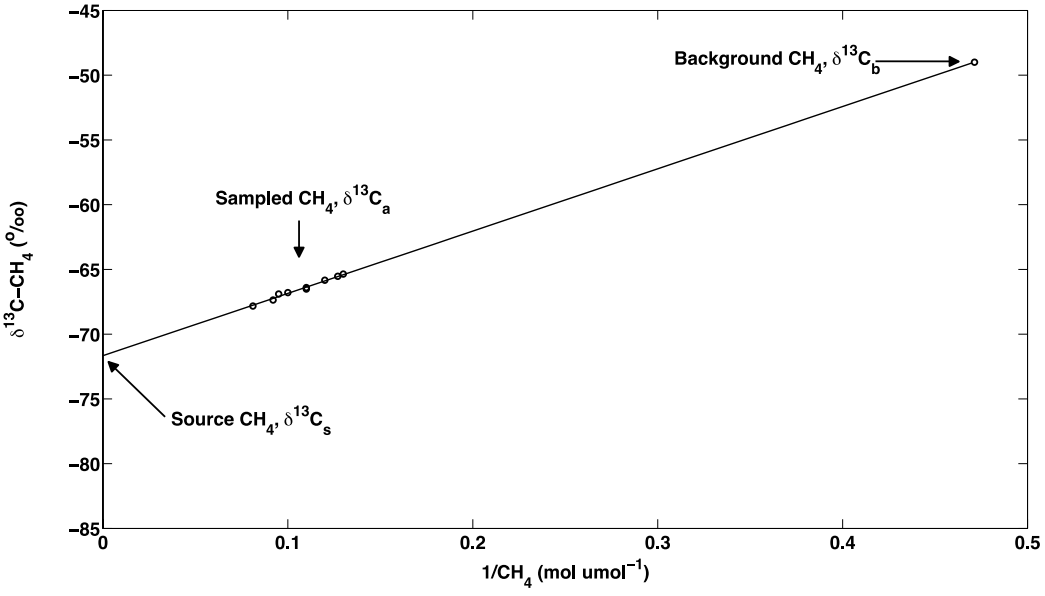

Figure 2-2: The Keeling Plot method as described by Equation 10. Inverse CH_4 concentrations (mol μmol^{-1}) are plotted vs. isotope $^{13}C/^{12}C$ ratios (‰). The isotopic signatures of sampled CH_4 ($\delta^{13}C_a$) and background CH_4 ($\delta^{13}C_b$) are shown with open circles. The y-intercept (-71.7 ‰) is interpreted as the isotopic signature of the CH_4 source, $\delta^{13}C_s$.

2.3.4 Redox potential measurements

As CH_4 production and consumption processes are microbially mediated, they require specific reduction-oxidation conditions for maximum activity levels. For example, strongly reducing conditions (<-200 mV) are favourable for the activity of methanogens, which are obligate anaerobes (Table 2-1; Zhi-Guang 1985, Mansfeldt 2003, Vorenhout *et al.* 2004). Methanotrophs, however, require O_2 as an electron acceptor and thus peak in activity under oxidizing conditions (>400 mV). Accordingly, the redox status of the peat substrate is an important parameter for investigating the spatial and temporal variability of CH_4 production potential. Measurements of the voltage difference between the peat substrate and a standard reference electrode represent the peat redox potential (Eh, mV) (Vorenhout *et al.* 2004). Redox potential indicates the ability of the peat substrate to gain or lose electrons and can range from +800 to -600 mV. Recent technological advances provide the opportunity for automated and continuous redox potential measurements from multiple locations in peatlands (Vorenhout *et al.* 2004, Vorenhout *et al.* 2011). With a field deployable multichannel datalogger and probe system, Eh profiles and temperature can be continuously monitored (e.g. 10 min frequency) and help inform the spatial and temporal variability of potential CH_4 production as a function of variation in temperature, microbial activity, WT position, and other environmental factors.

2.3.5 Pore water collection and analysis

To elucidate peat processes and associated turnover patterns at depth, vertical concentration profiles of chemical species in peatland pore water are commonly used (Blodau 2001, Blodau & Moore 2002). These pore water profiles allow for the quantification of processes along specific depth intervals, where the mass balance between these depths enhances process understanding of peat layers (Blodau 2001). Peatland pore water has historically been collected in situ by using equilibrium diffusion chambers ("peepers") or suction samplers. As introduced by Hesslein (1976), the peeper technique relies on diffusive equilibration principles for in situ pore water collection without sample degassing or oxidation (Steinmann & Shotyk 1996, Gao *et al.* 2012). The peeper itself is typically constructed of Plexiglas or some sort of acrylic body that is equipped with a continuous series of dialysis chambers at certain depth intervals and dialysis membranes that separate the chambers from the surrounding peat. The chambers, which are filled with deionized water before installation, equilibrate with the surrounding pore water through diffusion of dissolved constituents (Steinmann & Shotyk 1996, Gao *et al.* 2012). While the peeper technique produces higher resolution concentration profiles, it requires long equilibration times of 27-270 hours at minimum (Gao *et al.* 2012). These peepers can also disturb the peat plot into which they are installed, and they come at a high cost. This hinders the technique's utility for investigating temporal variations in pore water composition at multiple plots simultaneously and at the same plot multiple times.

The suction method of pore water extraction was thus developed to enable repeated sample collection from the same research plot. Pore water sampling via suction requires the installation of tubular samplers into the site peat, followed by the application

of weakly negative pressure to the tube for sample collection (Gao *et al.* 2012). Blodau and Moore (2002) found that retrieving peat pore water through suction could result in a mix of pore water from various depths and pore sizes. When compared to pore water collected from a peeper, the pore water collected via suction had higher dissolved inorganic carbon (DIC) concentrations with larger variability in values and more gradual concentration gradients (Blodau & Moore 2002). Thus, peat pore water extracted through suction techniques could produce concentration patterns that are partially confounded by macroporosity effects including preferential flow patterns. However, these sampling devices do not cause disruption to the peat layers to the same extent as larger peepers. In addition, pore water from suction samplers can be collected without device removal and does not require long equilibration times thus allowing for higher frequency measurements and more constrained temporal investigations. For deeper pore water, simple stand-pipe piezometers can be used, as they are less expensive and easier to install than peepers (Waddington *et al.* 2009, Gao *et al.* 2012). In a study investigating whether the presence of piezometers impacts below-surface pore water CH_4 concentrations at two peatlands, Waddington *et al.* (2009) concluded that pore water obtained from open piezometers had significantly lower CH_4 concentrations than pore water from sealed samplers. The open piezometers created preferential flow paths in the peat, allowing CH_4 to vent to the atmosphere (Waddington *et al.* 2009). Although piezometers can alter peatland gas dynamics, the disturbance is minimized with sealed piezometers. Therefore, to enhance understanding of both spatial and temporal variability of pore water constituents and their role in peatland CH_4 dynamics, the suction sampling technique and

use of sealed piezometers are viable alternatives to the classic equilibrium diffusion chambers.

The present study focuses in particular on the differences in CH_4 cycling dynamics among plant community types during a wet summer at the Mer Bleue ombrotrophic bog in Ottawa, Ontario, Canada. It aims to provide a more detailed examination of indicators of CH_4 production, storage and transport processes for three dominant vegetative communities at Mer Bleue through the analysis of CH_4 fluxes in conjunction with measurements of emitted stable isotope signatures, pore water depth profiles and redox potential. Previous studies at this site have examined the spatial and temporal variability of CH_4 emissions (Lai *et al.*2014a, Moore *et al.* 2011), ecosystem-scale CH_4 emissions (Brown *et al.* 2014), and belowground CH_4 dynamics (Blodau 2001, Blodau & Moore 2003a, Blodau & Moore 2003b, Blodau *et al.* 2007), yet none have simultaneously investigated the high frequency temporal variability of CH_4 emissions with pore water characteristics in conjunction with isotopic techniques across the main vegetative communities. The current study hopes to provide further understanding of the production, storage and transport processes that control CH_4 emissions at Mer Bleue.

3.0 METHODS

3.1 Site description

The Mer Bleue peatland complex is located 10 km east of Ottawa, Ontario (45.41°N, 75.48°W) covering a 28 km^2 area (Figure 3-1) (Roulet *et al* 2007, Moore *et al.* 2011, Lai *et al.* 2012). The region is characterized by a cool continental climate with a mean annual air temperature of 6.4 ± 0.8°C and mean annual precipitation of 943 mm, 47% of which falls during the growing season between May and September (1981-2010, Environment Canada 2014). Westerly winds blow most frequently, with an average annual velocity of 13 km h^{-1}. Each year, the first fall frost arrives ~October 7 at Mer Bleue and the last spring frost occurs ~April 30, with ~210 days where the air temperature is above freezing (Environment Canada 2014). While winter snow cover conditions vary widely between years, peak snow packs tend to range between 60 and 80 cm with snow cover present from December through March (Lafleur *et al.* 2003).

The progression of events leading to the formation of Mer Bleue bog is described in detail by Roulet *et al.* (2007). While the oldest lake sediments of the Mer Bleue peatland basin are ~9000 years old, the conditions for the peatland's formation began prior to 13,200 years ago when regional ice retreat enabled the invasion of Glacial Lake Iroquois. By 13,100 years ago, the Champlain Sea invaded this area and laid down 40-50 m of silty clay marine sediments. Freshwaters were dominant again in this basin around 10,600 years ago. Between 12,000 and 9500 years ago, outbursts from the Ottawa River eroded the postglacial channel system (in which Mer Bleue now lies) into the former floor of the Champlain Sea basin. The Mer Bleue peatland's formation spanned the last 8400 years,

with initial development as a fen, which replaced the existing lake. This was followed by bog phase initiation between 7100 and 6800 years ago (Roulet *et al.* 2007, Moore *et al.* 2011).

The northwestern arm of the Mer Bleue peatland complex is dominated by a dome-shaped ombrotrophic bog (Figure 3-1), which has hosted a long-term C cycling research program for 17 years. This area has an undulating hummock-lawn-hollow microtopography with a 0.25 m mean difference in elevation between hummock and hollow (Lafleur *et al.* 2003). The peat depth varies by ~5 m from the center (5-6 m) to the margins (<0.3 m) where a band of beaver ponds encircles the bog (Roulet *et al.* 2007). The bog surface is covered by *Sphagnum* moss (primarily *Sphagnum capillifolium, Sphagnum magellanicum* and *Sphagnum angustifolium)* with some *Polytrichum strictum* present. At an average height of 0.2-0.3 m, the dominant evergreen and deciduous shrubs include: *Chamaedaphne calyculata, Ledum groenlandicum (=Rhododendron groenlandicum), Kalmia angustifolia* and *Vaccinium myrtilloides.* Sedges (*Eriophorum vaginatum)* and select small trees on hummocks (*Larix laricina* and *Betula populifolia)* add sparse cover to the bog surface (Moore *et al.* 2011). Mer Bleue is considered to be a relatively dry bog, as indicated by the 1998-2014 mean growing season WT depth of 42 cm below hummock top at the tower site. Over this 16-year period, the mean growing season WT position ranged from 33 to 50 cm below peat surface, with observed daily WT minimum and maximum of 78 and 23 cm below the peat surface respectively.

Figure 3-1: Location of the tower site, gas analyzers and logging equipment, and chamber area at the Mer Bleue research site. The star, representing the tower site, is located at 45°24′33″N, 75°31′07″W. Map data: Google, Digital Globe (Imagery Date: 9/24/2013).

3.1.1 Sampling Area

The research sampling area was composed of 6 automated chamber and 3 manual chamber plots located approximately 50 m south of the eddy covariance tower (Figure 3-1). The autochambers were chosen to be representative of the dominant vascular plant communities including *Chamaedaphne*- and *Ledum*-dominated communities (plots C-A 1, 2, and 3 and plots L-A 1, 2 and 3, respectively), while manual chambers were chosen to represent the *Eriophorum*-dominated community (plots E-M 1, 2, and 3). While the number of sampling chambers was limited by the existing infrastructure and physical arrangement of dominant plant communities, the nine selected chambers also captured this peatland's range in microtopography and WT. The autochamber and manual chamber plots were accessed via wooden boardwalks to minimize peat damage and vegetation disturbance. Each chamber was located < 15 m from the gas analyzers and logging equipment (Figure 3-1). The characteristics of each chamber plot, including dominance of vascular and nonvascular species and leaf area index (LAI), are presented in Table 3-1. Leaf area index was measured weekly at each chamber as m^2 leaf area per m^2 ground area (m^2 m^{-2}) using two methods. First, biomass LAI was measured using a Plant Canopy Analyzer (LAI-2000, LI-COR Inc., Lincoln, NE). This instrument calculates the ratio of foliage area to ground area based on radiation measurements made above (2 measurements) and below (3 measurements) the standing plant canopy but does not include the LAI associated with creeping species or moss. It also cannot distinguish between living and dead foliage and simply gives a measure of canopy light interception. Green LAI was determined using the point intercept method. The point intercept frame (60 x 60 cm) had a fishing line grid of 5 x 5 cm squares for a total of 121 grid points.

The frame was leveled and centered above each sampling collar and a metal rod (8 mm diameter) was dropped at alternating grid points such that it was perpendicular to and touching the moss carpet (Adkinson 2009). The number of times the rod came in contact with a living vascular plant organ (leaf, stem, flower, shoot) for each species was recorded over 35 and 9 grid points for automated and static chamber collars, respectively (Larmola *et al.* 2013). The % cover and species composition of the vascular and nonvascular canopy was also determined (Table 3-1). All chambers plots had 100% or near 100% moss cover for the duration of the growing season.

Table 3-1: Vegetation characteristics at the 9 chamber plots including dominance (%) of vascular and nonvascular plant species, growing season maximum biomass leaf area index (LAI, m^2 m^{-2}), total and *Eriophorum vaginatum (EV)* green LAI, and maximum percent of *EV* cover.

Chamber	***Vascular plant species*** *(% dominance)* [a]	***Nonvascular plant species*** *(% dominance)*[a]	***Max. biomass LAI*** *(m^2 m^{-2})*[b]	***Max. total green LAI*** *(m^2 m^{-2})* [b]	***Max. EV green LAI*** *(m^2 m^{-2})*[b]	***Max. % EV cover***
Chamaedaphne						
C-A 1	CC 53%, EV 27%, LG 10%, VO 5%, VM 3%, MT 2%	SP 63%, P 37%	2.83	6.03	2.03	34
C-A 2	CC 84%, LG 8%, VO 5%, MT 2%, VM 1%	P 60%, SP 40%	3.61	6.83	0	0
C-A 3	EV 50%, CC 42%, LG 6%, VM 2%	P 57%, SP 11%	7.24	10.54	6.34	60
Ledum						
L-A 1	LG 40%, EV 40%, MT 10%, CC 9%, VO 1%	SP 96%, P 4%	6.56	5.32	2.66	53
L-A 2	EV 74%, LG 18%, KA 3%, VO 3% MT 2%	SP 87%, P 8%	5.19	10.74	8.71	82
L-A 3	EV 68%, LG 22%, MT 7%, VO 3%	SP 67%, P 31%	4.22	8.09	5.83	74
Eriophorum						
E-M 1	EV 97%, LG 1%, CC 1%, MT 1%	SP 70%, P 6%	5.33	21	20.44	99
E-M 2	EV 83%, CC 9%, VO 5%, MT 3%	SP 64%, P 22%	4.18	12.11	11.11	93
E-M 3	EV 89%, VO 6%, KA 2%, CC 2%, LG 1%	SP 94%, P 0%	4.14	12.78	12.11	96

[a] *CC: Chamaedaphne calyculata, EV: Eriophorum vaginatum, KA: Kalmia angustifolia, LG: Ledum (rhododendron) groenlandicum, MT: Maianthemum trifolium, VM: Vaccinium myrtilloides, VO: Vaccinium oxycoccos, AP: Andromeda polifolia, P: Polytrichum moss, SP: Sphagnum moss.*

[b] From DOY 133 to DOY 239.

3.2 Data collection

3.2.1 Autochamber CH_4 flux measurements

The existing autochamber system (Figure 3-2) was used to collect chamber flux measurements 24 h day^{-1} between May 1 and October 1, 2014. Each autochamber (see Appendix A Section 7.0) was constructed using a PVC collar (height=0.385 m) inserted into the peat and attached to a clear Plexiglas® dome by an aluminum frame (see Lai *et al.* 2012 for full description). The collars enclosed a surface area of 0.21 m^2 (internal diameter=0.52 m) with collars inserted to a depth of 0.16 to 0.31 m (Figure 3-4), which minimized air leakage through the peat. The autochamber domes were 0.205 m high and were sealed when closed by a partially-deflated bicycle tube and foam gasket. The chamber headspace air was mixed by a small brushless fan fixed to the inside of the dome. Pressure equilibration between external and internal environments was achieved during autochamber flux measurements through a 0.50 m long vent tube that was coiled, open at both ends and emerged from the dome top.

The autochamber system was controlled by a datalogger (CR23X, Campbell Scientific) and was programmed to close the chamber domes sequentially every half hour for 2.5 minutes during the day (09:00-21:00 EST) to minimize plant stress, and 15 minutes at night (21:00-09:00 EST) to minimize bias introduced by atmospheric turbulence (Lai *et al.* 2012). This produced a measured flux value for all chambers each half hour during the day and every 4 hours at night. An oil-free air compressor and pneumatic cylinder system powered the opening and closing of chambers. Sampling tubes drew the gases from the appropriate chamber to a sampling manifold where CH_4

concentrations were measured using a fast CH_4 analyzer using off-axis integrated cavity output spectroscopy (model DLT-100, Los Gatos Inc., Mountain View, CA), and CO_2 concentrations were measured by a closed-path infrared gas analyzer (LI-6262, LI-COR Inc.) in a temperature controlled housing. Sampled once per second and averaged every 5 seconds, gas analyzer data were automatically sent to a computer in an enclosed hut at the nearby tower site (Figure 3-1). The gas analyzers and autochambers were maintained regularly, particularly at the beginning of the season (e.g. replaced tubing, patched leaks, repaired fans). The system's equipment (gas analyzers, data logger, air compressor and manifold and pump system) was located under a shelter at the junction of the primary and secondary boardwalks (Figure 3-5).

Figure 3-2: Photos of a) the autochamber system at Mer Bleue used to measure CH_4 fluxes at b) the plant community scale with c) a Plexiglas® dome fitted to a PVC collar.

Flux data were processed in Matlab 8.1.0.604 (The Math Works, Inc., 2013). Only nighttime data were used as the autochambers closed for 15 minute periods, which reduced the flux underestimations caused when winds flush the near surface peat and there is an associated decrease in headspace turbulence during deployment (Lai *et al.* 2012). When deployment periods are too short (< 13 minutes), these turbulence conditions influence headspace CH_4 concentrations after the chamber closes. As a result, we used only the last 250 seconds of data to calculate nighttime CH_4 fluxes. CH_4 fluxes (F_{CH4}, nmol m^{-2} s^{-1}) were calculated as:

$$F_{CH4} = \frac{\rho V}{R^* T_{air} A} \frac{dC}{dt} \quad (11)$$

where ρ is air pressure (Pa), V is chamber volume (m^3), R^* is the ideal gas constant (8.314 J K^{-1} mol^{-1}), T_{air} is mean air temperature (°K), A is chamber surface area (m^2), and dC/dt is the rate of change in CH_4 mixing ratio in the chamber over the measurement period (nmol mol^{-1} dry air s^{-1}). The mixing ratio of CH_4 takes into consideration the effects of water vapour dilution and was calculated using the headspace mole fraction of CH_4 and the water vapour mole fraction measured by the LI-6262 gas analyzer. A negative CH_4 flux indicates uptake by the peatland while a positive flux indicates CH_4 loss to the atmosphere.

3.2.2 Static chamber CH_4 flux measurements

As there were no existing autochamber plots representative of the *Eriophorum*-dominated community, 3 *Eriophorum* plants for manual CH_4 flux measurement were selected in close proximity to the autochamber system (Figure 3-3).

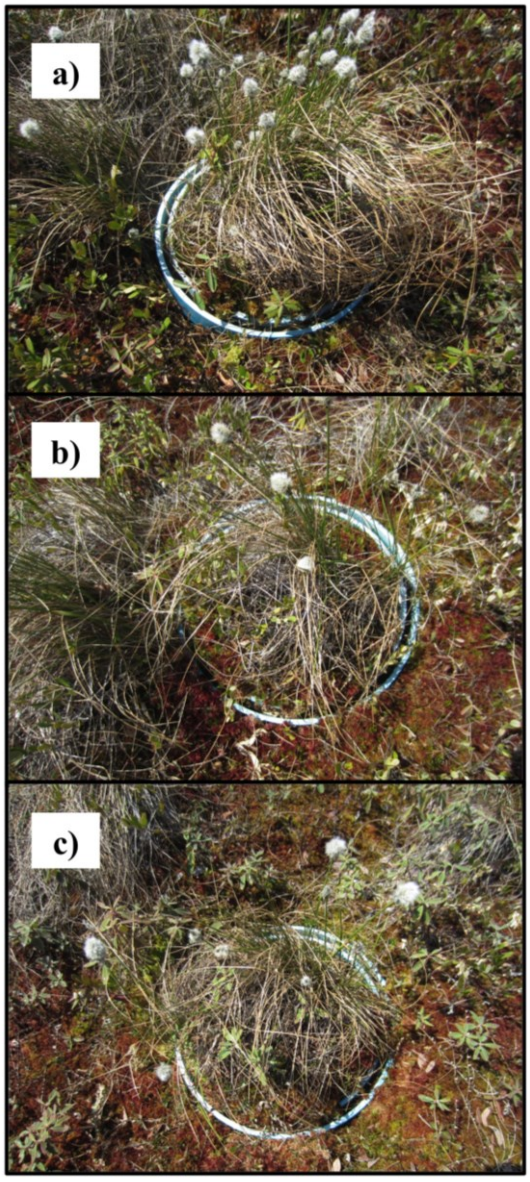

Figure 3-3: Photos of manual chamber collars inserted into the peat at a) E-M 1, b) E-M 2 and c) E-M 3 *Eriophorum* plants.

Grooved collars of 0.24 m internal diameter (surface area= 0.05 m^2) were inserted ~10 cm into the peat to be compatible with existing 18 L opaque chambers at the site. All manual chambers were covered with aluminum foil tape to minimize temperature increase during measurement (Bubier *et al.* 1995a). Flux measurements were made at least twice weekly (2-3 rounds per sampling day) between 07:00 and 15:00 EST. A seal was created between collar and chamber during the measurement period by filling the collar grooves with water. The air in these static chambers was sampled at 5 min intervals for a total of 20 min starting at time 0. First, 60 cc of air was pumped between a sealed syringe and the chamber via tubing 3 times to mix the headspace air. Next 24 cc of air was extracted and injected via syringe and needle to an evacuated 12 cc vial with a small amount of magnesium perchlorate as a desiccant. Vials were analyzed for CH_4 mixing ratio on a Varian CP-3800 gas chromatograph at Carleton University, with methods described in detail by Wilson & Humphreys (2010). The gas chromatograph used flame-ionization detection and methanizer technology at 300°C and 350°C, respectively, with a He carrier gas at an injection rate of 30 ml min^{-1}. Quality control was maintained during gas sampling using three replicates of five standards (439.2-15212.6 ppm CO_2, 1.08-19.4 ppm CH_4) and He blanks. The chamber was removed for at least 2 minutes between successive rounds of flux measurements.

The slope of the regression between CH_4 concentration and time during the 20-minute sampling period was used to calculate CH_4 fluxes (Roulet *et al.* 2007) following Equation 11. Samples were rejected when CO_2 and CH_4 concentrations remained close to ambient concentrations for the duration of the sampling period when a substantial flux was expected given the measurements from that chamber during a particular time period,

indicating contamination of the sample with ambient air through a possible chamber or vial leak. Samples were also rejected when there was a large initial spike in CO_2 and CH_4 concentrations, as this suggested that the placement of the chamber on the collar disturbed the peat and caused a rapid degassing of trace gases to the chamber headspace. Approximately 17% of samples were rejected.

Although there were some inherent differences among the chamber sampling methods (static vs. circulating flow, collar area, chamber headspace, slope determinations), we were confident that the two methods were comparable as the magnitude and temporal variability of fluxes from the *Eriophorum* plots were very similar to those presented by Lai *et al.* (2014a) when the autochambers had been located on *Eriophorum* plants near the static chamber plots used in this study.

3.2.3 Pore water collection

Weekly pore water collection occurred between 07:00 and 15:00 EST starting on June 4 and ending on September 12, 2014. In order to minimize vegetation and subsurface peat disturbance within sampling collars, pore water was collected at least 20 cm from the collar edge in an area with similar moss and vegetation cover. The order of pore water collection for each sampling plot was randomized week-to-week. A portable pore water sipper (Figure 3-5a) was used to collect pore water directly below the WT on each sampling day. The sipper was inserted into the peat at the required depth and a 60 ml syringe was attached to the top of the sipper with a 3-way stopcock. The syringe was used to pull up and flush out 30 ml of pore water. After flushing, 30 ml of pore water was collected and the stopcock was closed to the atmosphere.

Pore water at 50, 65 and 80 cm below the peat surface was collected using permanent pore water samplers (Figure 3-4 , Figure 3-5b). Pore water "seepers" were constructed from a section of PVC piping (length=15 cm, internal diameter=2.54 cm) with rows of holes at 1 cm intervals drilled 10 cm from the sealed end of the seeper and covered in fine mesh. Rubber stoppers were inserted at both ends of the seeper and two small holes were drilled through the top stopper so that two Bev-A-Line tubes could be installed for sample extraction and nitrogen pressure equalization. A 3-way stopcock was added at the end of each tube to enable the use of a syringe above the peat surface. Pore water seepers were installed at 50, 65 and 80 cm on June 4, 2014 at each plot. Pore water was collected from seepers using a similar method to the sipper procedure. A 60 ml syringe was attached to the stopcock of the sample extraction tube emerging from the peat. A Tedlar bag (volume=1L) filled with nitrogen was attached to the second tube's stopcock for pressure equilibration. After opening the stopcocks to enable nitrogen flow to depth and pore water flow to surface, a syringe was used to pull up and flush out 30 ml of pore water. The 30 ml pore water sample was then collected and both stopcocks were closed.

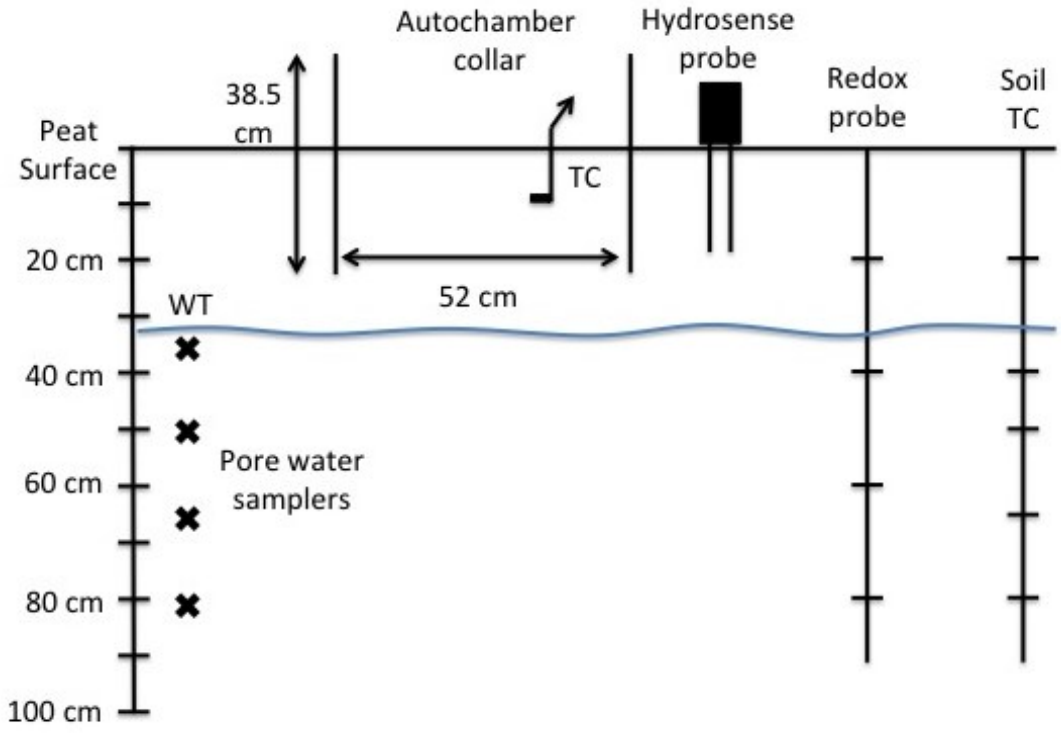

Figure 3-4: Example setup of instrumentation at an autochamber collar showing sampling depths for pore water samplers, Hydrosense probe, redox probe and soil thermocouples (TC) inside and outside the chamber collar. Note that only a single soil thermocouple profile was installed and was located near the flux tower ~ 50 m from the autochambers. All other sensor placements and depths are to scale.

A secondary pore water sampler was designed and installed on August 6, 2014 at 50, 65 and 80 cm for each plot. This fat sipper design consisted of a piezometer for each sampling depth (internal diameter=1.91 cm) with holes drilled at the appropriate depth, a cap sealing the bottom and a cap and septa at the top (Figure 3-5c). Before the first sampling, piezometers were flushed with nitrogen via tubing and a 22-gauge (0.7 mm x 25 mm) needle piercing the septa in the top cap (a second needle was inserted into the septa to allow for pressure equilibration). Samples were obtained by removing the top septa and cap, inserting a sipper and collecting pore water as per the sipper and syringe

method described above. After pore water extraction, the piezometers were sealed and flushed with nitrogen to limit O_2 entry to the subsurface.

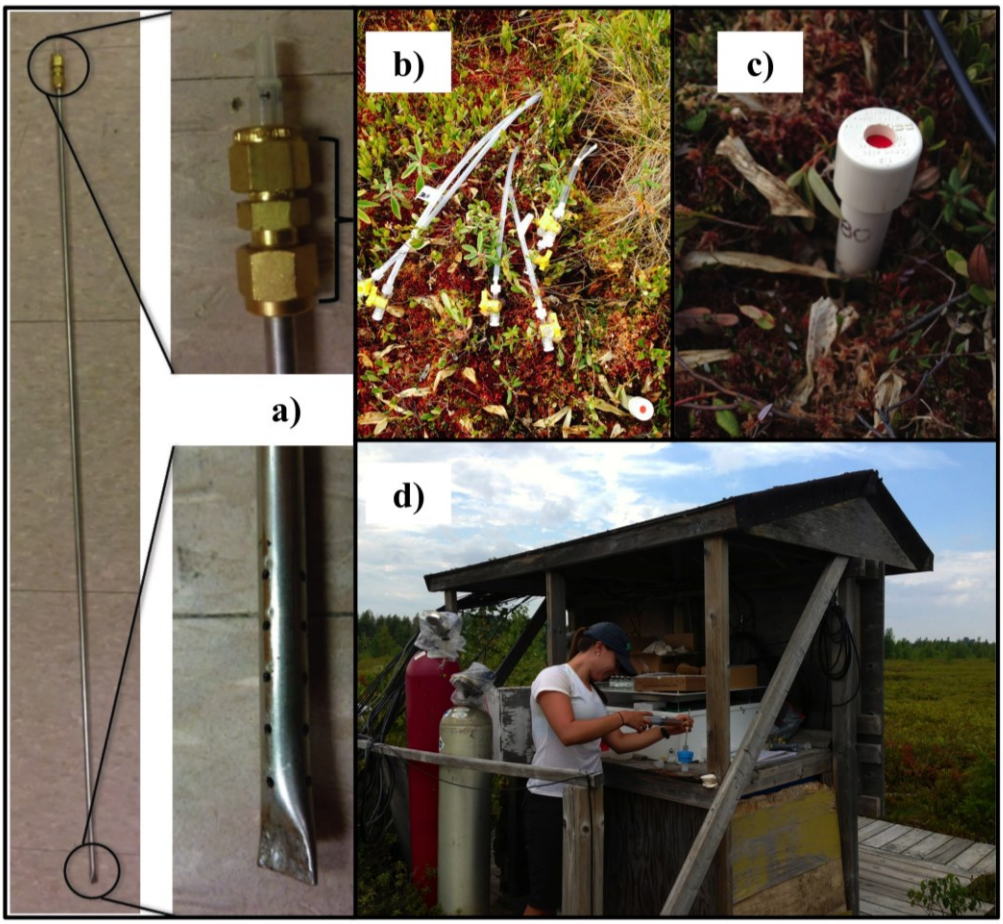

Figure 3-5: Photos of pore water sampling instrumentation where a) a pore water sipper was used to collect pore water from depths < 50 cm below peat surface and permanent b) pore water seepers and c) piezometers were used to collect pore water at 50, 65 and 80 cm. After samples were collected, d) pore water filtration and equilibration for isotope analysis was carried out in the field at a small equipment hut.

Once a 30 ml pore water sample was obtained in a 60 ml syringe using the above methods, the remaining 30 ml of the syringe was filled with ambient air. The stopcock was then closed to the atmosphere and the syringe was shaken for 2 minutes to equilibrate liquid and gas CH_4 concentrations. The syringe headspace was pushed through a 22-gauge needle to displace saltwater in a 30 ml vial (sealed and crimped) until

15 ml of headspace remained in the syringe. The remaining 15 ml of headspace sample air was used to overpressurize the saltwater solution. 2.5 ml of gas in the headspace was analyzed for CH_4 on the Varian CP-3800 as described above. The water remaining in the syringe was then filtered through a 0.40μm glass fiber filter (diameter=47 mm) and stored in a 20 ml scintillation vial in the fridge for DOC analysis. Pore water CH_4 concentrations (μmol L^{-1}) were calculated according to the equations found in Appendix B Section 7.0.

Pore water samples were analyzed on a Shimadzu TOC/TN-V_{CSN} analyzer at McGill University for DOC (mg L^{-1}) and total dissolved nitrogen, TDN (mg L^{-1}) using the combustion catalytic oxidation method at 680°C. The carbon to nitrogen ratio (C/N) was calculated as the ratio between DOC and TDN. UV absorbance (m^{-1}) was determined at 250, 254 and 365 nm on an Agilent Cary 60 UV-Vis spectrophotometer with a fiber optic dip probe in dual beam mode at a scan rate of 600 nm/min. The aromaticity of DOC was approximated by calculating specific ultraviolet absorbance at 254 nm, $SUVA_{254}$ (L m^{-1} mg^{-1} DOC), as:

(12) $$SUVA_{254} = \frac{UV\ Absorbance\ at\ 254\ nm\ (m^{-1})}{DOC\ (mg\ L^{-1})}$$

where the UV absorbance at 254 nm (m^{-1}) is divided by the DOC concentration (mg L^{-1}).

3.2.4 Storage Change

Each pore water CH_4 measurement was representative of a peat layer based on sampling depth (20 cm, below WT, 50 cm, 65 cm, 80 cm). For example, the pore air sample taken at 20 cm represented the aerated zone from the peat surface to the average WT position at each individual chamber. The average WT from DOY 155-255 was determined for each chamber and used to calculate the unique thickness of peat layers for each sampling depth at each chamber. Methane concentration values were weighted for each specific peat layer thickness.

These depth-weighted CH_4 concentration values were used for storage change calculations at specific depths (i.e. 50 cm sampling depth had associated peat layer thickness of 15 cm), or after summing over a total depth of 1 m. Units were converted from μmol cm^{-2} to mg cm^{-2}, and a plot of depth-weighted CH_4 concentrations (mg cm^{-2}) over time (DOY) was constructed for each chamber. Linear regressions were then applied to obtain chamber-specific slope values, where slope represented the change in CH_4 storage over time for that chamber (mg cm^{-2} d^{-1}). These values were converted to units of mg m^{-2} h^{-1} to obtain final storage change values (S_{CH4}, mg m^{-2} h^{-1}). The average CH_4 flux ($F_{CH4,}$ mg m^{-2} h^{-1}) was then calculated for each chamber over the pore water sampling period using manual sampling day data.

3.2.5 Headspace sample collection

Weekly headspace sample collection occurred on pore water sampling days between July 31 and September 12, 2014. At the end of autochamber and static chamber measurements, 30 ml headspace samples were obtained using the septum-stopcock extraction method with a 22-gauge needle and syringe. These 30 ml gas samples were injected into evacuated, sealed and crimped 30 ml vials.

Headspace gas samples were analyzed at Arizona State University on a Picarro G2201-*i* CRDS (Cavity Ring-down Spectroscopy) Analyzer in combined mode for isotopic C in CO_2 and CH_4. This instrument had a simultaneous mode precision of <0.16‰ for $\delta^{13}C\text{-}CO_2$ and <1.15‰ for $\delta^{13}C\text{-}CH_4$, and maximum peak-to-peak drift of <0.6‰ for $\delta^{13}C\text{-}CO_2$ and <1.5‰ for $\delta^{13}C\text{-}CH_4$ (Picarro, Inc. 2015). The sample flow rate was <50 sccm (typical ~25 sccm) at 101.3 kPa. The isotopic composition and concentration of sample and background CH_4 were used to calculate $\delta^{13}C\text{-}CH_4$ source signatures at each chamber through the Keeling Plot approach (Equation 10).

3.2.6 Redox potential measurements

This study used a HYPNOS 3 datalogger for redox measurements. The HYPNOS logger measured the difference in potential between the soil matrix and an Ag/AgCl reference probe (QM710X from Q-I-S) with 3 M KCl filling solution. Nine fiberglass probes with platinum sensor tips and temperature sensors (DS18B20, ±5°C accuracy from 10 to 85°C) at 20, 40, 60 and 80 cm (Figure 3-4) were installed adjacent to each chamber on July 18, 2014. The reference probe was installed close to the junction of the main and secondary boardwalks, near the equipment hut (Figure 3-1). The data were

stored on an SD card (Vorenhout *et al.* 2011). Readings were recorded every 10 minutes and data were downloaded from the SD card every ~2 weeks.

Standardized redox potential values (Eh, mV) were calculated according to:

(13) $$E_h = E_m + E_{ref}$$

where E_h is the standardized redox potential, E_m is the measured redox potential, and E_{ref} is the potential of the reference probe (Vorenhout *et al.* 2011). As the Ag/AgCl reference probe had a 3M KCl filling solution, the linear relation between E_{ref} and temperature (Langmuir 1971) was used to determine temperature-specific E_{ref} values for the calculation of E_h values. These standardized redox potentials were then adjusted for pH according to:

(14) $$E_{h\text{-}corrected} = E_h + 59(pH - 7)$$

where the pH was assumed to be stable at 4.

3.2.7 Environmental variables

Ancillary field measurements included environmental variables presented in Table 3-2. These variables were measured at varying frequency, as indicated in the table, and employed both manual and automated methods. They served to characterize the microclimate and vegetation for each sampling chamber and to quantify differences between vegetative communities.

Wells were established at each sampling plot for the manual measurement of WT position. Depth to WT was measured manually at each plot using a “bubbler” each day

that manual flux measurements were obtained. WT was also measured at 30 min intervals at each plot throughout the season using automatic capacitive water level loggers installed in wells adjacent to each chamber. Rainfall was measured at 2 rain gauges (NE and S of main tower site hut) every day that fieldwork was conducted. An existing tipping bucket rain gauge near the eddy covariance tower also measured rainfall at the site, and was calibrated for under-catching using a relationship developed with manual measurements.

Peat temperature was measured continuously at 10 cm depth using chromel-constantan thermocouples installed in each collar as of May 29, 2014. An existing thermocouple profile at the tower site measured peat temperature at 20, 40, 50, 65 and 80 cm below the peat surface.

A datalogger (CR7X, Campbell Scientific) and existing instrumentation at the eddy covariance tower site recorded additional climate variables including air temperature, atmospheric pressure, and photosynthetic photon flux density. Lafleur *et al*. (2003) provide a description of instruments; measurements were recorded every 5 s and averaged over 30 min.

Air temperature (°C) and rainfall (mm) data collected at Mer Bleue were compared to 30-yr Ottawa climate normals (1981-2010, Environment Canada 2014) measured at the Ottawa International Airport, located approximately 20 km southwest of the research site. Each month's daily average temperature and standard deviation were analyzed along with total monthly rainfall from May through September.

Table 3-2: Frequency and method of manual and automated measurements for environmental variables.

Variable	***Measurement frequency***	***Measurement Method***
WT depth	2-3 times per week 30 min	1 well per chamber§ Odyssey capacitive water level logger
Rainfall	3-4 times per week Variable	2 rain gauges§ Tipping bucket rain gauge*
Peat temperature (10, 20, 40, 50, 65, 80 cm)	5s (averaged every 30 min)	Chromel-constantan thermocouples
Air temperature (0.5 m height)	5s (averaged every 30 min)	Chromel-constantan thermocouples*
Atmospheric pressure	5s (averaged every 30 min)	Barometer*
Photosynthetic photon flux density	5s (averaged every 30 min)	Quantum sensor*
Biomass LAI	1 time per week	LAI-2000 Plant canopy analyzer§
Green LAI	1 time per week	Point intercept method§
Moss moisture	2 times per week	Peat tabs §
Moss live sampling	1 time per week	Manual collection outside chamber§
Moss volumetric water content	2 times per week	HydroSense soil water sensor§

Note: LAI=leaf area index.
§manual measurement
*existing instrumentation at eddy covariance tower site.

3.2.8 Statistical analyses

All statistical analyses were completed using JMP 12.0.1 (SAS Institute Inc.). For seasonal analyses, the data were separated into late spring (LSp, DOY 132-154), early summer (ES, DOY 155-189), mid-summer (MS, DOY 190-221), and late summer (LS, DOY 222-255) measurement periods. Fluxes were available for the late spring period, while pore water data collection started with the early summer period. Redox potential measurements were only active during the late summer period. All data were tested prior to analyses for assumptions of normality and equal variances. Data that did not meet the assumption of normality were transformed. While this did not fully correct the distribution in all cases, the restricted maximum likelihood (REML) method used in mixed model analysis is robust to deviations from normality (Fung & Xu 2010). Statistical analyses were tested at the significance level of 0.05, unless otherwise stated.

A simple linear regression analysis was applied to examine the relationship between mean seasonal depth to WT and log CH_4 flux. Averages were determined based on manual static chamber sampling day data to ensure completeness of flux data at *Eriophorum* plots. The relationship between mean 50 cm CH_4 storage change and mean CH_4 flux was examined using a Pearson's correlation analysis and nonlinear regression for manual sampling days during the pore water collection period. The relationships among indicators of CH_4 production, storage and transport were examined when all variables were available between DOY 212-255. Analyses of calculated averages of these variables at the 50 cm depth included a principal components analysis (PCA), and multiple correlation analysis using Pearson correlations.

Repeated measures analyses using mixed models were applied to investigate CH_4 fluxes throughout the growing season, pore water CH_4 concentrations during the pore water sampling period (DOY 155-255), and the $\delta^{13}C$-CH_4 isotopic signatures for headspace sampling days. The model was fit using restricted maximum likelihood (REML) method in the standard least squares personality to view the variation in intercepts and slopes. The REML method is the commonly accepted method for fitting mixed models, as it provides accurate results regardless of whether the data is balanced or not (JMP 7 Statistics and Graphics Guide 2007). The "chamber" variable was designated as a random effect and nested within vegetative community since the chamber plots were randomly selected from the vegetation populations. The fixed effects were analyzed to a factorial degree of 2 in order to examine interaction effects (JMP 7 Statistics and Graphics Guide 2007).

4.0 RESULTS

4.1 Environmental conditions

The environmental conditions for the 2014 season at Mer Bleue were analyzed in reference to the 1981-2010 climate normals (Environment Canada 2014) (Figure 4-1). The daily average air temperatures were comparable with Ottawa climate normals for the early summer 2014 period, while the mid- to late-summer periods were slightly cooler than the long-term average. Mer Bleue experienced a wet summer compared to the last 30 years, with particularly heavy rainfall events in June contributing to a total rainfall of 569.0 mm from May through September in comparison to the climate normal of 440.4 mm for the same period (Figure 4-1). The WT recorded near the tower (where the long term record has been maintained since 1998) reflected these wet conditions and was high relative to the long-term average (Figure 4-2).

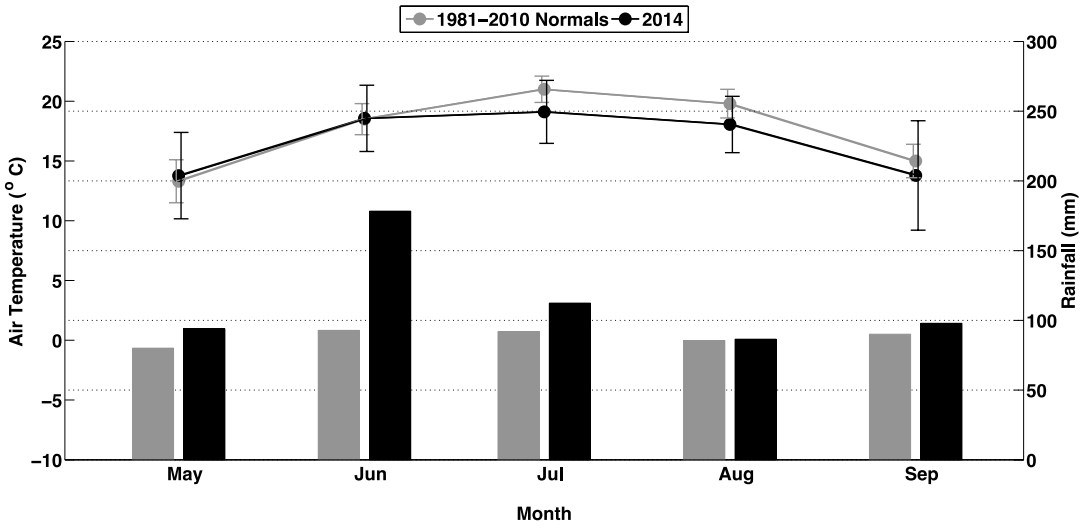

Figure 4-1: Mean (±1 SD) daily average air temperature (lines) and total monthly rainfall (bars) from May through September 2014 at Mer Bleue peatland in reference to 1981-2010 climate normals measured at the Ottawa Macdonald-Cartier International Airport (Environment Canada 2014).

The 2014 WT at a given location varied by only 10 cm from the mean and was thus restricted to a narrow fluctuation range compared to previous years. During 2014, the WT never reached mid-summer depths typical at Mer Bleue. Differences in WT among plant communities were a result of microtopography: *Chamaedaphne* plants were located on hummock tops while *Ledum* and *Eriophorum* were in hollows or depressions between hummocks (Figure 4-2). As a result, the *Chamaedaphne* community's WT was on average 10 cm lower than *Ledum* and *Eriophorum* communities. Note that the *Chamaedaphne* community and the tower site had very similar WT depth patterns because of their similar microtopographic position, while *Ledum* and *Eriophorum* communities both had WT closer to the surface due to their relatively low position. The

Eriophorum community had the shortest WT measurement period due to the timing of instrument installation and removal.

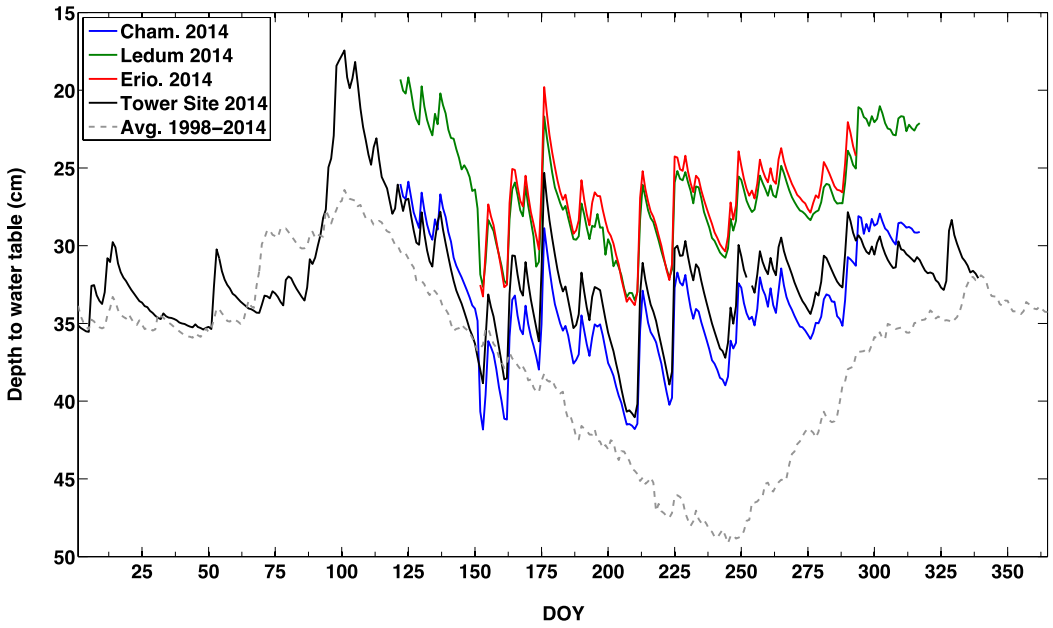

Figure 4-2: Mean daily depth to water table from peat surface (cm) measured at *Chamaedaphne*, *Ledum* and *Eriophorum*-dominated communities and tower site at Mer Bleue, 2014. The long-term mean water table position recorded at the tower site between 1998 and 2014 is shown for comparison.

The 10 cm peat temperatures followed daily mean air temperature patterns with slightly dampened day-to-day variations at this depth (Figure 4-3). With increased depth from the peat surface, temperatures were cooler with fewer extreme values as the dampening of day-to-day variations in peat temperature increased with depth (Figure 4-4). At 20 cm and below, peat temperature consistently increased over the 2014 measurement period to DOY 255.

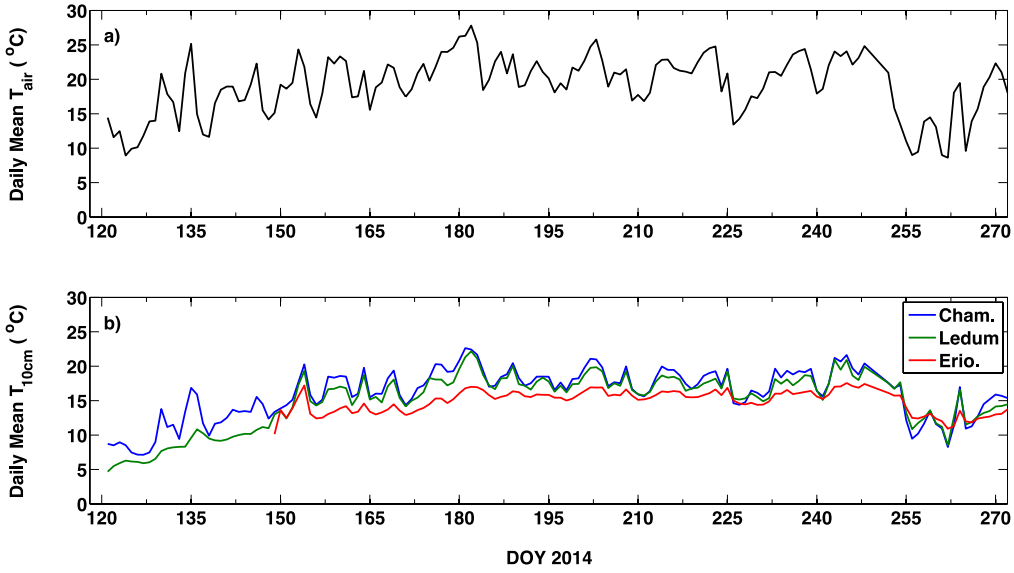

Figure 4-3: Daily mean a) air temperature (T_{air} ,°C) and b) 10 cm peat temperature (T_{10cm} ,°C) for the *Chamaedaphne*, *Ledum* and *Eriophorum*-dominated communities during the 2014 measurement period.

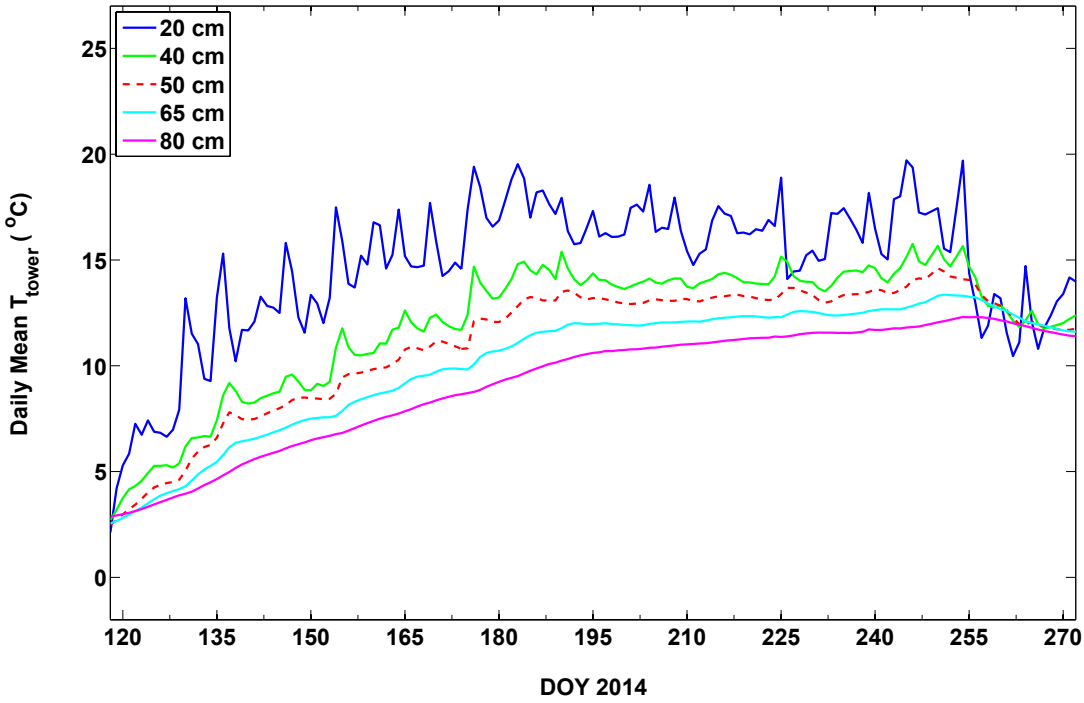

Figure 4-4: Daily mean peat temperature at the tower site (T_{tower}, °C) measured at 20, 40, 50, 65, and 80 cm below peat surface during the 2014 measurement period.

4.2 Methane fluxes

The *Chamaedaphne*-dominated autochamber community had the lowest mean daily CH_4 emissions compared to the *Ledum*- and *Eriophorum*-dominated communities (Figure 4-5). The *Eriophorum* community had the most temporally variable fluxes and by late July (~DOY 210) this community represented a CH_4 emission hot spot. The *Ledum* and *Eriophorum* communities' emissions demonstrated a clear seasonal increase to roughly mid-July (~ DOY 195) after which emission rates remained high until mid-September (~DOY 255). In contrast, the *Chamaedaphne* community's emissions increased more modestly with fluxes remaining relatively small. The manual static chamber sampling days, indicated by the open black circles in Figure 4-5, were representative of the overall trends for the *Chamaedaphne* and *Ledum* communities.

By splitting the season into late spring, early summer, mid-summer and late summer periods, differences in CH_4 fluxes between communities were apparent (Table 4-1). In particular, by mid- to late-summer, the *Ledum* and *Eriophorum* communities had mean daily CH_4 flux values that were at least 3 times greater than *Chamaedaphne* fluxes.

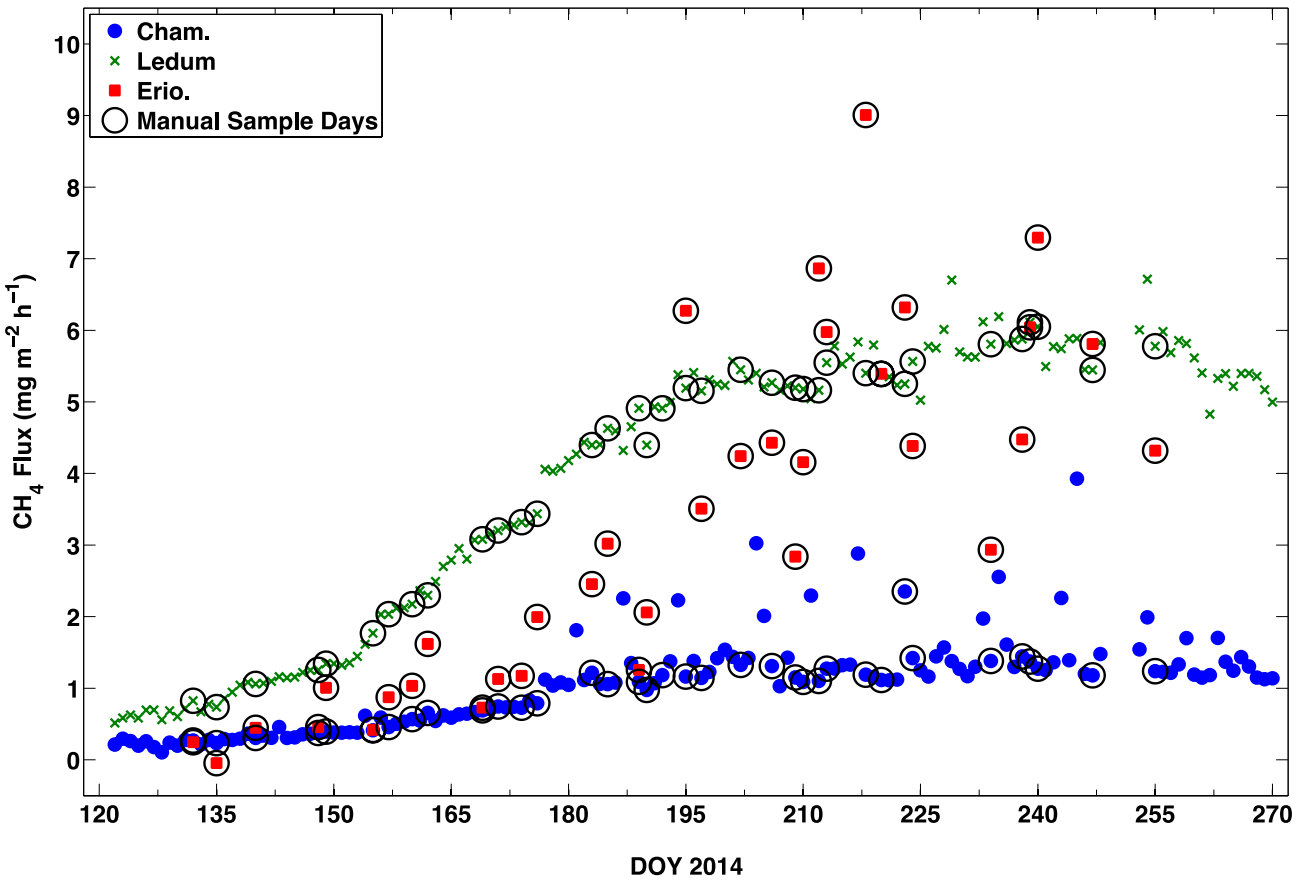

Figure 4-5: Mean daily CH_4 flux (mg m^{-2} h^{-1}) for *Chamaedaphne*, *Ledum* and *Eriophorum*-dominated communities at Mer Bleue during the 2014 measurement period (DOY 120-270). Open circles indicate days when manual static chamber flux sampling measurements were collected at the *Eriophorum* community chambers.

Table 4-1: Comparison of mean daily CH_4 flux, water table (WT) and 50 cm peat temperature at the tower site (T_{50cm}) for *Chamaedaphne*, *Ledum* and *Eriophorum*-dominated communities at Mer Bleue, 2014. Standard deviation is given in parentheses. CH_4 fluxes with different superscripts across a row are significantly different at the α=0.10 level when accounting for the chamber as a random effect (or repeated measure) in a mixed model and using Student's *t*-test post-hoc analysis. Similarly, WT depths with different superscripts across a row are significantly different at the α=0.10 level when accounting for the chamber as a random effect (or repeated measure) in a mixed model and using Student's *t*-test post-hoc analysis.

Chamaedaphne		*Ledum*		*Eriophorum*		
CH_4 Flux (mg CH_4 m^{-2} h^{-1})	WT (cm)	CH_4 Flux (mg CH_4 m^{-2} h^{-1})	WT (cm)	CH_4 Flux (mg CH_4 m^{-2} h^{-1})	WT (cm)	T_{50cm} (°C)
Whole Period (DOY 132-255, n=891)						
0.99^{b} (0.82)	36.5^{a} (6.7)	4.13^{a} (2.13)	28.8^{b} (3.7)	2.95^{ab} (3.57)	28.5^{b} (3.6)	11.1 (3.0)
Late Spring (DOY 132-154, n=129)						
0.32^{a} (0.30)	35.2^{a} (7.0)	1.04^{b} (0.39)	27.3^{a} (3.6)	0.52^{NA} (0.51)	N/A	6.6 (1.8)
Early Summer (DOY 155-189, n=281)						
0.77^{b} (0.54)	36.0^{a} (7.2)	3.21^{a} (1.26)	28.3^{ab} (4.0)	1.39^{b} (1.45)	27.5^{b} (3.7)	11.3 (1.2)
Mid Summer (DOY 190-221, n=223)						
1.17^{b} (0.52)	37.0^{a} (6.5)	5.19^{a} (1.53)	29.7^{b} (3.3)	4.46^{ab} (4.15)	29.2^{b} (3.7)	13.2 (0.2)
Late Summer (DOY 222-255, n=185)						
1.46^{b} (1.24)	37.1^{a} (6.2)	5.74^{a} (1.82)	29.2^{b} (3.4)	5.12^{a} (4.11)	29.2^{b} (2.8)	13.6 (0.4)

From a chamber-specific perspective, CH_4 emissions for the *Ledum* were greatest for autochambers L-A 2 and 3 (Figure 4-6). While classified as part of the *Ledum* community, L-A 2 and 3 had *Eriophorum* plants within the chamber collar that constituted 74% and 68% of total LAI, respectively. In contrast, autochamber L-A 1 had a tightly constrained CH_4 emission pattern with moderate fluxes at about half the emission rates of the L-A 2 and 3 autochambers. E-M 1 was the driver of the highest daily *Eriophorum* fluxes, while the other two *Eriophorum* plots were characterized by less frequently elevated flux values. Autochambers C-A 1, 2, and 3, predominantly composed of *Chamaedaphne* shrubs, had the lowest CH_4 emissions despite sporadic higher flux events from C-A 1. While these nine chambers were selected from a relatively small sampling area within the peatland, the spatial variability of summer CH_4 fluxes was slightly larger than the temporal variability (Figure 4-6). For example, for any given manual flux sampling date, the coefficient of variation ranged from 52-102% (as a measure of spatial variation), while the coefficient of variation ranged from 28-87% for a given chamber across all 36 sampling dates (as a measure of temporal variation). Greatest temporal coefficients of variation were associated with the *Eriophorum* community plots (73 – 87%) compared to the *Ledum* (28 – 49%) and *Chamaedaphne* (45– 66%) plots.

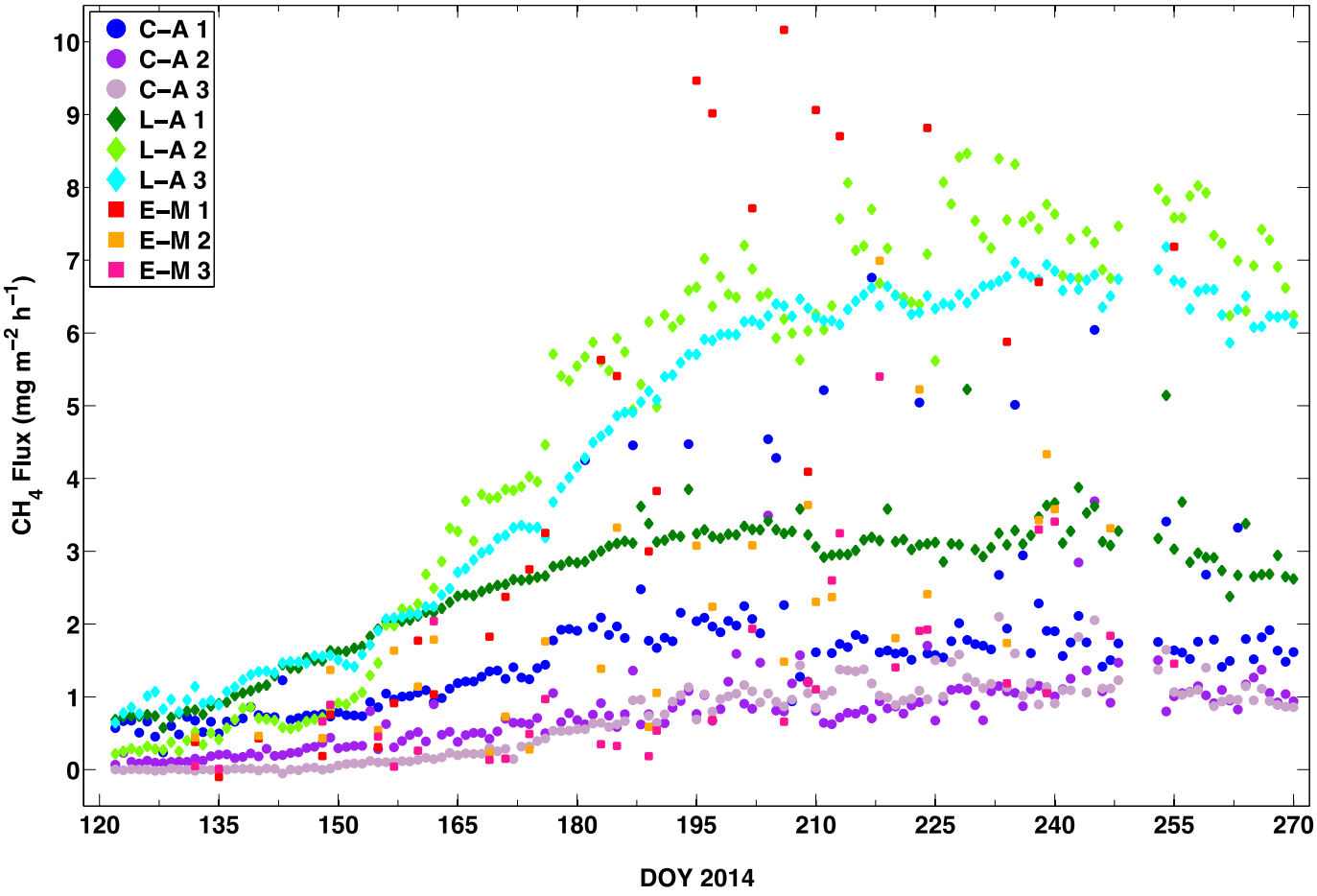

Figure 4-6: Mean daily CH_4 flux (mg m^{-2} h^{-1}) emitted from 3 *Chamaedaphne*-dominated autochambers (C-A 1, 2, 3) (circles), 3 *Ledum*-dominated autochambers (L-A 1, 2, 3) (diamonds) and 3 *Eriophorum*-dominated manual chambers (E-M 1, 2, 3) (squares) at Mer Bleue during the 2014 measurement period (DOY 120-270).

To better understand the factors influencing spatial and temporal variations in CH_4 emissions, the log transform of CH_4 fluxes for manually sampled days were analyzed using a mixed model with community as a fixed effect, chamber as a random effect (to account for repeated measures on the same location over time) and with the following variables as covariates: barometric pressure, 10 cm peat temperature and WT from each chamber, and 50 cm peat temperature from the tower location. There was no statistically significant effect of 10 cm peat temperature as a covariate of CH_4 fluxes ($F(1,794) = 2.6170$, $p = 0.1061$). For example, the *Chamaedaphne* community plots' 10 cm peat temperatures varied greatly while there was a relatively restricted range of low CH_4 fluxes (Figure 4-7). There was a smaller temperature range and wider range of measured CH_4 fluxes for the *Ledum* community. The *Eriophorum* community demonstrated greatest variability among chambers in both temperature and CH_4 fluxes with greatest fluxes for E-M 1 despite little temperature variation at 10 cm while E-M 2 reached the highest temperatures but did not produce the greatest CH_4 fluxes. The day-to-day variation in 10 cm peat temperature obscures the relationship with CH_4 flux, such that peat temperature at 10 cm depth is not useful for analyzing CH_4 flux patterns **(**Figure 4-7). However, deeper peat temperatures 40-50 cm below the surface have been successfully applied in an examination of controls on CH_4 emissions (Moore *et al.* 2011, Lai *et al.* 2014a). There was a statistically significant effect of 50 cm peat temperature ($F(1,791.8)=523.8658$, $p<0.0001$) with a significant interaction effect of vegetation community and 50 cm peat temperature ($F(2,791.1)=62.7842$, $p<0.0001$). There was a positive relationship between 50 cm peat temperature and CH_4 flux (Figure 4-8) suggesting that peat temperature near the WT may be an important environmental control

on CH_4 emissions although the relationship between CH_4 flux and 50 cm peat temp varies among the vegetative communities.

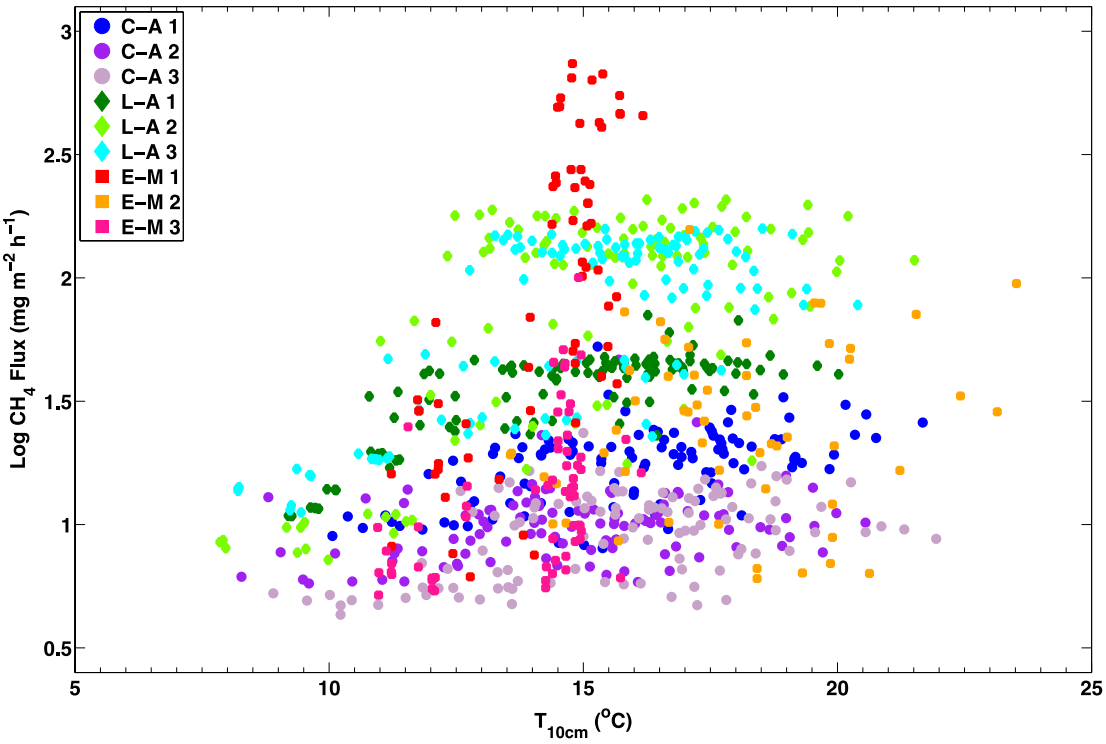

Figure 4-7: The relationship between 10 cm peat temperature (T_{10cm} ,°C) and log CH_4 flux (mg m^{-2} h^{-1}) emitted from 3 *Chamaedaphne*-dominated autochambers (C-A 1, 2, 3) (circles), 3 *Ledum*-dominated autochambers (L-A 1, 2, 3) (diamonds) and 3 *Eriophorum*-dominated manual chambers (E-M 1, 2, 3) (squares) at Mer Bleue for manual sampling day data (DOY 132-255).

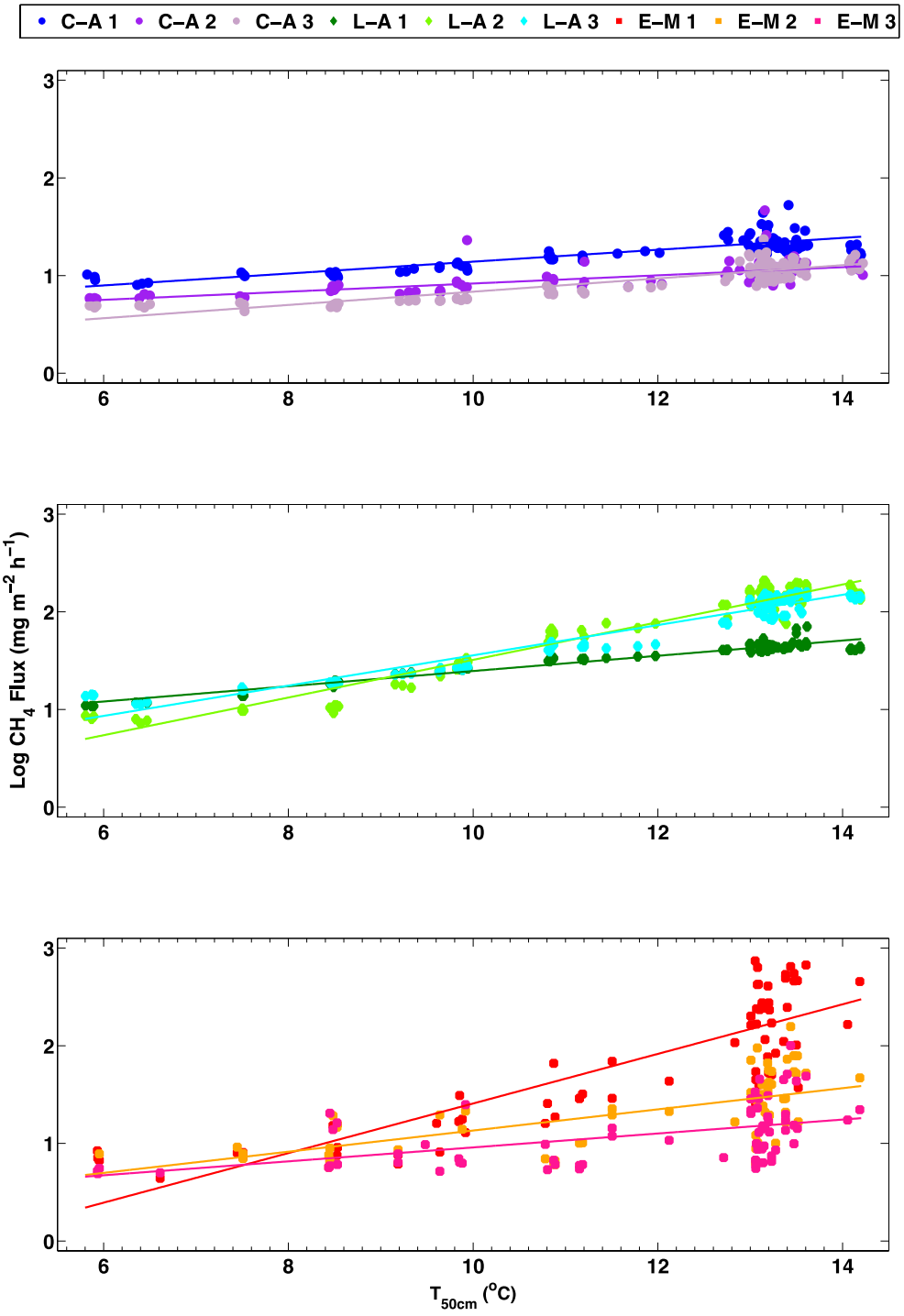

Figure 4-8: The relationship between 50 cm peat temperature (T_{50cm} ,°C) and log CH_4 flux (mg m^{-2} h^{-1}) emitted from 3 *Chamaedaphne*-dominated autochambers (C-A 1, 2, 3) (circles), 3 *Ledum*-dominated autochambers (L-A 1, 2, 3) (diamonds) and 3 *Eriophorum*-dominated manual chambers (E-M 1, 2, 3) (squares) at Mer Bleue for manual sampling day data (DOY 132-255).

Overall, as WT rose, CH_4 flux increased when examining all daily chamber flux values (Figure 4-9) and all seasonal averages (Figure 4-10). As a covariate, WT had a significant relationship with CH_4 fluxes for manual sampling day data ($F(1,793.8)=5.7958$, $p=0.0163$). For the seasonal averages, the significant relationship between log CH_4 flux and chamber-specific WT is 2.435 mg m^{-2} h^{-1} + 0.03162 (WT) mg m^{-2} h^{-1} cm^{-1} ($F(1,816) = 169.77$, $p < 0.001$, $R^2 = 0.172$).

However, for a given chamber, there was little relationship with WT, which was expected given the small range in WT variation through the growing season. As a result, microtopography effects on WT drove the spatial variations observed in Figure 4-9 and Figure 4-10. For example, C-A 2 (a *Chamaedaphne* shrub hummock) had the lowest seasonal WT and lowest CH_4 fluxes, while L-A 3 and E-M 1 had WT closer to the surface and produced some of the largest CH_4 fluxes (Figure 4-10).

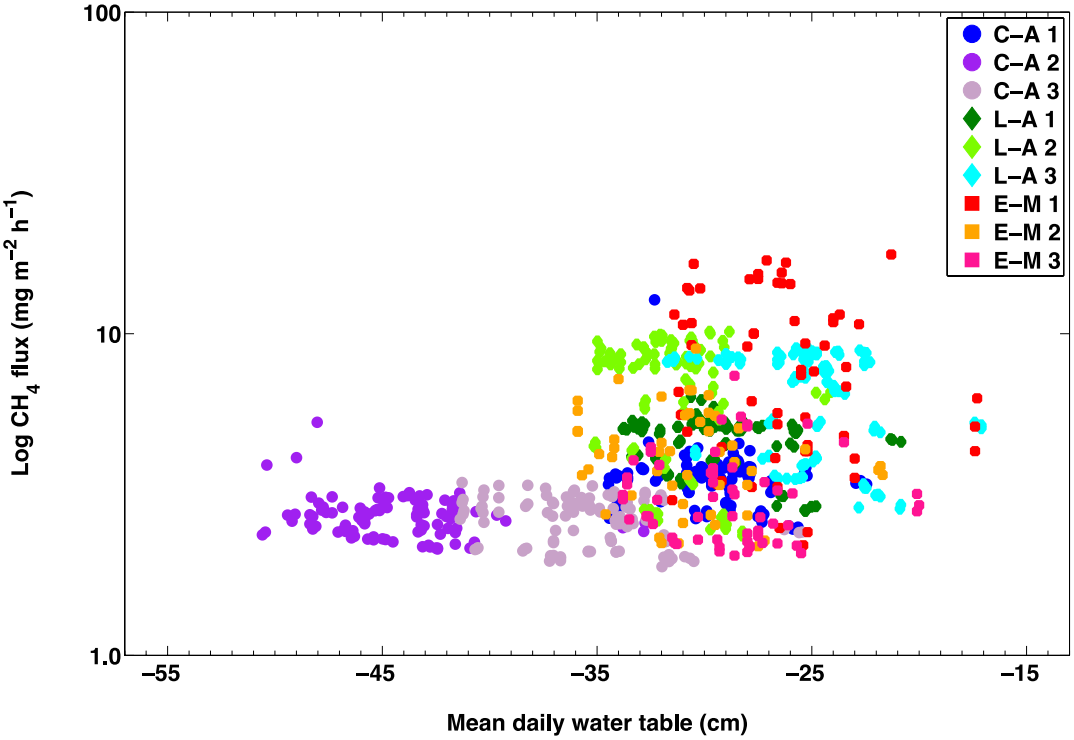

Figure 4-9: Relationship between mean depth to water table (cm) and log CH_4 flux (mg m^{-2} h^{-1}) from 3 *Chamaedaphne*-dominated autochambers (C-A 1, 2, 3) (circles), 3 *Ledum*-dominated autochambers (L-A 1, 2, 3) (diamonds) and 3 *Eriophorum*-dominated manual chambers (E-M 1, 2, 3) (squares) at Mer Bleue for manual static chamber sampling days (DOY 132-255) during the 2014 measurement period.

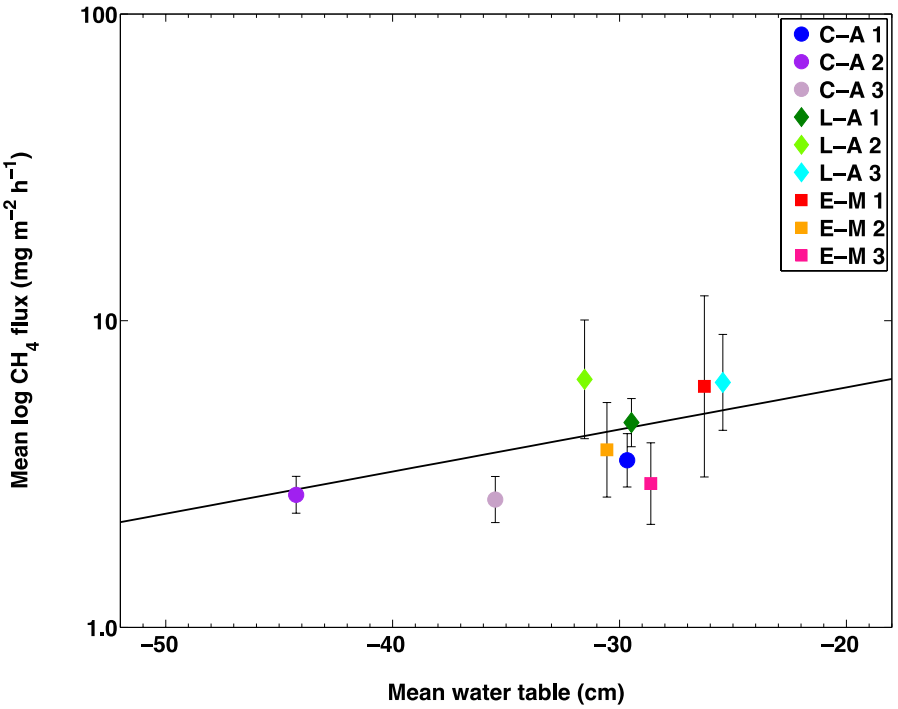

Figure 4-10: Relationship between mean seasonal depth to water table (cm) and mean (±SD) seasonal log CH_4 flux (mg m^{-2} h^{-1}) from 3 *Chamaedaphne*-dominated autochambers (C-A 1, 2, 3) (circles), 3 *Ledum*-dominated autochambers (L-A 1, 2, 3) (diamonds) and 3 *Eriophorum*-dominated manual chambers (E-M 1, 2, 3) (squares) at Mer Bleue for manual static chamber sampling days (DOY 132-255) 2014. The solid black line shows the linear regression calculated to predict log CH_4 flux based on mean daily water table, where predicted log CH_4 flux is equal to 2.435 + 0.03162 (WT) mg m^{-2} h^{-1} when WT is measured in cm from the peat surface at each chamber.

4.3 Redox potential measurements

Examples of redox potential measurements recorded at E-M 1 and E-M 2 are presented in Figure 4-11 and Figure 4-12 respectively. As the boundary between reduction and oxidation conditions is controlled by the position of the WT, the mean daily depth to WT is important to consider. Both chambers had WT below 20 cm for the late summer–fall sampling period. This is reflected by the average standardized redox

potential value of ~600 mV at 20 cm, which indicates aerated conditions and the predominance of O_2 (Table 2-1). In both of these cases, redox potential reached the most negative values at a depth of 40 cm – the depth closest to but still below the WT. At E-M 1, the 40 cm Eh value of -200 mV suggests the activity of methanogens for the reduction of CO_2 to CH_4. At E-M 2, the redox potential at 40 cm is similar to that at 60 and 80 cm (-100 to 0 mV), suggesting a greater proportion of alternate terminal electron acceptors higher up the cascade of redox pairs in the soil, such as sulfate (SO_4^{2-}) and ferric iron (Fe^{3+}) (Table 2-1).

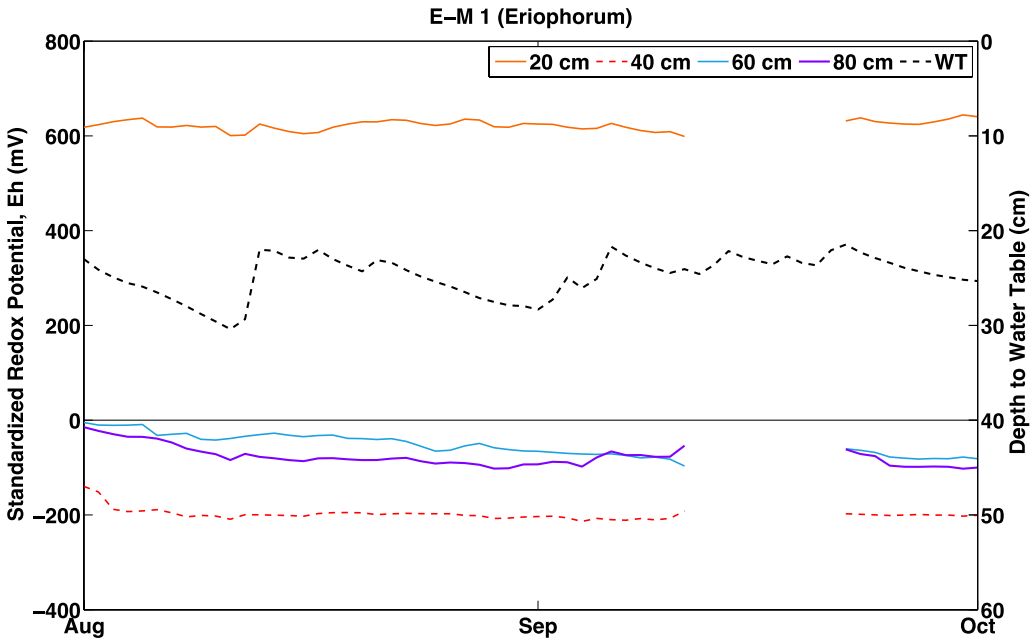

Figure 4-11: Mean daily redox potential (mV) referenced to Ag/AgCl reference electrode with 3 M KCl filling solution and corrected for pH of 4. Sampled at chamber E-M 1 (*Eriophorum*) for peat depths of 20cm, 40 cm, 60 cm, and 80 cm at Mer Bleue, 2014. Mean daily depth to water table (cm) is shown for reference (dotted black line) on the secondary y-axis.

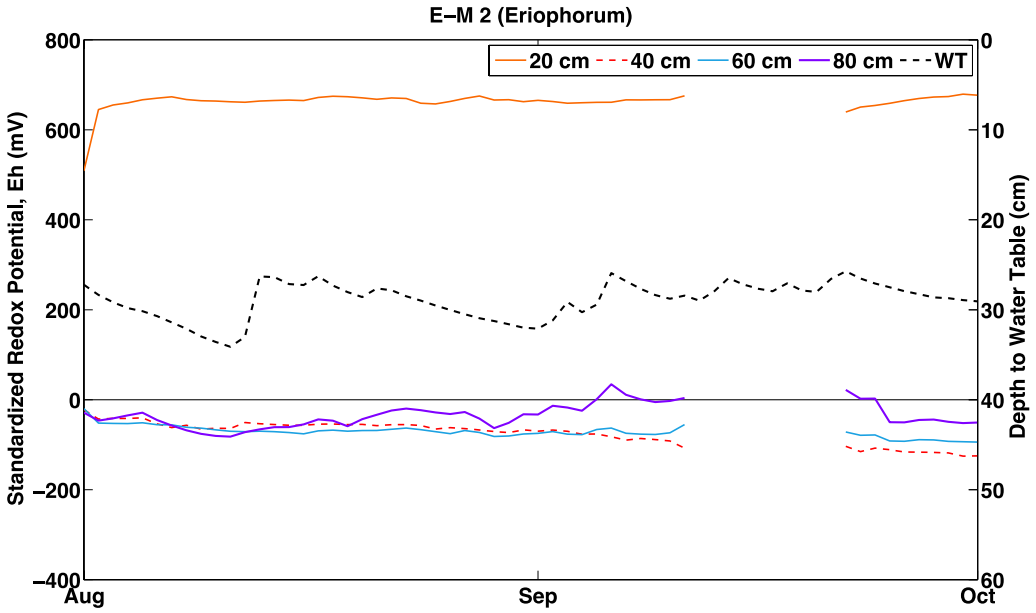

Figure 4-12: Mean daily redox potential (mV) referenced to Ag/AgCl reference electrode with 3 M KCl filling solution and corrected for pH of 4. Sampled at chamber E-M 2 (*Eriophorum*) for peat depths of 20cm, 40 cm, 60 cm, and 80 cm at Mer Bleue, 2014. Mean daily depth to water table (cm) is shown for reference (dotted black line) on the secondary y-axis.

4.4 Pore water analyses

For temporal pore water analyses, DOC (mg L^{-1}), TDN (mg L^{-1}), $SUVA_{254}$ (L m^{-1} mg^{-1} DOC) and C/N ratio were averaged across all chambers for four sampling depths and presented in Figure 4-13. There was an increasing seasonal concentration of DOC and TDN observed in pore water (Figure 4-13). When DOC concentrations were lowest at the beginning of the summer, $SUVA_{254}$ was at its highest.

The pore water C/N ratio did not have as much seasonal variation as both DOC and TDN increased throughout the summer, yet it did appear to mimic the variation in peat C/N ratio, which decreases with depth (Hornibrook *et al.* 2000b, Malmer & Wallén 2004, Rydin & Jeglum 2013, Wang *et al.* 2015). By constructing the same figure using data from *Eriophorum* plots only (Figure 4-14) the patterns have much greater variation over the season and with depth. In addition, the trend for these variables in the *Eriophorum* plots at 50 cm did not clearly increase or decrease over the season.

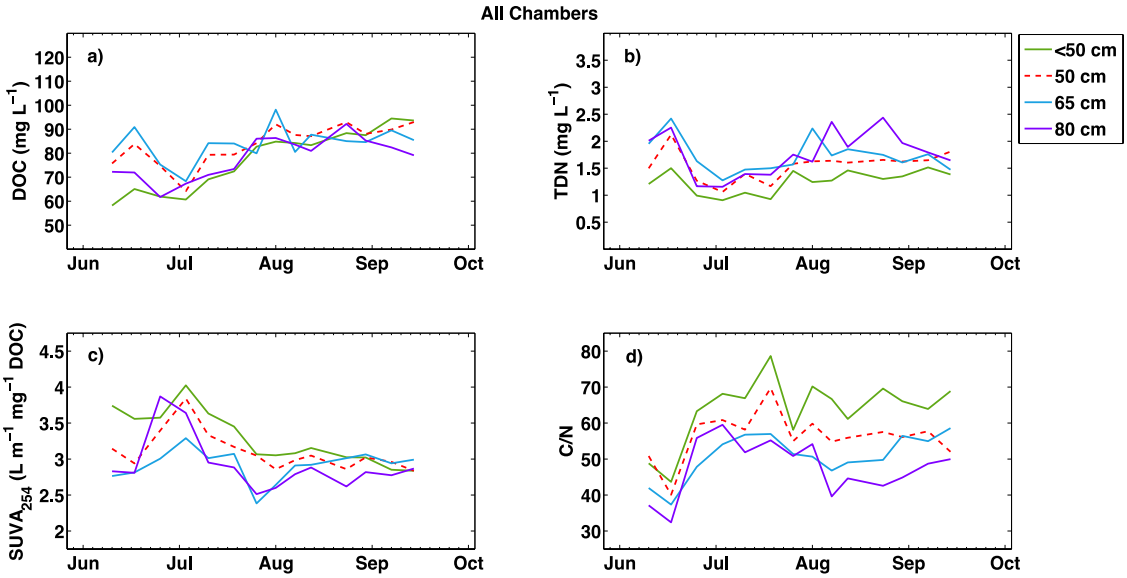

Figure 4-13: Mean daily (a) dissolved organic carbon (DOC, mg L^{-1}), (b) total dissolved nitrogen (TDN, mg L^{-1}), (c) specific ultraviolet absorbance at 254 nm ($SUVA_{254}$,L m^{-1} mg^{-1} DOC), and (d) carbon to nitrogen ratio (C/N) for all chambers at various depths during the 2014 measurement period.

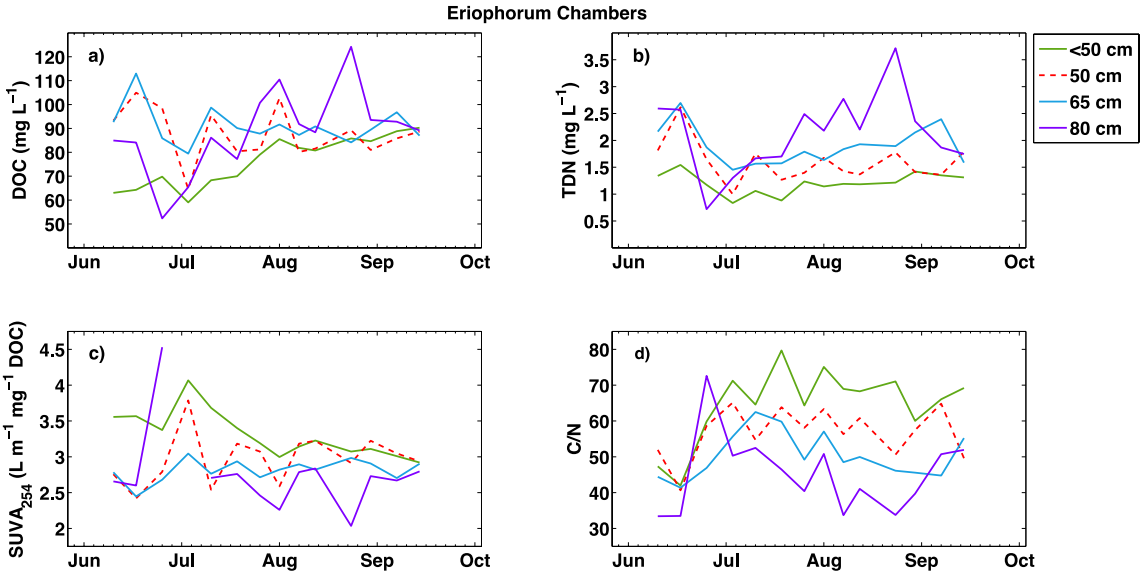

Figure 4-14: Mean daily (a) dissolved organic carbon (DOC, mg L^{-1}), (b) total dissolved nitrogen (TDN, mg L^{-1}), (c) specific ultraviolet absorbance at 254 nm ($SUVA_{254}$,L m^{-1} mg^{-1} DOC), and (d) carbon to nitrogen ratio (C/N) for *Eriophorum*-dominated chambers at various depths during the 2014 measurement period.

Pore water CH_4 concentrations generally increased with depth to a peak at 50 cm during the late summer season. Samples obtained 20 cm below peat surface, which was in the aerobic zone above the WT, had small, near-ambient CH_4 concentrations. However, a few higher CH_4 concentrations (in the range of 100-230 μmol L^{-1}) were observed at 20 cm, particularly for the *Chamaedaphne* community in late summer. This could provide evidence for ebullition events (Figure 4-15). Pore water CH_4 was analyzed using a mixed model with chamber as a random effect and DOC, TDN, depth-specific peat temperature and WT as covariates, and depth and community as fixed effects. There was no statistically significant effect of community ($F(2, 8.53)=1.4098$, $p=0.2958$) or sampling depth ($F(1,445.2)=0.4707$, $p=0.4930$) on pore water CH_4 concentrations over the entire sampling period (DOY 155-255). However, when only later summer sampling days were considered (DOY 212-255), there was a statistically significant effect of community ($F(2, 9.669)=4.7589$, $p=0.0364$) where *Chamaedaphne* had significantly higher pore water CH_4 concentrations than the *Ledum* community.

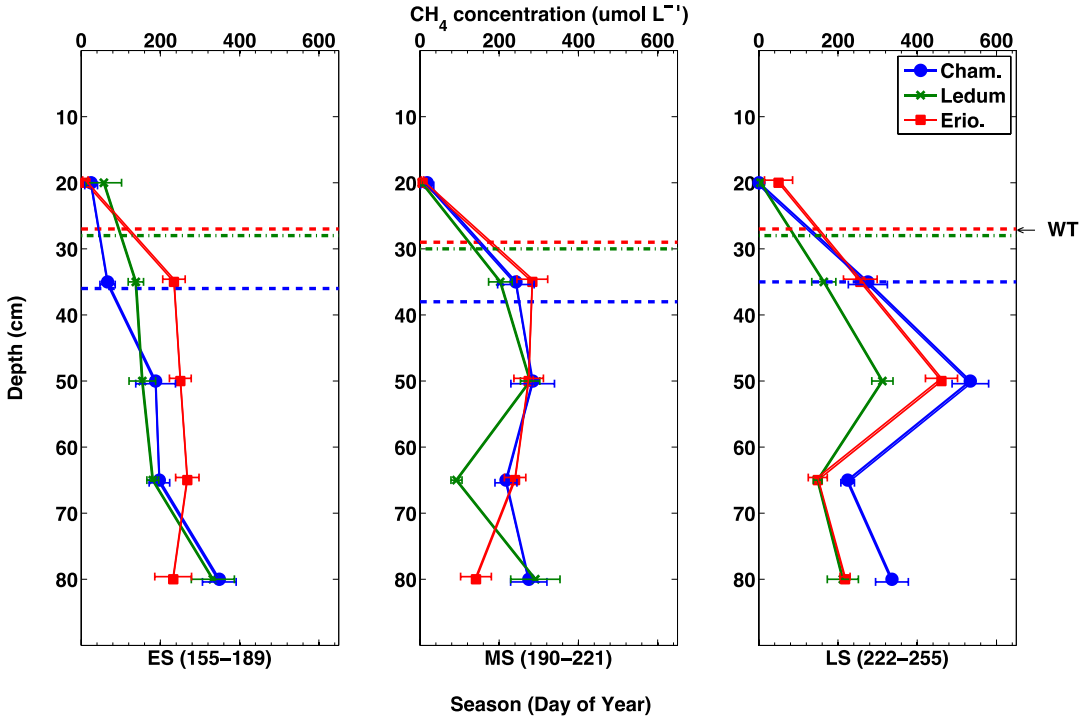

Figure 4-15: Pore water profiles of mean (± SE) dissolved CH_4 concentrations (µmol L^{-1}) for three vegetation communities at Mer Bleue. Depth was measured from peat surface (cm). Horizontal lines indicate mean depth to water table (cm) for each community. Note: ES, early summer (DOY 155-189); MS, mid-summer (DOY 190-221); LS, late summer (DOY 222-255) for the 2014 measurement period.

Only at 50 cm was there a tendency for pore water CH_4 concentrations to increase through the growing season (Figure 4-16). This trend seemed to be largely driven by several high pore water CH_4 concentrations sampled in late August and early September. To further investigate the importance of the 50 cm depth, CH_4 concentrations ($\mu mol\ L^{-1}$) at 50 cm were analyzed on a plot basis (Figure 4-17). Methane concentrations appeared to increase over the summer, but there was large variability among chambers. In particular, C-A 3 fluctuated substantially but reached the highest 50 cm CH_4 concentrations of all chambers by late summer. The least variability among the *Ledum* chambers was L-A 3. E-M 1 was variable but produced the largest CH_4 concentrations among the *Eriophorum* chambers for most of the summer. Collectively, the largest increase in CH_4 concentration at 50 cm over time was in the *Chamaedaphne* plots.

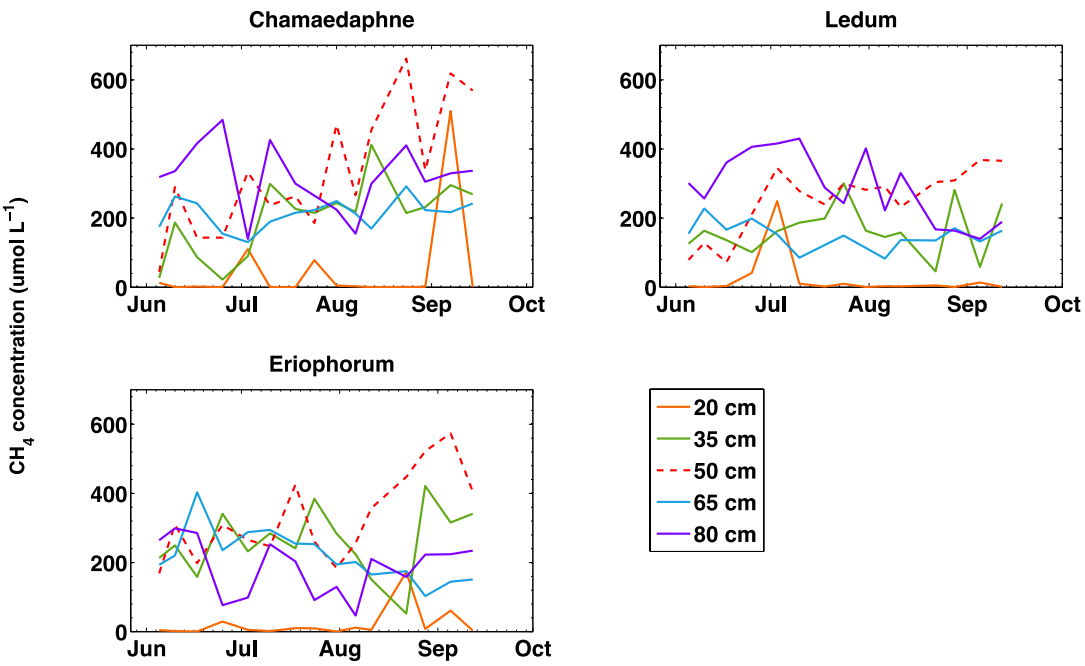

Figure 4-16: Seasonal dissolved pore water CH_4 concentrations (µmol L^{-1}) at 20, 35, 50, 65 and 80 cm for *Chamaedaphne*, *Ledum* and *Eriophorum*-dominated communities at Mer Bleue during 2014.

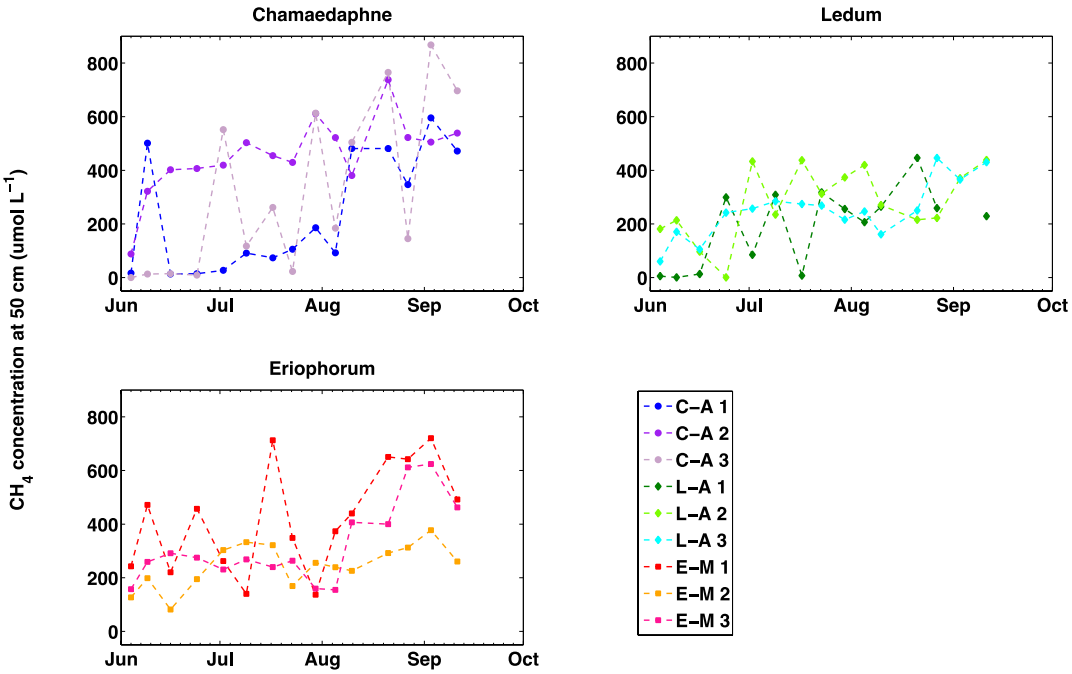

Figure 4-17: Seasonal dissolved pore water CH_4 concentrations (µmol L^{-1}) at 50 cm depth for 3 *Chamaedaphne*-dominated autochambers (C-A 1, 2, 3) (circles), 3 *Ledum*-dominated autochambers (L-A 1, 2, 3) (diamonds) and 3 *Eriophorum*-dominated manual chambers (E-M 1, 2, 3) (squares) at Mer Bleue during the 2014 measurement period.

4.5 CH_4 production pathway

CH_4 production pathways were investigated using the Keeling Plot approach to discern the dominant CH_4 production pathway (Figure 4-18). The $\delta^{13}C$-CH_4 source signatures were restricted to a narrow range of depleted values (~ -81 to -71 ‰) for all chambers. Taking into account the random effect of chamber (as a repeated measure), there was no statistically significant effect of community on $\delta^{13}C$-CH_4 source signatures ($F(2, 5.668)=0.2107$, $p= 0.8161$). The $\delta^{13}C$-CH_4 source signatures for all three communities provided evidence for the CO_2 reduction pathway of CH_4 production, which produces a relatively ^{13}C-depleted signature (-110 to -60 ‰) compared to the acetate fermentation (-65 to -50 ‰) pathway (Whiticar *et al.* 1986) (Figure 4-18).

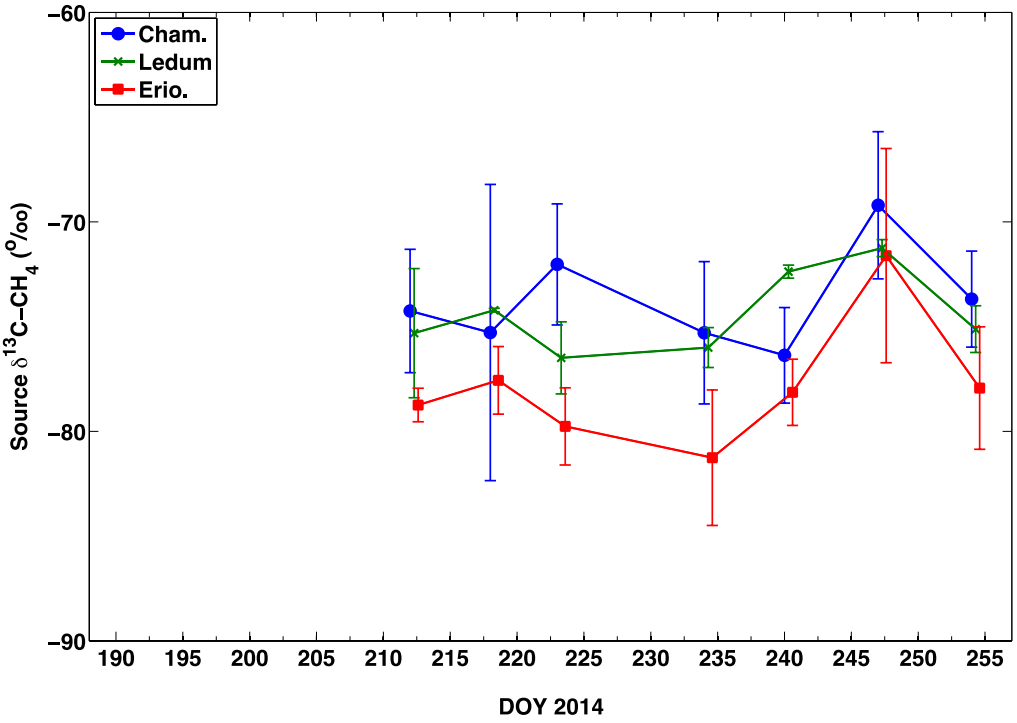

Figure 4-18: Mean (± SD) $\delta^{13}C$- CH_4 isotopic signatures (‰) for CH_4 emitted from *Chamaedaphne*, *Ledum* and *Eriophorum*-dominated communities at Mer Bleue during the mid- to late-summer 2014 measurement period.

4.6 Estimates of seasonal CH_4 storage change

The change in pore water CH_4 storage over time was explored with a focus on multiple peat depths and combinations of sampling depths along with different time periods. Week-to-week analyses were confounded by high variability in pore water CH_4 concentrations, while the temporal variations in pore water CH_4 at 50 cm dominated the storage term. Changes in storage of CH_4 computed using only the 50 cm depth (over a 15 cm layer) over the entire pore water sampling period revealed the most distinct differences among communities. C-A 3 (*Chamaedaphne*) had the largest increase in CH_4 storage (0.71 mg m^{-2} h^{-1}) at the 50 cm depth (Figure 4-19). C-A 1 (*Chamaedaphne*) also had a relatively large increase in CH_4 storage (0.44 mg m^{-2} h^{-1}). However, the remaining *Chamaedaphne* autochamber, C-A 2, had only moderate CH_4 storage change (0.34 mg m^{-2} h^{-1}) in comparison to the other two *Chamaedaphne* chambers over the season. This chamber's deep WT position (~ 45 cm below peat surface) and the corresponding thick aerobic peat layer, which provides increased potential for CH_4 consumption, likely contributed to this difference. E-M 2 demonstrated the smallest change in CH_4 storage (0.16 mg m^{-2} h^{-1}). The remaining chambers showed moderate CH_4 storage increase over the season ranging from 0.20 to 0.33 mg m^{-2} h^{-1}.

A linear relationship between CH_4 storage change at 50 cm and mean CH_4 flux for manual sampling days during the pore water collection period was not significant (Figure 4-20) ($r = -0.4438$, $N=9$, $p=0.2315$). However, an exponential function fit the data (Figure 4-20) ($p = 0.0024$), reflecting the pattern of greater fluxes with less change in CH_4 storage in the pore water. For example, the chamber with the greatest CH_4 storage change

had very low fluxes (C-A 3) and some of the highest emitters (L-A 2, 3) had low CH_4 storage change.

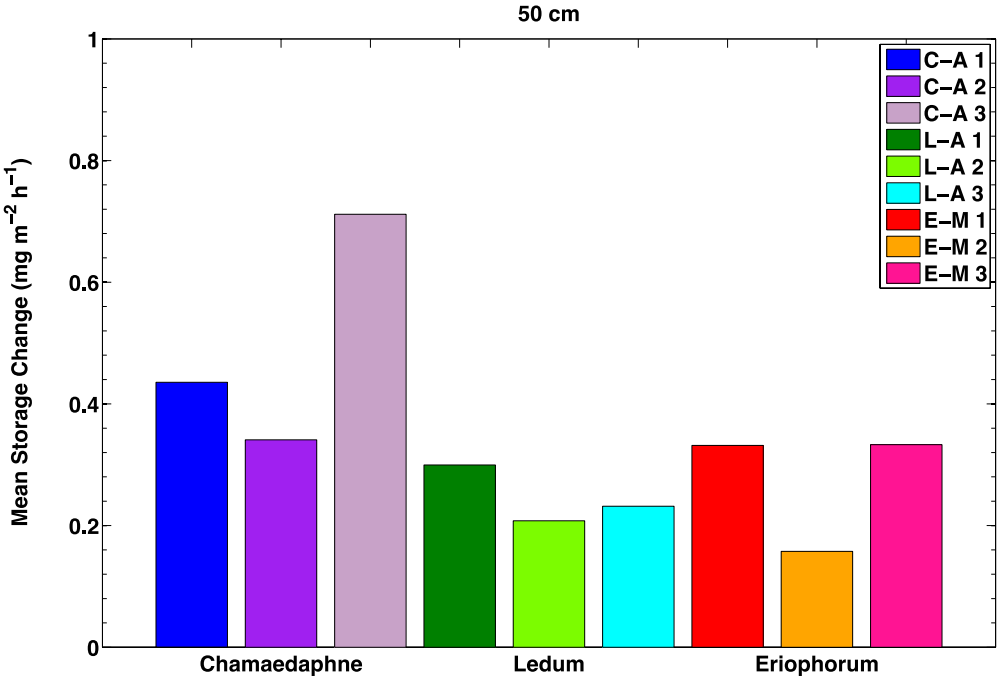

Figure 4-19: Mean CH_4 storage change (mg m^{-2} h^{-1}) for 3 *Chamaedaphne*-dominated autochambers (C-A 1, 2, 3), 3 *Ledum*-dominated autochambers (L-A 1, 2, 3) and 3 *Eriophorum*-dominated manual chambers (E-M 1, 2, 3) at the 50 cm depth (15 cm thickness) during the pore water sampling period (DOY 155-255).

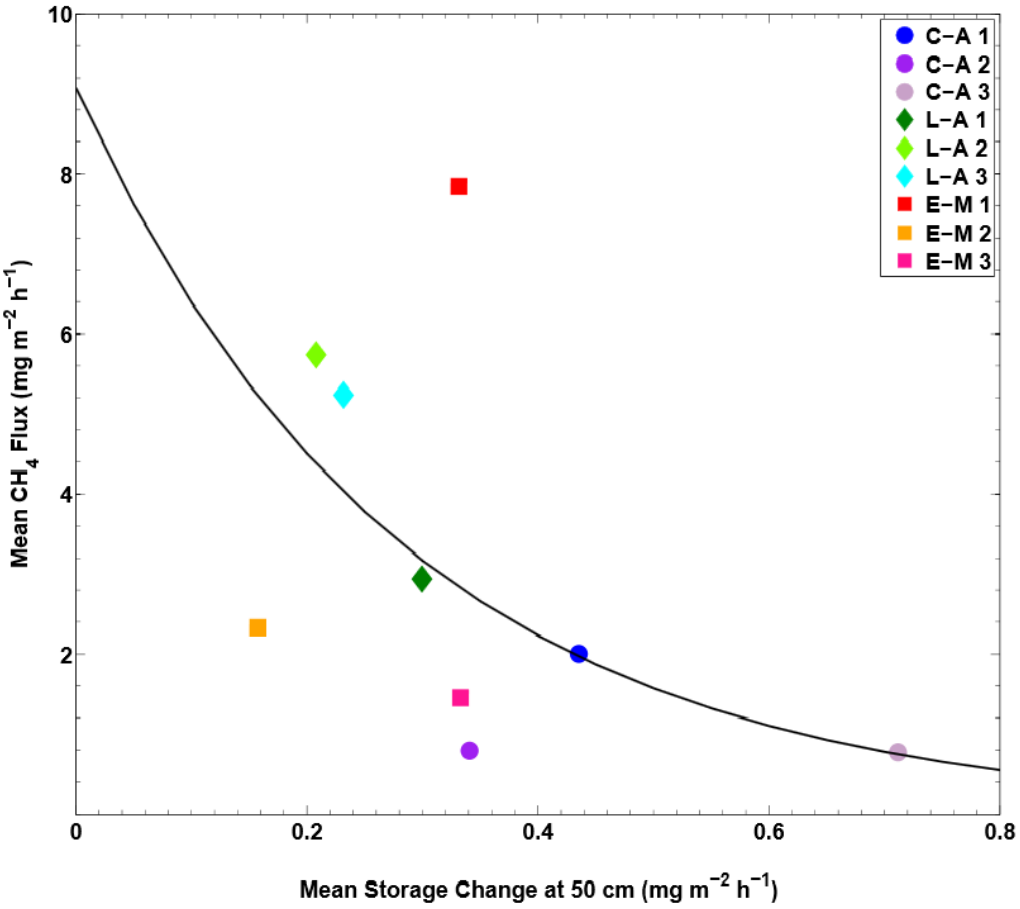

Figure 4-20: Relationship between mean storage change at 50 cm (mg m^{-2} h^{-1}) and mean CH_4 flux (mg m^{-2} h^{-1}) for 3 *Chamaedaphne*-dominated autochambers (C-A 1, 2, 3) (circles), 3 *Ledum*-dominated autochambers (L-A 1, 2, 3) (diamonds) and 3 *Eriophorum*-dominated manual chambers (E-M 1, 2, 3) (squares) at Mer Bleue for manual sampling days during the pore water collection period 2014 (DOY 155-255). The solid black line shows the nonlinear regression calculated to predict mean CH_4 flux based on storage change at 50 cm, where predicted mean CH_4 flux (mg m^{-2} h^{-1}) is equal to $9.08 \times 0.03^{S_{CH4}}$ where S_{CH4} is storage change measured in mg m^{-2} h^{-1}.

4.7 Relationships among indicators of CH_4 production, storage and transport

Overall, on a plot scale during the mid- to late-summer periods when all variables were available for analysis, vegetation community type can be related to a number of variables associated with the production, storage and transport of CH_4 (Figure 4-21 and Table 4-2). Although vegetation classification is subject to the user's classification scheme, *Eriophorum vaginatum*, as an important species with mechanistic implications to CH_4 transport and production, correlated strongly to community type (where *Chamaedaphne* = community 1, *Ledum* = community 2, and *Eriophorum* = community 3). More *Eriophorum* was associated with shallower WT, greater CH_4 emissions and more depleted $\delta^{13}C$-CH_4 source signature (Figure 4-21 and Table 4-2). These variables tended to be associated with the first principle component, which explained 38.1% of the variation in the data (Figure 4-21). However, neither community nor % LAI attributed to *Eriophorum vaginatum* (*EV*%) correlated with 50 cm pore water characteristics (Figure 4-21 and Table 4-2). The second principle component explained 28.1% of the variance and tended to associate with below ground characteristics. For this set of variables, a measure of biomass (LAI-2000) correlated with some of these pore water characteristics (positive correlation with TDN and negative correlation with C/N). Many of these pore water characteristics also closely related to each other. For example, greater TDN was associated with lower $SUVA_{254}$ and C/N, as was also demonstrated with the temporal and spatial (depth) trends in Figure 4-13. Only WT weakly correlated with pore water CH_4 concentrations (p-value =0.07) with deeper WT having greater CH_4 concentrations (characteristic of the non-*Eriophorum* plots although not correlating to any vegetation metrics). As with previous analyses, there was no significant correlation ($p < 0.05$)

between CH_4 storage change (calculated from pore water CH_4 from DOY 155 to 255) and any measure of community type or any other variable. However, there was a weak negative relationship ($p = 0.09$) between storage change and community type, where more sedge has less storage change and a negative relationship between storage change and flux ($p = 0.09$). Similarly, weak relationships between total LAI (perhaps as a proxy for plant productivity) and pore water characteristics included a negative correlation with DOC ($p = 0.08$) and a positive correlation with SUVA ($p = 0.09$).

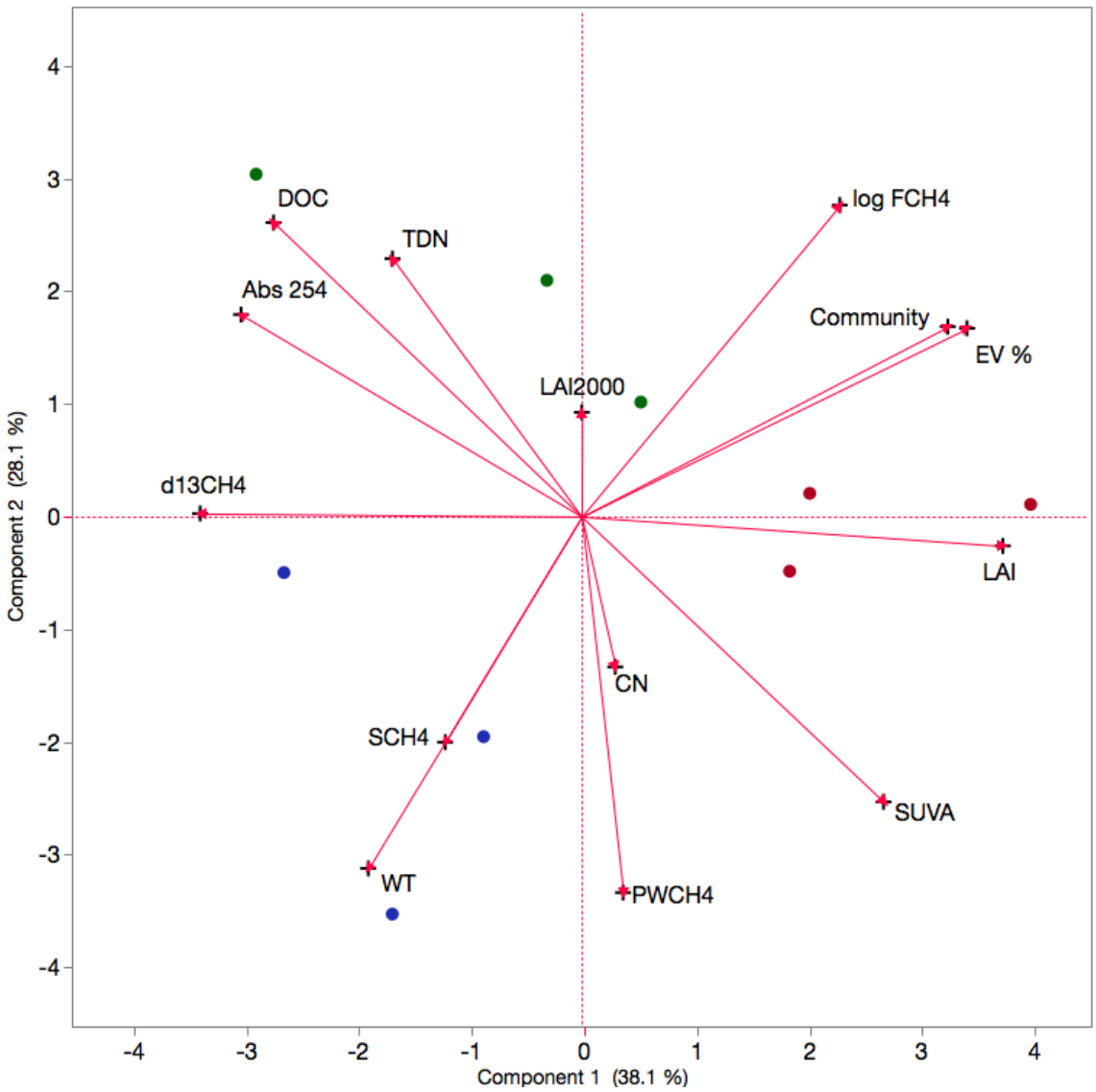

Figure 4-21: Principal component analysis for averaged chamber-specific variables between DOY 212 and 255. N = 9. All pore water and temperature variables are from the 50 cm depth. Variables include: community type, total green hits LAI (LAI), percent LAI attributed to *Eriophorum vaginatum* (EV %), total biomass LAI as measured with the LAI-2000 (LAI2000), CH_4 flux (F_{CH4}), storage change of pore water CH_4 (S_{CH4}), pore water CH_4 concentration (PW_{CH4}), $\delta^{13}C$-CH_4 source signature ($\delta^{13}C$-CH_4), water table depth (WT), dissolved organic carbon (DOC), total dissolved nitrogen (TDN), carbon to nitrogen ratio (CN), absorbance at 254 nm (Abs_{254}), and specific ultraviolet absorbance at 254 nm ($SUVA_{254}$) . Chambers are dots and grouped according to community type: *Chamaedaphne* = blue, *Ledum* = green, and *Eriophorum* = red.

Table 4-2: Pearson correlations for averaged chamber-specific variables between DOY 212 and 255. All pore water and temperature variables are from the 50 cm depth. Correlations in bold ($p < 0.05$) and italics ($p<0.10$) are significant. N = 9. Variables include: community type, total green hits LAI (LAI), percent LAI attributed to *Eriophorum vaginatum* (EV %), total biomass LAI as measured with the LAI-2000 (LAI2000), CH_4 flux (F_{CH4}), storage change of pore water CH_4 (S_{CH4}), pore water CH_4 concentration (PW_{CH4}), $\delta^{13}C$-CH_4 source signature ($\delta^{13}C$-CH_4), water table depth (WT), dissolved organic carbon (DOC), total dissolved nitrogen (TDN), carbon to nitrogen ratio (CN), absorbance at 254 nm (Abs_{254}), and specific ultraviolet absorbance at 254 nm ($SUVA_{254}$).

	Community	LAI-2000	LAI	EV %	WT	DOC	TDN	CN	Abs_{254}	$SUVA_{254}$	$\delta^{13}C$-CH_4	PW_{CH4}	S_{CH4}	log F_{CH4}
Community	**1.00**													
LAI2000	0.00	**1.00**												
LAI	**0.68**	0.16	**1.00**											
EV %	**0.87**	0.18	**0.77**	**1.00**										
WT	**-0.70**	-0.03	-0.39	**-0.81**	**1.00**									
DOC	-0.27	0.18	*-0.61*	-0.30	-0.23	**1.00**								
TDN	-0.21	**0.68**	-0.33	-0.12	-0.16	*0.64*	**1.00**							
CN	0.04	**-0.74**	-0.01	-0.04	0.05	-0.19	**-0.86**	**1.00**						
Abs_{254}	-0.46	0.02	**-0.75**	-0.49	0.05	**0.79**	0.40	-0.02	**1.00**					
$SUVA_{254}$	0.26	-0.18	*0.59*	0.28	0.25	**-0.99**	*-0.66*	0.21	**-0.71**	**1.00**				
$\delta^{13}C$-CH_4	*-0.59*	-0.45	**-0.94**	**-0.72**	0.30	0.55	0.09	0.28	*0.63*	-0.56	**1.00**			
PW_{CH4}	-0.38	0.12	0.30	-0.28	*0.63*	-0.52	-0.24	-0.03	-0.56	0.48	-0.28	**1.00**		
S_{CH4}	*-0.59*	0.42	-0.06	-0.33	0.42	0.01	0.16	-0.15	-0.12	-0.05	-0.01	**0.69**	**1.00**	
log F_{CH4}	*0.65*	0.05	0.54	**0.72**	**-0.80**	0.06	0.14	-0.17	-0.05	-0.04	-0.51	-0.46	*-0.60*	**1.00**

5.0 DISCUSSION

Vegetation community characteristics are often used as a predictor for CH_4 emissions in peatlands, with sedge-dominated vegetation expected to have greater emissions than shrub, herb or moss dominated plots (Ward *et al.* 2013). At Mer Bleue, community type or % LAI attributed to *Eriophorum* (*EV*%), more specifically, was an important variable associated with greater CH_4 emissions, more depleted $\delta^{13}C\text{-}CH_4$ source signature, and less storage change of CH_4 although perhaps surprisingly, there was no direct relationship between *EV*% and pore water characteristics. WT correlated well with community type and the *EV*% (Figure 4-21). WT at Mer Bleue is a good indicator of the potential magnitude of CH_4 emissions (Moore *et al.* 2011, Brown *et al.* 2014, Lai *et al.* 2014a). WT is also a good indicator of the vegetation community composition, where sedge cover (*Eriophorum vaginatum*) increased as the average WT depth approached the surface, and dwarf shrubs (*Chamaedaphne calyculata*) dominated in drier hummock positions (Bubier *et al.* 2006).

The $\delta^{13}C\text{-}CH_4$ source signatures for all nine chambers ranged from -81 to -71 ‰, all well within the -110 to -60‰ range, suggesting the dominance of the CO_2 reduction pathway for CH_4 production at Mer Bleue (Whiticar *et al.* 1986). Although the vegetation community composition did not have a significant effect on the source signature when accounting for the random effects of the repeated measurements on a chamber (Figure 4-18), a simple negative correlation with the *EV*% suggested the influence of transport effects on source signature, as increased sedge cover allows for increased plant-mediated CH_4 transport. Plant-mediated transport processes, as well as diffusion processes,

preferentially remove the lighter ^{12}C-CH_4 (Chanton 2005). However, the distance CH_4 diffuses through the oxidation zone will also impact the $\delta^{13}C$-CH_4 value due to the substantial fractionation (5-30‰) of C by methanotrophs (i.e. microbes preferentially consume ^{12}C-CH_4) (Whiticar 1999). In a study investigating C fractionation by methanotrophs, Coleman *et al.* (1981) found evidence for a microbial preference for the consumption of lighter ^{12}C-CH_4, leaving residual CH_4 enriched with heavier ^{13}C after CH_4 oxidation. Thus, Figure 4-18 suggests that the presence of *Eriophorum* allows the direct transport of lighter, more depleted CH_4 to the atmosphere by bypassing the CH_4 consumption zone and associated fractionation by methanotrophs.

Optimal CH_4 production conditions are likely related to input and output dynamics of potential substrates (Kalbitz *et al.* 2000, Preston *et al.* 2011), as organic C substrate and a source of N are necessary for methanogenic activity. The instantaneous DOC and TDN concentrations obtained from pore water are a function of production processes involving multiple sources (e.g. litter and humus, root exudates, microbial biomass), consumption through microbial activity, and transport dynamics (e.g. flushing, adsorption) (Kalbitz *et al.* 2000, Preston *et al.* 2011). While TDN comprises ammonium (NH_4^+), nitrate (NO_3^-) and dissolved organic nitrogen (DON), a previous study showed that the majority of TDN in Mer Bleue pore water is in the organic DON form (Rattle 2006). As such, there is an interaction between C and N cycling, and patterns in TDN are related to DOC dynamics (Rattle 2006). The current study demonstrated increasing pore water concentrations of DOC and TDN over the season (Figure 4-13). During the spring, snowmelt at Mer Bleue flushes the peat with small concentrations of DOC and TDN. As peat temperature increases throughout the growing season, decomposition processes

accelerate and both DOC and TDN are released into pore water (Moore & Dalva 1993, Kalbitz *et al.* 2000, Moore & Dalva 2000, Lai 2009). This likely contributes to the increasing seasonal pattern in DOC and TDN observed at all depths over 2014 at Mer Bleue.

The C/N ratio was assumed to be equal to the DOC/TDN ratio since TDN in pore water is dominated by DON at Mer Bleue (Rattle 2006). The pore water C/N ratio demonstrated limited temporal variation, which reflects the seasonal increases in both DOC and TDN (Figure 4-13). The pore water C/N ratio decreased with depth, similar to patterns in peat C/N ratio found in previous studies (Hornibrook *et al.* 2000b, Malmer & Wallén 2004, Rydin & Jeglum 2013, Wang *et al.* 2015). This can be attributed to a loss of C (i.e. consumption of carbohydrates) and fixation of N by microorganisms with depth (Hornibrook *et al.* 2000b, Rydin & Jeglum 2013). The peak TDN, and corresponding trough in C/N ratio, that occurred in June may have been a function of spring thawing and microbial turnover (Moore & Dalva 2000).

The quality of the DOC substrate was assessed using $SUVA_{254}$ measurements, which have a positive linear relation with DOC aromaticity (Weishaar *et al.* 2003, Olefeldt & Roulet 2012). Thus, greater $SUVA_{254}$ for pore water DOC indicates greater aromaticity of the DOC molecule (Weishaar *et al.* 2003). Measured $SUVA_{254}$ values fell within the commonly reported range of 0.5-6.0 L m^{-1} mg^{-1} DOC, corresponding to a percent aromaticity of 5-45% (Weishaar *et al.* 2003). The current results indicate an inverse relation between DOC and $SUVA_{254}$ measurements, with $SUVA_{254}$ (and thus DOC aromaticity) decreasing as the season progressed (Figure 4-13). This suggests that at low initial DOC concentrations at the beginning of the season, DOC is more aromatic

in nature. Since methanogens favour simple, relatively labile DOC molecules, this could limit CH_4 production during this early summer period (Blodau 2001). The increasing DOC concentration and lability over the 2014 summer at Mer Bleue supports findings by Kane *et al.* (2014), where increased temperature (1.9 ± 0.4°C) in poor fen plots produced increased concentrations of more labile DOC in pore water.

One reason neither community type nor *EV*% directly related to pore water characteristics may have been due to the significant variability in pore water characteristics for *Eriophorum* community plots (Figure 4-14). This could be the result of the deeper rooting zone of sedges, which add labile C and other organic substrates to the anaerobic zone, potentially contributing to the increased variability in TDN and DOC quantity and quality.

The increasing seasonal DOC and TDN pore water concentrations, in conjunction with the presence of more labile DOC as the summer progressed, likely contributed to the spatial and temporal variability of pore water CH_4 concentrations at depth. The pore water CH_4 concentrations measured in this study were in range with those measured by Blodau *et al.* (2007) during 2003-2004, which yielded CH_4 concentrations in the range of 0-600 μmol L^{-1}. In this study, pore water CH_4 concentrations peaked at 50 cm by late summer (Figure 4-15). Similarly Blodau *et al.* (2007) also found increasing concentrations over the summer months, with a peak CH_4 concentration at 40 - 55 cm by September/October in 2003 but a general trend of increasing concentrations with depth in 2004 (to 60 cm). This could be attributed to differences in moisture conditions where 2003 and 2004 WT reached depths 10-14 cm deeper than in 2014 and may have resulted in a deeper zone of CH_4 production. Also, sampling methods differed, where Blodau *et*

al. (2007) used the peeper technique and the current study used suction sampling and closed piezometer techniques. As previously detailed (Section 1.1.1), the peeper technique requires long equilibration times; from June 2003 to December 2004, Blodau *et al.* (2007)'s peepers were only sampled 12 times, for example. The shorter weekly interval between samples in the current study may have captured CH_4 concentration depth patterns that were not apparent with monthly sampling (i.e. spatial variability at a shorter time scale). Redox potential measurements obtained during the late-summer period supported the importance of the 50 cm peak in the CH_4 concentration profile, as they indicated strongly reducing conditions (<-100 mV) (Zhi-Guang 1985) at around this depth for most chambers.

In general, plots with smaller fluxes tended to have greater increases in CH_4 storage over the measurement period. For example, the *Chamaedaphne* community produced some of the largest pore water CH_4 concentrations at depth in late summer (Figure 4-15). Yet, this community consistently had the lowest CH_4 fluxes throughout the summer (Table 4-1, Figure 4-5). Since it is unlikely production rates were greater in *Chamaedaphne* plots, this suggests the influence of restrictive transport of CH_4 to the atmosphere and/or greater CH_4 consumption within the aerated peat at *Chamaedaphne* plots. As discussed earlier, there is evidence of *Eriophorum* providing a direct pathway to the atmosphere through aerenchymatous tissue such that more *Eriophorum* plants may enhance transport and limit the build-up of CH_4 in the pore water, with the opposite occurring in *Chamaedaphne*-dominated plots where diffusion through the peat (or ebullition) are the dominant pathways.

Although there is no direct measure of production rates in this study, production may have been lower in *Chamaedaphne*-dominated plots and greater in plots with more *Eriophorum* despite the greater pore water concentrations of CH_4 in *Chamaedaphne* plots. *Eriophorum* is usually associated with enhanced C and substrate addition leading to increased CH_4 production (Strack *et al.* 2008). The *Eriophorum* community produced a relatively restricted pore water CH_4 profile in early summer, with the late-summer profile demonstrating a more clear peak in CH_4 concentrations at 50 cm despite chamber E-M 2 having very low late-summer CH_4 concentrations at 50 cm and drawing the community average down. This chamber was also associated with very high 10 cm soil temperature (Figure 4-7), moderate fluxes and redox potential values in the -100 to 0 mV range during late summer, indicating a lack of strongly reducing conditions associated with CO_2 reduction to CH_4 (Figure 4-12). This implies that methanogenic activity was not optimized at the 40-50 cm production zone for E-M 2. While this redox status does not indicate the predominance of O_2 (>400 mV), it may provide evidence that CO_2 reduction processes are being suppressed by the consumption of more favourable terminal electron acceptors such as iron or sulfur (Table 2-1) (Deppe *et al*. 2010b, Bridgham *et al.* 2013). In contrast, strongly reducing conditions (~ -200 mV) were found at 40-50 cm depth for E-M 1 (Figure 4-11) where both CH_4 fluxes and 50 cm concentrations were high mid- to late-summer. Below this depth, decomposition is likely limited by substrate supply, possibly leading to a greater proportion of terminal electron acceptors higher up the redox pair cascade (i.e. SO_4^{2-}, Fe^{3+}) and redox potential measurements that are less negative. Although E-M 3 also showed evidence for strongly reducing conditions (~ -200 mV) and produced large 50 cm CH_4 concentrations late in the season, it consistently had the lowest

CH_4 fluxes of the *Eriophorum* chambers throughout the summer. This *Eriophorum* plant was sitting atop a hummock that was ~9 cm above the top of the collar and surrounding peat surface. This possibly exposed a greater surface area of peat to the atmosphere in the top 9 cm and contributed to increased CH_4 consumption potential as the CH_4 diffused up through the aerobic zone. C-A 1 and 3 both showed relatively large mean seasonal storage change, while C-A 2 had a value similar to other chambers in the *Ledum* and *Eriophorum* communities (Figure 4-19). As this *Chamaedaphne* chamber had the deepest WT of all chambers, it is likely that oxidation processes were again consuming CH_4 in the aerobic peat layer, yielding small CH_4 fluxes and a smaller than expected increase in CH_4 storage over the season.

The seasonal increase in 50 cm CH_4 concentrations is likely tied to increasing trends in DOC and TDN, which are required for methanogen metabolism. As 50 cm temperatures increased as the summer progressed, decomposition rates would have been expected to increase. Previous studies have addressed the importance of peat temperature for CH_4 dynamics, where CH_4 production rates are positively related to peat temperature (Dunfield *et al.* 1993, Valentine *et al.*1994). CH_4 oxidation processes, however, are not as sensitive to temperature (Dunfield *et al.* 1993). In an examination of northern fens, a peatland hydrologic model by Roulet *et al.* (1992) predicted that an increase in air temperature of 3°C and associated increase in 10 cm peat temperature of 0.8°C could produce a CH_4 flux increase of 5-40%. In the current study, peat temperature at 10 cm was not a significant control on CH_4 fluxes over the 2014 sampling period (Figure 4-7). The pattern in 10 cm peat temperature was influenced by day-to-day variation, with patterns very similar to daily air temperature (Figure 4-3). Moore *et al*. (2011) found 40

cm peat temperature at Mer Bleue was significantly correlated with CH_4 flux, with WT representing a control on seasonal differences in CH_4 flux. The present study found 50 cm peat temperature to relate best with CH_4 flux (Figure 4-8), presumably because this depth is where CH_4 production is greatest (Blodau *et al.* 2007) and it is this mechanism that is likely most important in determining CH_4 emission rates. Although, warmer temperatures may also enhance CH_4 transport processes and reduce storage in pore water.

The statistically significant interaction effect of vegetation community and 50 cm peat temperature on CH_4 flux suggested that vegetation communities' CH_4 dynamics differed in their response to increased peat temperature. Previous studies have suggested that increased peat temperature could enhance ebullition CH_4 flux by increasing bubble volume (Fechner-Levy & Hemond 1996). It is possible that this increased ebullition flux response disproportionately impacts low-lying plots with WT close to the surface, as bubbles would have a thinner aerobic layer to traverse and would thereby have reduced potential for consumption through CH_4 oxidation. Increased peat temperature has also been suggested to enhance plant CH_4 transport through increased aerenchyma ventilation (Groβe 1996). This further underlines the influence of *Eriophorum* on CH_4 transport and emission rates.

6.0 CONCLUSION

Upon examination of a variety of potential mechanisms associated with CH_4 dynamics and inferred differences in CH_4 production, storage and transport processes for dominant vegetative communities during a wet summer at Mer Bleue, the following conclusions can be drawn in reference to thesis hypotheses:

1. During the growing season, both spatial and temporal variability in CH_4 emissions were high but temporal variations were greatest in the plots dominated by *Eriophorum* plants likely due to the combined effects of temporal variability in substrate production for methanogens and the influence of aerenchymatous tissues on CH_4 transport to the atmosphere.

2. Pore water biogeochemistry suggested increasing substrate availability and CH_4 production rates as peat temperature and plant growth increased throughout the growing season. Conditions for CH_4 production via CO_2 reduction were optimized near the 50 cm depth, as this depth is characterized by strongly reducing conditions and is close enough to the long-term average WT at Mer Bleue for sufficient organic C substrate supply.

3. The nonlinear relationship between mean 50 cm CH_4 storage change and mean CH_4 flux provided support for the hypothesis that plots with smaller storage increase are associated with larger CH_4 emissions. However, the lack of a significant linear relationship highlights the complexity of CH_4 dynamics in peatlands, and suggests a varying influence of CH_4 transport and consumption processes among chambers and communities at Mer Bleue.

Considering the uncertainty surrounding the global CH_4 budget, and the significance of CH_4 emissions from northern peatland ecosystems in particular, this study contributes a site-specific examination of CH_4 dynamics at the plant community scale for a temperate ombrotrophic bog that confirms the importance of plant community characteristics on CH_4 emissions through factors influencing production, storage and transport. Future studies could employ isotopic analyses of pore water samples from key depths to track the movement and transformations of CH_4 through the peat profile over the growing season, and enhance understanding of the relative importance of CH_4 production, consumption, and transport processes at Mer Bleue. Depth profiles could also be sampled at a higher temporal and spatial resolution in conjunction with full-season redox potential measurements to confirm the presence/importance, and spatial and seasonal variability of a critical zone below the water table for CH_4 production through methanogenic activity. If CH_4 production processes can be primarily related to a particular depth/zone in the peat profile regardless of the peatland, this would simplify modeling efforts to improve our understanding of the role peatlands play in the global CH_4 budget. Similarly, there is a need to focus not only on the influence of warmer peat on CH_4 production potential, but also on the response of CH_4 transport pathways to warmer peat in the context of global climate change.

7.0 APPENDICES

Appendix A Autochamber photographs

Chamaedaphne-dominated autochamber (C-A 1) on June 18, 2014.

Chamaedaphne-dominated autochamber (C-A 2) on June 18, 2014.

Chamaedaphne-dominated autochamber (C-A 3) on June 18, 2014.

Ledum-dominated autochamber (L-A 1) on June 18, 2014.

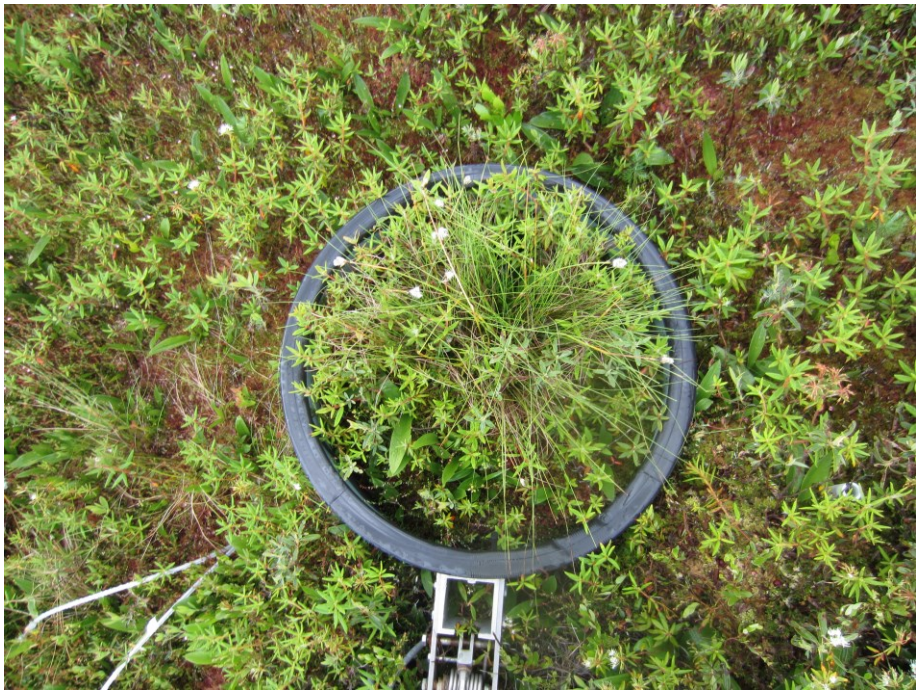

Ledum-dominated autochamber (L-A 2) on June 18, 2014.

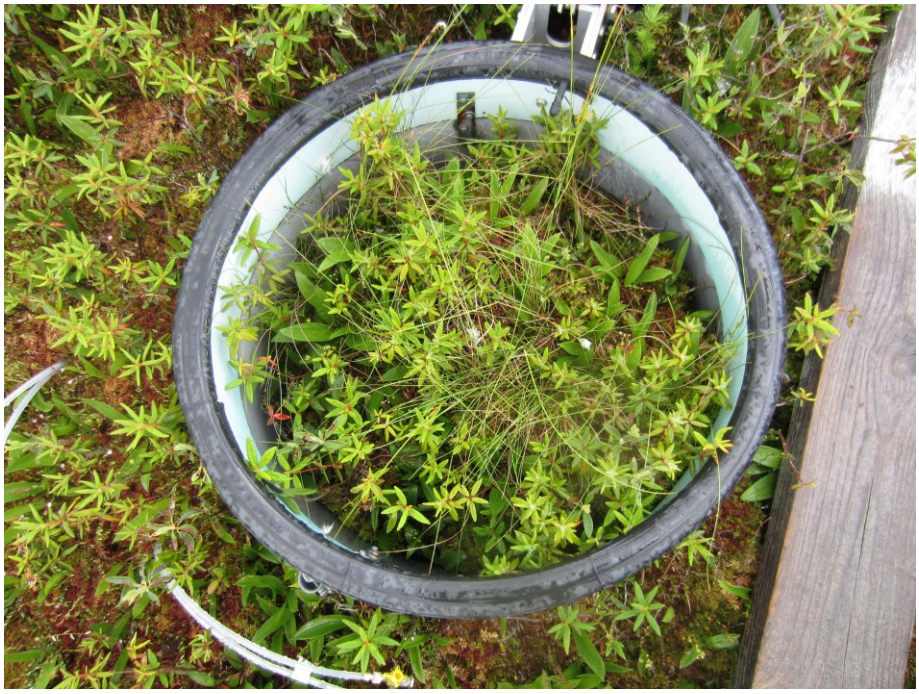

Ledum-dominated autochamber (L-A 3) on June 18, 2014.

Appendix B Calculating concentrations of pore water constituents

B.1 Units, conversions and constants

Relevant base and supplementary SI units (Brock & Richardson 2001).

Physical Quantity	*Unit Name*	*Symbol*
Length	meter	m
Mass	kilogram	kg
Time	second	s
Thermodynamic temperature	kelvin	K
Amount of substance	mole	mol
Plane angle	radian	rad

Relevant derived units (Brock & Richardson 2001).

Derived Quantity	*Unit Name*	*Symbol*	*SI Base Unit*	*Derived Unit*
Pressure, stress	pascal	Pa	kg m^{-1} s^{-2}	N m^{-2}
Energy, work, heat	joule	J	kg m^2 s^{-2}	N m
Force	newton	N	kg m s^{-2}	
Power	watt	W	kg m^2 s^{-3}	J s^{-1}
Area	square meter	A	m^2	
Volume	cubic meter	V	m^3	

Relevant units in continuous use with SI system of units (Brock & Richardson 2001).

Unit Name	*Symbol*	=
Minute	min	60 s
Hour	h	3600 s
Day	d	86 400 s
Degree	°	(π/180) rad
Minute	′	(1/60)°
Second	″	(1/60)′
Liter	L	10^{-3} m^3

Relevant universal constants.

Universal Constant	*Symbol*	*Value*	*Reference*
Air density (0°C, 100 kPa)	ρ_a	1.275 kg m^{-3}	Brock & Richardson 2001
Water density (0°C, liquid)	ρ_w	1000 kg m^{-3}	Brock & Richardson 2001
Ideal gas constant	R^*	8.3144261 J mol $^{-1}K^{-1}$	Brock & Richardson 2001
Standard atmospheric pressure		101.33 kPa	Oke 1987

Pressure unit conversion table.

	mbar	*bar*	*Torr (mm Hg)*	*Pa*	*kPa*	*atm*
1 mbar =	1					
1 bar =	10^3	1				
1 Torr =	1.333	1.333×10^{-3}	1			
1 Pa =	10^{-2}	10^{-5}	7.5006×10^{-3}	1		
1 kPa =	10^1	10^{-2}	7.5006	10^3	1	
1 atm =	1.01325×10^3	1.01325	7.60×10^2	1.01325×10^5	1.01325×10^2	1

Other common conversions

Unit	*Gas*	*Solution*
Part per million (ppm)	µmol mol^{-1}	mg/L
Part per billion (ppb)	nmol mol^{-1}	µg/L

Constants for the calculation of CO_2 solubility (mol L^{-1} atm^{-1}) from moist air at a total pressure of 1 atm (Weiss & Price 1980).

Constants	*Value (mol L^{-1} atm^{-1})*
A_1	-160.7333
A_2	215.4152
A_3	89.8920
A_4	-1.47759
B_1	0.029941
B_2	-0.027455
B_3	0.0053407

Constants for the calculation of temperature (°K) and salinity (‰) dependent CH_4 Bunsen solubility coefficient (L L^{-1} atm^{-1}) (Wanninkhof 1992).

Constants	*Value (L L^{-1} atm^{-1})*
A_1	-68.8862
A_2	101.4956
A_3	28.7314
B_1	-0.076146
B_2	0.043970
B_3	-0.0068672

B.2 Calculating CO_2 concentration in pore water

B.2.1 CO_2 solubility

As defined by Weiss & Price (1980), the solubility of CO_2 in water (F, mol L^{-1} atm^{-1}) as a function of temperature and salinity, including all nonideality effects, is calculated as:

$$\ln F = A_1 + A_2(100/T) + A_3 \ln(T/100) + A_4(T/100)^2 + S[B_1 + B_2(T/100) + B_3(T/100)^2] \quad (1)$$

$$F = e^{\ln F} \quad (2)$$

where A and B values are constants (mol L^{-1} atm^{-1}) defined in Section A.1, T is absolute temperature (K) and S is salinity in parts per thousand (‰).

B.2.2 CO_2 in headspace

The amount of CO_2 in the headspace (CO_{2_h}, µmol) after equilibration is calculated as:

$$[CO_2]_{RES} = [CO_2]_{GC} - [CO_2]_{AMB} \quad (3)$$

$$CO_{2_h} = \left([CO_2]_{RES} \frac{PV_h}{R * T} \right) \frac{1m^3}{1000L} \quad (4)$$

where $[CO_2]_{GC}$ is the headspace concentration of CO_2 (µmol CO_2 mol^{-1}), as measured on the gas chromatograph, $[CO_2]_{AMB}$ is the ambient concentration of CO_2 (µmol CO_2 mol^{-1}) at the time of sampling, $[CO_2]_{RES}$ is the residual concentration of CO_2 in the headspace (µmol CO_2 mol^{-1}) after subtracting the ambient influence, P is the pressure at

equilibration (Pa), V_h is the headspace volume after equilibration (L), R^* is the ideal gas constant 8.3144261 (J mol $^{-1}$ K^{-1}) as given in Section A.1, and T is the absolute air temperature at equilibration (K).

B.2.3 CO_2 in water

The amount of CO_2 in the water (CO_{2_w}, μmol) after equilibration is calculated as:

(5) $$CO_{2_w} = F \times [CO_2]_{RES} \times P \times V_w$$

where F is the CO_2 solubility (mol L^{-1} atm^{-1}, Equation 1 and 2), $[CO_2]_{RES}$ is the residual concentration of CO_2 in the headspace (μmol CO_2 mol $^{-1}$) as per Equation 3, P is the pressure at equilibration (atm), and V_w is the water volume after equilibration (L).

B.2.4 Total CO_2 concentration in pore water

The total concentration of CO_2 in the pore water ($[CO_2]_{PW}$, μmol CO_2 L^{-1}) can thus be calculated as:

(6) $$[CO_2]_{PW} = \frac{CO_{2_h} + CO_{2_w}}{V_w}$$

where CO_{2_h} and CO_{2_w} are the amount of CO_2 in the headspace and water respectively after equilibration (μmol CO_2), and V_w is the water volume after equilibration (L).

B.2.5 Sample CO_2 pore water concentration calculations

The above procedure was applied for sample input variables, and the calculated concentration values of CO_2 in pore water are provided in the table below.

Sample calculations for determining the concentration of CO_2 in pore water according to the procedure detailed in Sections A.2.1 through A.2.4.

Variable	*Units*	*Sample #1*	*Sample #2*	*Sample #3*
T	K	283.15	293.15	303.15
S	‰	0	0	0
F	mol L^{-1} atm^{-1}	5.28×10^{-2}	3.81×10^{-2}	2.85×10^{-2}
$[CO_2]_{GC}$	µmol CO_2 mol^{-1}	8.15×10^{2}	1.01×10^{4}	3.13×10^{2}
$[CO_2]_{AMB}$	µmol CO_2 mol^{-1}	4.02×10^{2}	4.02×10^{2}	4.02×10^{2}
$[CO_2]_{RES}$	µmol CO_2 mol^{-1}	4.13×10^{2}	9.65×10^{3}	3.09×10^{4}
P	Pa	1.0076×10^{5}	1.0076×10^{5}	1.0076×10^{5}
P	atm	9.94423×10^{-1}	9.94423×10^{-1}	9.94423×10^{-1}
V_h	L	3.0×10^{-2}	3.0×10^{-2}	3.0×10^{-2}
V_w	L	3.0×10^{-2}	3.0×10^{-2}	3.0×10^{-2}
CO_{2h}	µmol CO_2	5.31×10^{-1}	1.20×10^{1}	3.70×10^{1}
CO_{2w}	µmol CO_2	6.51×10^{-1}	1.10×10^{1}	2.62×10^{1}
$[CO_2]_{PW}$	**µmol CO_2 L^{-1}**	**3.94×10^{1}**	**7.66×10^{2}**	**2.11×10^{3}**

B.3 Calculating CH_4 concentration in pore water

B.3.1 CH_4 solubility

The Bunsen solubility coefficient of CH_4 (β, mol L^{-1} atm^{-1}) can be calculated as a function of temperature and salinity (Wanninkhof 1992), where:

(7) $$\ln\beta = A_1 + A_2(100/T) + A_3\ln(T/100) + S\left[B_1 + B_2(T/100) + B_3(T/100)^2\right]$$

(8) $$\beta = e^{\ln\beta}\frac{101325}{R^*(298.15)}\times 0.001$$

where *A* and *B* values are constants (L L^{-1} atm^{-1}) defined in Section A.1, *T* is absolute temperature (K) and *S* is salinity in parts per thousand (‰). Equation 8 converts this solubility value from L CH_4 L^{-1} water atm^{-1} to units of mol L^{-1} atm^{-1}.

B.3.2 CH_4 in headspace

The amount of CH_4 in the headspace (CH_{4_h}, μmol) after equilibration is calculated as:

(9) $$[CH_4]_{RES} = [CH_4]_{GC} - [CH_4]_{AMB}$$

(10) $$CH_{4_h} = \left([CH_4]_{RES} \frac{PV_h}{R^* T} \right) \frac{1m^3}{1000L}$$

where $[CH_4]_{GC}$ is the headspace concentration of CH_4 (μmol CH_4 mol $^{-1}$), as measured on the gas chromatograph, $[CH_4]_A$ is the ambient concentration of CH_4 (μmol CH_4 mol $^{-1}$) at the time of sampling, $[CH_4]_{RES}$ is the residual concentration of CH_4 in the headspace (μmol CH_4 mol $^{-1}$) after subtracting the ambient influence, P is the pressure at equilibration (Pa), V_h is the headspace volume after equilibration (L), R^* is the ideal gas constant 8.314 4261 (J K^{-1} mol $^{-1}$) as given in Section A.1, and T is the absolute air temperature at equilibration (K).

B.3.3 CH_4 in water

The amount of CH_4 in the water (CH_{4_w}, μmol) after equilibration is calculated as:

(11) $$CH_{4_w} = \beta \cdot [CH_4]_{RES} \cdot P \cdot V_w$$

where β is the Bunsen solubility coefficient of CH_4 (mol L^{-1} atm^{-1}, Equation 6 and 7), $[CH_4]_{RES}$ is the residual concentration of CH_4 in the headspace (μmol CH_4 mol $^{-1}$), P is the pressure at equilibration (atm), and V_w is the water volume after equilibration (L).

B.3.4 Total CH_4 concentration in pore water

The total concentration of CH_4 in the pore water ($[CH_4]_{PW}$, µmol CH_4 L^{-1}) can thus be calculated as:

$$[CH_4]_{PW} = \frac{CH_{4_h} + CH_{4_w}}{V_w} \quad (12)$$

where CH_{4_h} and CH_{4_w} are the amount of CH_4 in the headspace and water respectively after equilibration (µmol CH_4), and V_w is the water volume after equilibration (L).

B.3.5 Sample CH_4 pore water concentration calculations

The above procedure was applied for sample input variables, and the calculated concentration values of CH_4 in pore water are provided in the table below.

Sample calculations for determining the concentration of CH_4 in pore water according to the procedure detailed in sections A.3.1 through A.3.4.

Variable	*Units*	*Sample #1*	*Sample #2*	*Sample #3*
T	K	283.15	293.15	303.15
S	‰	0	0	0
β	mol L^{-1} atm^{-1}	1.80×10^{-3}	1.40×10^{-3}	1.20×10^{-3}
$[CH_4]_{GC}$	µmol CH_4 mol^{-1}	1.15×10^{2}	5.43×10^{3}	1.99×10^{4}
$[CH_4]_{AMB}$	µmol CH_4 mol^{-1}	1.90×10^{0}	1.90×10^{0}	1.90×10^{0}
$[CH_4]_{RES}$	µmol CH_4 mol^{-1}	1.13×10^{2}	5.42×10^{3}	1.99×10^{4}
P	Pa	1.0076×10^{5}	1.0076×10^{5}	1.0076×10^{5}
P	atm	9.94423×10^{-1}	9.94423×10^{-1}	9.94423×10^{-1}
V_h	L	3.0×10^{-2}	3.0×10^{-2}	3.0×10^{-2}
V_w	L	3.0×10^{-2}	3.0×10^{-2}	3.0×10^{-2}
CH_{4h}	µmol CH_4	1.45×10^{-1}	6.73×10^{0}	2.38×10^{1}
CH_{4w}	µmol CH_4	6.07×10^{-3}	2.26×10^{-1}	7.12×10^{-1}
$[CH_4]_{PW}$	**µmol CH_4 L^{-1}**	**5.04** $\times 10^{0}$	**2.32** $\times 10^{2}$	**8.17** $\times 10^{2}$

Appendix C Seasonal CH_4 Fluxes

C.1 Comparison of CH_4 fluxes among seasons

Comparison of mean daily CH_4 flux (mg CH_4 m^{-2} h^{-1}), WT (cm) and 50 cm peat temperature (T_{50cm}, °C) from *Chamaedaphne* (C-A 1,2,3), *Ledum* (L-A 1,2,3) and *Eriophorum* (E-M 1,2,3)-dominated communities at Mer Bleue, 2014. Standard deviation is given in parentheses. Note: WP, whole period (DOY **120**-155); LSp, late spring (DOY **120**-154); ES, early summer (DOY 155-189); MS, mid-summer (DOY 190-221); LS, late summer (DOY 222-255) for the 2014 measurement period.

Whole Period (DOY 120-255)			
	CH_4 Flux (mg m^{-2} h^{-1})	**WT (cm)**	**T_{50cm} (°C)**
Chamaedaphne	*1.03 (0.65)*	*36.4 (3.2)*	11.1 (3.0)
C-A 1	1.68 (1.14)	29.1 (2.4)	
C-A 2	0.75 (0.55)	43.8 (3.1)	
C-A 3	0.65 (0.54)	34.6 (3.2)	
Ledum	*3.81 (1.98)*	*28.5 (3.2)*	
L-A 1	2.55 (0.97)	28.8 (2.9)	
L-A 2	4.56 (2.78)	31.1 (2.2)	
L-A 3	4.25 (2.27)	24.6 (2.8)	
Eriophorum	*3.27 (2.42)*	*28.4 (3.1)*	
E-M 1	6.16 (4.88)	25.8 (2.8)	
E-M 2	2.13 (1.56)	30.1 (2.7)	
E-M 3	1.27(1.22)	28.2 (2.6)	
Late Spring (DOY 120-154)			
Chamaedaphne	*0.31 (0.10)*	*34.9 (3.2)*	6.6 (1.8)
C-A 1	0.68 (0.16)	27.9 (2.5)	
C-A 2	0.22 (0.14)	43.4 (3.3)	
C-A 3	0.01 (0.03)	32.9 (3.4)	
Ledum	*0.99 (0.33)*	*26.9 (2.9)*	
L-A 1	1.12 (0.38)	27.3 (3.3)	
L-A 2	0.59 (0.27)	29.8 (2.4)	
L-A 3	1.20 (0.30)	23.1 (2.9)	
Eriophorum	*0.42 (0.34)*	*N/A*	
E-M 1	0.33 (0.32)	30.2 (1.6)	
E-M 2	0.68 (0.46)	34.0 (1.5)	
E-M 3	0.40 (0.44)	31.9 (1.4)	

Early Summer (DOY 155-189)			
	CH_4 Flux (mg m^{-2} h^{-1})	**WT (cm)**	**T_{50cm} (°C)**
Chamaedaphne	*0.88 (0.38)*	*37.8 (3.4)*	11.3 (1.2)
C-A 1	1.60 (0.80)	29.1 (1.7)	
C-A 2	0.62 (0.21)	43.7 (3.5)	
C-A 3	0.38 (0.25)	34.3 (2.9)	
Ledum	*3.41 (0.90)*	*27.9 (2.5)*	
L-A 1	2.60 (0.42)	28.6 (2.6)	
L-A 2	4.04 (1.39)	31.2 (2.3)	
L-A 3	3.36 (1.02)	24.4 (2.5)	
Eriophorum	*1.58 (0.72)*	*27.8 (3.6)*	
E-M 1	2.57 (1.71)	25.0 (2.9)	
E-M 2	1.22 (0.91)	29.4 (2.8)	
E-M 3	0.49 (0.57)	27.5 (2.7)	
Mid Summer (DOY 190-221)			
Chamaedaphne	*1.44(0.50)*	*37.4 (2.6)*	13.2 (0.2)
C-A 1	2.29 (1.29)	30.4 (2.3)	
C-A 2	0.99 (0.53)	45.1 (2.6)	
C-A 3	1.03 (0.20)	36.7 (2.8)	
Ledum	*5.33 (0.23)*	*30.5 (3.2)*	
L-A 1	3.22 (0.19)	30.6 (2.2)	
L-A 2	6.56 (0.62)	32.5 (1.6)	
L-A 3	6.11 (0.37)	26.6 (2.6)	
Eriophorum	*5.27 (1.83)*	*28.8 (3.4)*	
E-M 1	9.57 (3.77)	27.0 (2.6)	
E-M 2	2.80 (1.66)	31.4 (2.6)	
E-M 3	1.88 (1.52)	29.3 (2.5)	
Late Summer (DOY 222-255)			
Chamaedaphne	*1.58 (0.57)*	*35.6 (2.5)*	13.6 (0.4)
C-A 1	2.23 (1.16)	28.9 (2.3)	
C-A 2	1.22 (0.61)	43.0 (2.7)	
C-A 3	1.27 (0.32)	34.7 (2.5)	
Ledum	*5.83(0.35)*	*28.7 (3.1)*	
L-A 1	3.35 (0.55)	28.6 (2.4)	
L-A 2	7.41 (0.65)	31.1 (1.8)	
L-A 3	6.64 (0.22)	24.3 (2.0)	
Eriophorum	*5.20(1.41)*	*28.9 (2.4)*	
E-M 1	10.04 (3.32)	25.1 (2.4)	
E-M 2	3.43 (1.15)	29.2 (2.2)	
E-M 3	2.01 (0.89)	27.5 (2.2)	

Comparison of mean daily CH_4 flux (mg CH_4 m^{-2} h^{-1}), WT (cm) and 50 cm peat temperature (T_{50cm}, °C) from *Chamaedaphne* (C-A 1,2,3), *Ledum* (L-A 1,2,3) and *Eriophorum* (E-M 1,2,3)-dominated communities at Mer Bleue, 2014. Standard deviation is given in parentheses. Note: WP, whole period (DOY **120**-155); LSp, late spring (DOY **120**-154); ES, early summer (DOY 155-189); MS, mid-summer (DOY 190-221); LS, late summer (DOY 222-255) for the 2014 measurement period.

Chamaedaphne		*Ledum*		*Eriophorum*		T_{50cm} (°C)
CH_4 Flux (mg CH_4 m^{-2} h^{-1})	WT (cm)	CH_4 Flux (mg CH_4 m^{-2} h^{-1})	WT (cm)	CH_4 Flux (mg CH_4 m^{-2} h^{-1})	WT (cm)	
Whole Period (DOY 120-255, n=1116)						
1.03^{b} (0.65)	36.4^{a} (3.2)	3.81^{a} (1.98)	28.5^{ab} (3.2)	3.26^{ab}(2.42)	28.0^{b} (2.7)	11.1 (3.0)
Late Spring (DOY 120-154, n=207)						
0.31^{b} (0.09)	34.9^{a} (3.2)	0.99^{a} (0.33)	26.9^{a} (2.9)	0.42^{NA}(0.34)	N/A	6.6 (1.8)
Early Summer (DOY 155-189, n=207)						
0.88^{b} (0.38)	37.8^{a} (3.4)	3.41^{a}(0.90)	27.9^{a} (2.5)	1.58^{b} (0.72)	27.3^{a} (2.8)	11.3 (1.2)
Mid Summer (DOY 190-221, n=207)						
1.44^{b} (0.50)	37.4^{a} (2.6)	5.33^{a} (0.23)	30.5^{a} (3.2)	5.27^{ab} (1.82)	29.2^{a} (2.6)	13.2 (0.2)
Late Summer (DOY 222-255, n=207)						
1.58^{b} (0.57)	35.6^{a} (2.5)	5.83^{a} (0.35)	28.7^{a} (3.1)	5.20^{a} (1.40)	27.3^{a} (2.3)	13.6 (0.4)

Appendix D Repeated measures analysis using mixed models in JMP

D.1 Mixed model analysis of factors affecting CH_4 fluxes

Output of JMP mixed model analysis where the log transform of CH_4 fluxes for manually sampled days is treated as the response with community as a fixed effect, chamber as a random effect and covariates including: barometric pressure, 10 cm peat temperature and WT from each chamber, and 50 cm peat temperature from the tower.

Response log(CH4+2) (mg/m2/hr)

Whole Model

Effect Summary

Source	LogWorth	PValue
Ttower_50cm	88.657	0.00000
Community*Ttower_50cm	25.308	0.00000
BarometricP	6.818	0.00000
Community*BarometricP	5.169	0.00001
Tsoil_10cm_chamber*Ttower_50cm	3.142	0.00072
WT_Chamber	1.788	0.01629
Tsoil_10cm_chamber*BarometricP	1.295	0.05065
Community	1.110	0.07770
Tsoil_10cm_chamber	0.974	0.10612
BarometricP*Ttower_50cm	0.384	0.41309
BarometricP*WT_Chamber	0.334	0.46295
Tsoil_10cm_chamber*WT_Chamber	0.228	0.59097
Community*Tsoil_10cm_chamber	0.182	0.65788
Community*WT_Chamber	0.157	0.69711
WT_Chamber*Ttower_50cm	0.022	0.95003

Remove Add Edit Undo FDR

Summary of Fit

RSquare	0.865741
RSquare Adj	0.862359
Root Mean Square Error	0.180499
Mean of Response	1.429272
Observations (or Sum Wgts)	815

REML Variance Component Estimates

Random Effect	Var Ratio	Var Component	Std Error	95% Lower	95% Upper	Pct of Total
Chamber[Community]	2.9872185	0.0973232	0.0566209	-0.013652	0.2082981	74.920
Residual		0.0325799	0.0016413	0.0295879	0.0360522	25.080
Total		0.1299031	0.0566438	0.0643588	0.3860533	100.000

-2 LogLikelihood = -274.8156033

Note: Total is the sum of the positive variance components.

Total including negative estimates = 0.1299031

Covariance Matrix of Variance Component Estimates

Iterations

Fixed Effect Tests

Source	Nparm	DF	DFDen	F Ratio	Prob > F
Community	2	2	6.052	4.0135	0.0777
Tsoil_10cm_chamber	1	1	794	2.6170	0.1061
BarometricP	1	1	788.1	28.0691	<.0001*
WT_Chamber	1	1	793.8	5.7958	0.0163*
Ttower_50cm	1	1	791.8	523.8658	<.0001*
Community*Tsoil_10cm_chamber	2	2	792.2	0.4189	0.6579
Community*BarometricP	2	2	788.1	12.0836	<.0001*
Community*WT_Chamber	2	2	793.1	0.3610	0.6971
Community*Ttower_50cm	2	2	791.1	62.7842	<.0001*
Tsoil_10cm_chamber*BarometricP	1	1	789.2	3.8315	0.0506
Tsoil_10cm_chamber*WT_Chamber	1	1	788.7	0.2891	0.5910
Tsoil_10cm_chamber*Ttower_50cm	1	1	788.3	11.5246	0.0007*
BarometricP*WT_Chamber	1	1	788.2	0.5393	0.4630
BarometricP*Ttower_50cm	1	1	788.9	0.6706	0.4131
WT_Chamber*Ttower_50cm	1	1	788.8	0.0039	0.9500

D.2 Mixed model analysis of factors affecting pore water CH_4 concentrations

Output of JMP mixed model analysis where the pore water CH_4 concentration (DOY 155-255) is treated as the response with chamber as a random effect and DOC, TDN, depth-specific peat temperature and WT as covariates, and depth and community as fixed effects.

Response CH4_PW_Wanninkhof

Whole Model

Effect Summary

Source	LogWorth	PValue
Community*TDN	3.252	0.00056
DOC	2.647	0.00225
Depth*WT	2.569	0.00270
DOC*TDN	1.974	0.01062
Depth*daily_Tsoil_AC8_profile	1.885	0.01302
TDN*daily_Tsoil_AC8_profile	1.262	0.05474
Community*Depth	1.163	0.06871
TDN*WT	0.699	0.19995
Community*DOC	0.647	0.22545
TDN	0.564	0.27273
Community	0.529	0.29581
Community*daily_Tsoil_AC8_profile	0.517	0.30408
WT	0.504	0.31300
daily_Tsoil_AC8_profile	0.458	0.34828
DOC*daily_Tsoil_AC8_profile	0.457	0.34922
DOC*WT	0.443	0.36085
Depth	0.307	0.49301
Community*WT	0.244	0.57072
Depth*DOC	0.182	0.65758
WT*daily_Tsoil_AC8_profile	0.165	0.68367
Depth*TDN	0.126	0.74833

Remove Add Edit FDR

Summary of Fit

RSquare	0.249179
RSquare Adj	0.203828
Root Mean Square Error	146.3941
Mean of Response	246.1222
Observations (or Sum Wgts)	475

REML Variance Component Estimates

Random Effect	Var Ratio	Var Component	Std Error	95% Lower	95% Upper	Pct of Total
Chamber[Community]	0.0227175	486.86377	595.98604	-681.2474	1654.9749	2.221
Residual		21431.232	1441.7402	18864.108	24563.439	97.779
Total		21918.096	1531.1358	19201.481	25258.201	100.000

-2 LogLikelihood = 5984.5265908

Note: Total is the sum of the positive variance components.

Total including negative estimates = 21918.096

Covariance Matrix of Variance Component Estimates

Iterations

Fixed Effect Tests

Source	Nparm	DF	DFDen	F Ratio	Prob > F
Community	2	2	8.53	1.4098	0.2958
Depth	1	1	445.2	0.4707	0.4930
DOC	1	1	362.8	9.4639	0.0023*
TDN	1	1	446.9	1.2059	0.2727
WT	1	1	111.8	1.0272	0.3130
daily_Tsoil_AC8_profile	1	1	441.3	0.8816	0.3483
Community*Depth	2	2	445.7	2.6941	0.0687
Community*DOC	2	2	406.3	1.4951	0.2254
Community*TDN	2	2	446.2	7.6141	0.0006*
Community*WT	2	2	82.23	0.5647	0.5707
Community*daily_Tsoil_AC8_profile	2	2	446	1.1937	0.3041
Depth*DOC	1	1	435	0.1967	0.6576
Depth*TDN	1	1	447	0.1031	0.7483
Depth*WT	1	1	444.2	9.1017	0.0027*
Depth*daily_Tsoil_AC8_profile	1	1	446.2	6.2161	0.0130*
DOC*TDN	1	1	446.7	6.5832	0.0106*
DOC*WT	1	1	444.3	0.8367	0.3608
DOC*daily_Tsoil_AC8_profile	1	1	445.6	0.8781	0.3492
TDN*WT	1	1	446.6	1.6476	0.1999
TDN*daily_Tsoil_AC8_profile	1	1	446.3	3.7093	0.0547
WT*daily_Tsoil_AC8_profile	1	1	446.3	0.1662	0.6837

Output of JMP mixed model analysis where the pore water CH_4 concentration (DOY 212-255) is treated as the response with chamber as a random effect and DOC, TDN, depth-specific peat temperature and WT as covariates, and depth and community as fixed effects.

Response CH4_PW_Wanninkhof

Whole Model

Effect Summary

Source	LogWorth	PValue
Community*TDN	4.304	0.00005
TDN	2.206	0.00623
TDN*WT	1.916	0.01213
DOC*TDN	1.804	0.01571
Community	1.439	0.03640
TDN*daily_Tsoil_AC8_profile	0.740	0.18212
Community*DOC	0.594	0.25490
DOC*daily_Tsoil_AC8_profile	0.441	0.36264
DOC*WT	0.427	0.37370
Depth	0.394	0.40343
Community*daily_Tsoil_AC8_profile	0.354	0.44308
Depth*daily_Tsoil_AC8_profile	0.351	0.44606
daily_Tsoil_AC8_profile	0.296	0.50595
WT*daily_Tsoil_AC8_profile	0.225	0.59555
Depth*WT	0.108	0.77935
WT	0.108	0.77985
Community*WT	0.081	0.83010
Depth*DOC	0.066	0.85868
DOC	0.031	0.93113
Depth*TDN	0.017	0.96260
Community*Depth	0.017	0.96260

Remove Add Edit FDR

Summary of Fit

RSquare	0.307449
RSquare Adj	0.219661
Root Mean Square Error	148.2043
Mean of Response	261.9299
Observations (or Sum Wgts)	241

REML Variance Component Estimates

Random Effect	Var Ratio	Var Component	Std Error	95% Lower	95% Upper	Pct of Total
Chamber[Community]	-0.016774	-368.4243	468.19292	-1286.066	549.21696	0.000
Residual		21964.523	2150.2659	18291.801	26872.615	100.000
Total		21964.523	2150.2659	18291.801	26872.615	100.000

-2 LogLikelihood = 2944.9847446

Note: Total is the sum of the positive variance components.

Total including negative estimates = 21596.098

Covariance Matrix of Variance Component Estimates

Iterations

Fixed Effect Tests

Source	Nparm	DF	DFDen	F Ratio	Prob > F
Community	2	2	9.669	4.7589	0.0364*
Depth	1	1	211.9	0.7009	0.4034
DOC	1	1	148	0.0075	0.9311
TDN	1	1	209.3	7.6374	0.0062*
WT	1	1	18.74	0.0804	0.7798
daily_Tsoil_AC8_profile	1	1	211.8	0.4439	0.5059
Community*Depth	2	2	212.4	0.0381	0.9626
Community*DOC	2	2	75.69	1.3919	0.2549
Community*TDN	2	2	193.6	10.4347	<.0001*
Community*WT	2	2	15.81	0.1884	0.8301
Community*daily_Tsoil_AC8_profile	2	2	202.5	0.8173	0.4431
Depth*DOC	1	1	212.3	0.0318	0.8587
Depth*TDN	1	1	211.8	0.0022	0.9626
Depth*WT	1	1	212.2	0.0787	0.7793
Depth*daily_Tsoil_AC8_profile	1	1	191.3	0.5831	0.4461
DOC*TDN	1	1	212.9	5.9300	0.0157*
DOC*WT	1	1	209.8	0.7947	0.3737
DOC*daily_Tsoil_AC8_profile	1	1	212.5	0.8323	0.3626
TDN*WT	1	1	212.7	6.4007	0.0121*
TDN*daily_Tsoil_AC8_profile	1	1	213	1.7919	0.1821
WT*daily_Tsoil_AC8_profile	1	1	209.5	0.2826	0.5956

D.3 Mixed model analysis of factors affecting $\delta^{13}C\text{-}CH_4$ source signatures

Output of JMP mixed model analysis where the $\delta^{13}C\text{-}CH_4$ source signature is treated as the response with chamber as a random effect and mean pore water CH_4 concentration, log CH_4 flux, 10 cm peat temperature and WT as covariates, and community as a fixed effect.

Response d13Ch4

Whole Model

Effect Summary

Source	LogWorth	PValue
mean WT*mean CH4 PW wanninkhof	0.575	0.26584
mean CH4 PW wanninkhof*mean Tsoil 10 cm	0.344	0.45292
Community*mean CH4 PW wanninkhof	0.342	0.45474
mean CH4 PW wanninkhof	0.326	0.47248
mean Tsoil 10 cm	0.323	0.47520
mean WT*log Ch4 flux	0.264	0.54406
mean CH4 PW wanninkhof*log Ch4 flux	0.245	0.56859
mean WT	0.175	0.66821
mean WT*mean Tsoil 10 cm	0.147	0.71365
Community*mean WT	0.138	0.72845
Community	0.088	0.81605
Community*mean Tsoil 10 cm	0.084	0.82327
log Ch4 flux*mean Tsoil 10 cm	0.058	0.87430
log Ch4 flux	0.015	0.96521
Community*log Ch4 flux	0.000	0.99985

Remove Add Edit FDR

Summary of Fit

RSquare	0.404831
RSquare Adj	0.114505
Root Mean Square Error	4.83897
Mean of Response	-75.2857
Observations (or Sum Wgts)	62

REML Variance Component Estimates

Random Effect	Var Ratio	Var Component	Std Error	95% Lower	95% Upper	Pct of Total
Chamber[Community]	0.3836872	8.984279	11.203353	-12.97389	30.942447	27.729
Residual		23.415634	5.4230701	15.585278	39.105004	72.271
Total		32.399913	11.8092	17.696678	77.458618	100.000

-2 LogLikelihood = 390.27492445

Note: Total is the sum of the positive variance components.

Total including negative estimates = 32.399913

Covariance Matrix of Variance Component Estimates

Iterations

Fixed Effect Tests

Source	Nparm	DF	DFDen	F Ratio	Prob > F
Community	2	2	5.668	0.2107	0.8161
mean WT	1	1	34.36	0.1869	0.6682
mean CH4 PW wanninkhof	1	1	39.34	0.5263	0.4725
log Ch4 flux	1	1	9.521	0.0020	0.9652
mean Tsoil 10 cm	1	1	31.58	0.5223	0.4752
Community*mean WT	2	2	39.87	0.3194	0.7285
Community*mean CH4 PW wanninkhof	2	2	38.47	0.8044	0.4547
Community*log Ch4 flux	2	2	9.335	0.0002	0.9998
Community*mean Tsoil 10 cm	2	2	31.45	0.1957	0.8233
mean WT*mean CH4 PW wanninkhof	1	1	37.96	1.2754	0.2658
mean WT*log Ch4 flux	1	1	40.68	0.3743	0.5441
mean WT*mean Tsoil 10 cm	1	1	37.94	0.1367	0.7136
mean CH4 PW wanninkhof*log Ch4 flux	1	1	38.15	0.3307	0.5686
mean CH4 PW wanninkhof*mean Tsoil 10 cm	1	1	37.97	0.5751	0.4529
log Ch4 flux*mean Tsoil 10 cm	1	1	40.43	0.0253	0.8743

8.0 REFERENCES

Adkinson AC (2009) Responses of *Sphagnum* productivity and net ecosystem exchange of CO_2 to modifications of moss moisture content in an ombrotrophic bog. M.Sc. Thesis. Carleton University, Ottawa, ON.

Avery GB, Shannon RD, White JR, Martens CS, Alperin MJ (1999) Effect of seasonal changes in the pathways of methanogenesis on the delta-13C values of pore water in a Michigan peatland. *Global Biogeochemical Cycles*, **13**(2), 475-484.

Bain CG, Bonn A, Stoneman R *et al.* (2011) IUCN UK Commission of Inquiry on Peatlands. IUCN UK Peatland Programme, Edinburgh.

Bardgett RD, Manning P, Morriën E, De Vries FT (2013) Hierarchical responses of plant-soil interactions to climate change: consequences for the global carbon cycle. *Journal of Ecology,* **101**, 334-343.

Bartlett KB, Harriss RC (1993) Review and assessment of methane emissions from wetlands. *Chemosphere,* **26**(1-4), 261-320.

Bender M, Conrad R (1995) Effects of CH_4 concentrations and soil conditions on the induction of CH_4 oxidation activity. *Soil Biology and Biochemistry*, **27**(12), 1517-1527.

Bergman I, Klarqvist M, Nilsson M (2000) Seasonal variation in rates of methane production from peat of various botanical origins: effects of temperature and substrate quality. *Microbiology Ecology*, **33**(3), 181-189.

Blodau C (2001) Carbon biogeochemistry in northern peatlands: regulation by environmental and biogeochemical factors. Ph.D. Thesis. McGill University, Montréal, QC.

Blodau C (2002) Carbon cycling in peatlands-- a review of processes and controls. *Environmental Reviews,* **10**(2), 111-134.

Blodau C, Moore TR (2002) Macroporosity affects water movement and pore water sampling in peat soils. *Soil Science*, **167**(2), 98-109.

Blodau C, Moore TR (2003a) Experimental response of peatland carbon dynamics to a water table fluctuation. *Aquatic Sciences*, **65**, 47-62.

Blodau C, Moore TR (2003b) Micro-scale CO_2 and CH_4 dynamics in a peat soil during a water fluctuation and sulphate pulse. *Soil Biology and Biochemistry*, **35**, 535-547.

Blodau C, Roulet NT, Heitmann T *et al.* (2007) Belowground carbon turnover in a temperate ombrotrophic bog. *Global Biogeochemical Cycles,* **21**, GB1021.

Bridgham SD, Megonigal JP, Keller JK, Bliss NB, Trettin C (2006) The carbon balance of North American wetlands. *Wetlands*, **26**(4), 889-916.

Bridgham SD, Cadillo-Quiroz H, Keller JK, Zhuang Q (2013) Methane emissions from wetlands: biogeochemical, microbial, and modeling perspectives from local to global scales. *Global Change Biology,* **19**(5), 1325-1346.

Brock FV, Richardson SJ (2001) *Meteorological Measurement Systems*. Oxford University Press, New York.

Brown MG, Humphreys ER, Moore TR, Roulet NT, Lafleur PM (2014) Evidence for a nonlinear relationship between ecosystem-scale peatland methane emissions and water table depth. *Journal of Geophysical Research: Biogeosciences*, **119**, 826-835.

Bubier JL (1995) The relationship of vegetation to methane emission and hydrochemical gradients in northern peatlands. *Journal of Ecology*, **83**, 403–420.

Bubier JL, Moore TR, Juggins S (1995a) Predicting methane emissions from bryophyte distribution in northern Canadian peatlands. *Ecology*, **76**, 677–693.

Bubier JL, Moore TR, Bellisario L, Comer NT, Crill PM (1995b) Ecological controls on methane emissions from a northern peatland complex in the zone of discontinuous permafrost, Manitoba, Canada. *Global Biogeochemical Cycles,* **9**, 455-470.

Bubier JL, Moore TR, Crosby G (2006) Fine-scale vegetation distribution in a cool temperate peatland. *Canadian Journal of Botany*, **84**(6), 910-923.

Chanton JP, Whiting GJ (1995) Trace gas exchange in freshwater and coastal marine environments: Ebullition and transport by plants. In *Biogenic Trace Gases: Measuring Emissions from Soil and Water* (eds. Matson PA, and Harriss RC), pp. 98-125. Wiley-Blackwell, Oxford, UK.

Chanton JP (2005) The effect of gas transport on the isotope signature of methane in wetlands. *Organic Geochemistry*, **36**, 753-768.

Chanton JP, Chaser LC, Glasser P, Siegel D (2005) Chapter 6: Carbon and hydrogen isotopic effects in microbial methane from terrestrial environments. In *Stable Isotopes and Biosphere-Atmosphere Interactions: Processes and Biological Controls* (eds. Flanagan LB, Ehleringer JR, Pataki DE), pp. 85-105. Elsevier, Amsterdam, NL.

Chanton JP, Glaser PH, Chasar LS, *et al.* (2008) Radiocarbon evidence for the importance of surface vegetation on fermentation and methanogenesis in contrasting types of boreal peatlands. *Global Biogeochemical Cycles*, **22**, GB4022.

Chawanakul S, Chaiprasert P, Towprayoon S, Tanticharoen M (2009) Contributions of available substrates and activities of trophic microbial community to methanogenesis in vegetative and reproductive rice rhizospheric soil. *Journal of environmental biology,* **30**(1), 119-127.

Christensen TR, Jackowicz-Korczynski M, Aurela M *et al.* (2012) Monitoring the multi-year carbon balance of a subarctic palsa mire with micrometeorological techniques. *Ambio (Royal Swedish Academy of Sciences),* **41**(Supplement 3), 207-217.

Clark ID, Fritz P (1997) *Environmental Isotopes in Hydrogeology*. Lewis Publishers, Boca Raton.

Coleman DD, Risatti JB, Schoell M (1981) Fractionation of carbon and hydrogen isotopes by methane-oxidizing bacteria. *Geochimica et Cosmochimica Acta,* **45**, 1033-1037.

Coles JRP, Yavitt JB (2002) Control of methane metabolism in a forested northern wetland, New York State, by aeration, substrates, and peat size fractions. *Geomicrobiology Journal*, **19,** 293-315.

Couwenberg J, Thiele A, Tanneberger F *et al.* (2011) Assessing greenhouse gas emissions from peatlands using vegetation as a proxy. *Hydrobiologia*, **674**, 67–89.

Dawson TE, Siegwolf RTW (eds) (2007) *Stable isotopes as indicators of ecological change*. Academic Press-Elsevier, San Diego, CA.

Demidenko E (2004) *Mixed models: theory and applications.* John Wiley & Sons, New Jersey.

Deppe MA, Knorr KH, McKnight DM, Blodau C (2010a) Effects of short-term drying and irrigation on CO2 and CH4 production and emission from mesocosms of a northern bog and an alpine fen. *Biogeochemistry*, **100**, 89-103.

Deppe MA, McKnight DM, Blodau C (2010b) Effects of short-term drying and irrigation on electron flow in mesocosms of a northern bog and an alpine fen. *Environmental Science & Technology*, **44**, 80-86.

Dias ATC, Hoorens B, Van Logtestijn RSP, Vermaat JE, Aerts R (2010) Plant species composition can be used as a proxy to predict methane emissions in Peatland ecosystems after land-use changes. *Ecosystems*, **13**, 526-538.

Dorodnikov M, Marushchak M, Biasi C, Wilmking M (2013) Effect of microtopography on isotopic composition of methane in porewater and efflux at a boreal peatland. *Boreal Environment Research,* **18**, 269-279.

Dunfield P, Knowles R, Dumont R, Moore TR (1993) Methane production and consumption in temperate and subarctic peat soils: Response to temperature and pH. *Soil Biology and Biochemistry*, **25**(3), 321–326.

Environment Canada (2014) 1981-2010 Canadian Climate Normals and Averages.

Farquhar GD, Ehleringer JR, Hubick KT (1989) Carbon isotope discrimination and photosynthesis. *Annual Review of Plant Physiology and Plant Molecular Biology,* **40**, 503-537.

Fechner-Levy EJ, Hemond HF (1996) Trapped methane volume and potential effects on methane ebullition in a northern peatland. *Limnology and Oceanography*, **41**(7), 1375-1383.

Fenchel T, King GM, Blackburn TH (1998) *Bacterial Biogeochemistry*. Academic Press, London.

Frenzel P, Rudolph J (1998) Methane emission from a wetland plant: the role of CH_4 oxidation in *Eriophorum*. *Plant and Soil*, **202**(1), 27-32.

Friborg T, Christensen TR, Hansen BU, Nordstroem C, Soegaard H (2000) Trace gas exchange in a high-Arctic valley: 2. Landscape CH4 fluxes measured and modeled using eddy correlation data. *Global Biogeochemical Cycles*, **14**, 715–723.

Fung TWK, Xu XC (2010) Estimation and robustness of linear mixed models in credibility context. *Casualty Actuarial Society*, **2**(1), 66-80.

Galand PE, Saarnio S, Fritze H, Yrjälä K (2002) Depth related diversity of methanogen Archaea in Finnish oligotrophic fen. *FEMS Microbiology Ecology*, **42**, 441-449.

Galand PE, Fritze H, Conrad R, Yrjälä K (2005) Pathways for methanogenesis and diversity of methanogenic archaea in three boreal peatland ecosystems. *Applied and Environmental Microbiology*, **71**(4), 2195-2198.

Galand PE, Yrjälä K, Conrad R (2010) Stable carbon isotope fractionation during methanogenesis in three boreal peatland ecosystems. *Biogeosciences*, **7**, 3893-3900.

Gallego-Sala AV, Prentice IC (2013) Blanket peat biome endangered by climate change. *Nature Climate Change*, **3**, 152-155.

Gao F, Deng J, Li Q, Hu L, Zhu J, Hang H, Hu W (2012) A new collector for in situ pore water sampling in wetland sediment. *Environmental Technology*, **33**(3), 257-264.

Garcia JL, Patel BKC, Ollivier B (2000) Taxonomic, phylogenetic, and ecological diversity of methanogenic Archaea. *Anaerobe*, **6**(4), 205–226.

Glaser PH, Chanton JP, Morin P *et al.* (2004) Surface deformations as indicators of deep ebullition fluxes in a large northern peatland. *Global Biogeochemical Cycles*, **18**, GB1003.

Google Earth (2013). Mer Bleue bog, 45°24’30.06” N 75°31’07.95” W. Sep. 24, 2013.

Gorham E (1991) Northern peatlands: role in the carbon cycle and probable responses to climatic warming. *Ecological Applications,* **1**(2), 182-95.

Gorham E (1995) The biogeochemistry of northern peatlands and its possible response to global warming. In *Biotic Feedbacks in the Global Climatic System: Will the*

Warming Feed the Warming? (eds. Woodwell GM, Mackenzie FT), pp. 169-187. Oxford University Press, New York, NY.

Gray A, Levy PE, Cooper MDA *et al.* (2013) Methane indicator values for peatlands: a comparison of species and functional groups. *Global Change Biology,* **19**, 1141-1150.

Große W (1996) The mechanism of thermal transpiration (= thermal osmosis). *Aquatic Botany,* **54**(2–3), 101–110.

Hesslein RH (1976) An in-situ sampler for close interval pore water studies. *Limnology and Oceanography*, **21**(6), 912-914.

Hornibrook ERC, Longstaffe FJ, Fyfe WS (1997) Spatial distribution of microbial methane production pathways in temperate zone wetland soils: stable carbon and hydrogen isotope evidence. *Geochimica et Cosmochimica Acta,* **61**(4), 745-753.

Hornibrook ERC, Longstaffe FJ, Fyfe WS (2000a) Factors influencing stable isotope ratios in CH_4 and CO_2 within subenvironments of freshwater wetlands: implications for δ-signatures of emissions. *Isotopes in Environmental and Health Studies,* **36**, 151-176.

Hornibrook ERC, Longstaffe FJ, Fyfe WS, Bloom Y (2000b) Carbon-isotope ratios and carbon, nitrogen and sulfur abundances in flora and soil organic matter from a temperate-zone bog and marsh. *Geochemical Journal*, **34**, 237-245.

Houweling S, Dentener F, Leliveld J *et al.* (2000) The modeling of tropospheric methane: how well can point measurements be reproduced by a global model? *Journal of Geophysical Research*, **105**(D7), 8981-9002.

Hribljan JA (2012) The effect of long-term water table manipulations on vegetation, pore water, substrate quality, and carbon cycling in a northern poore fen peatland. Ph.D. Thesis. Michigan Technological University, Houghton, MI.

Hribljan JA, Kane ES, Pypker TG, Chimner RA (2014) The effect of long-term water table manipulations on dissolved organic carbon dynamics in a poor fen peatland. *Journal of Geophysical Research: Biogeosciences*, **119**, 577-595.

IPCC (2007) *Climate Change 2007: The Physical Science Basis. Contribution of Working Group 1 to the Fourth Assessment Report of the IPCC.* Cambridge University Press, Cambridge.

IPCC (2013) *Climate Change 2013: The Physical Science Basis. Contribution of Working Group 1 to the Fifth Assessment Report of the IPCC.* Cambridge University Press, Cambridge.

JMP 7 Statistics and Graphics Guide. SAS Institute Inc., Cary, North Carolina.

Kalbitz K, Solinger S, Park J-H, Michalzik B, Matzner E (2000) Controls on the dynamics of dissolved organic matter in soils: a review. *Soil Science*, **165**(4), 277-304.

Kamal S, Varma A (2008) Peatland microbiology. In *Microbiology of Extreme Soils* (eds. Dion P, Nautiyal CS), pp. 177–203. Springer-Verlag, Berlin Heidelberg. .

Kane ES, Mazzoleni LR, Kratz CJ, Hribljan JA, Johnson CP, Pypker TG, Chimner RA (2014) Peat porewater dissolved organic carbon concentration and lability increase with warming: a field temperature manipulation experiment in a poor-fen. *Biogeochemistry*, **119**, 161-178.

Keeling CD (1958) The concentration and isotopic abundances of atmospheric carbon dioxide in rural areas. *Geochemica et Cosmochimica Acta*, **13**, 322-334.

Keeling CD (1960) The concentration and isotopic abundances of carbon dioxide in the atmosphere. *Tellus A*, **12**, 200-203.

Kellner E, Price JS, Waddington JM (2004) Pressure variations in peat as a result of gas bubble dynamics. *Hydrological Processes*, **18**, 2599-2605.

Kettunen A, Kaitala V, Lehtinen A *et al.* (1999) Methane production and oxidation potentials in relation to water table fluctuations in two boreal mires. *Soil Biology & Biochemistry*, **31**, 1741-1749.

Kim Y, Ullah S, Moore TR, Roulet NT (2014) Dissolved organic carbon and total dissolved nitrogen production by boreal soils and litter: the role of flooding, oxygen concentration and temperature. *Biogeochemistry*, **118**, 35-48.

Kirschke S, Bousquet P, Ciais P *et al.* (2013) Three decades of global methane sources and sinks. *Nature Geoscience*, **6**, 813-823.

Kirstine WV, Galbally IE (2012) Ethanol in the environment: a critical review of its roles as a natural product, a biofuel, and a potential environmental pollutant. *Critical Reviews in Environmental Science and Technology*, **42**, 1735-1779.

Klass DL (1984) Methane from anaerobic fermentation. *Science*, **223**(4640), 1021-1028.

Knorr K, Oosterwoud MR, Blodau C (2008) Experimental drought alters rates of soil respiration and methanogenesis but not carbon exchange in soil of a temperate fen. *Soil Biology and Biochemistry*, **40**(7), 1781-1791.

Kobayashi H, Ryu Y, Baldocchi DD, Welles JM, Norman JM (2013) On the correct estimation of gap fraction: how to remove scattered radiation in gap fraction measurements? *Agricultural and Forest Meteorology*, **174-175**, 170-183.

Kopp BJ, Fleckenstein JH, Roulet NT, Humphreys E, Talbot J, Blodau C (2013) Impact of long-term drainage on summer groundwater flow patterns in the Mer Bleue peatland, Ontario, Canada. *Hydrology and Earth System Sciences*, **17**, 3485-3498.

Kotsyurbenko OR, Chin K-J, Glagolev MV *et al.* (2004) Acetoclastic and hydrogenotrophic methane production and methanogenic populations in an acidic West-Siberian peat bog. *Environmental Microbiology*, **6**(11), 1159-1173.

Kotsyurbenko OR, Friedrich MW, Simankova MV *et al.* (2007) Shift from acetoclastic to H2-dependent methanogenesis in a West Siberian peat bog at low pH values and isolation of an acidophilic *Methanobacterium* strain. *Applied and Environmental Microbiology*, **73**(7), 2344-2348.

Lafleur PM, Roulet NT, Bubier JL, Frolking S, Moore TR (2003) Interannual variability in the peatland-atmosphere carbon dioxide exchange at an ombrotrophic bog. *Global Biogeochemical Cycles,* **17**, 1036.

Lai DYF (2009) Methane dynamics in northern peatlands: a review. *Pedosphere*, **19**(4), 409-421.

Lai DYF, Roulet NT, Humphreys ER, Moore TR, Dalva M (2012) The effect of atmospheric turbulence and chamber deployment period on autochamber CO_2 and CH_4 flux measurements in an ombrotrophic peatland. *Biogeosciences*, **9**, 3305-22.

Lai DYF, Moore TR, Roulet NT (2014a) Spatial and temporal variations of methane flux measured by autochambers in a temperate ombrotrophic peatland. *Journal of Geophysical Research: Biogeosciences,* **5**(119), 864-880.

Lai DYF, Roulet NT, Moore TR (2014b) The spatial and temporal relationships between CO_2 and CH_4 exchange in a temperate ombrotrophic bog. *Atmospheric Environment*, **89**, 249-259.

Langmuir D (1971) Eh-pH determination. In *Procedures in sedimentary petrology* (ed. Carver RE), p.612. Wiley- Interscience, New York.

Larmola T, Bubier JL, Kobyljanec C *et al.* (2013) Vegetation feedbacks of nutrient addition lead to a weaker carbon sink in an ombrotrophic bog. *Global Change Biology*, **19**(12), 3729-3739.

Le Mer J, Roger P (2001) Production, oxidation, emission, and consumption of methane by soils: a review. *European Journal of Soil Biology*, **37**(1), 25-50.

Levy PE, Burden A, Cooper MDA *et al.* (2012) Methane emissions from soils: synthesis and analysis of a large UK data set. *Global Change Biology*, **18**(5), 1657-1669.

Limpens J, Berendse F, Blodau C *et al.* (2008) Peatlands and the carbon cycle: from local processes to global implications- a synthesis. *Biogeosciences*, **5**, 1475-1491.

Long KD, Flanagan LB, Cai T (2010) Diurnal and seasonal variation in methane emissions in a northern Canadian peatland measured by eddy covariance. *Global Change Biology*, **16**, 2420–2435.

Lou T, Xie H (2006) Photochemical alteration of the molecular weight of dissolved organic matter. *Chemosphere*, **65**, 2333-2342.

Malmer N, Wallén B (2004) Input rates, decay losses and accumulation rates of carbon in bogs during the last millennium: internal processes and environmental changes. *The Holocene,* **14**(1), 111-117.

Mansfeldt T (2003) In situ long-term redox potential measurements in a dyked marsh soil. *Journal of Plant Nutrition and Soil Science,* **166**, 210-219.

Matthews E, Fung I (1987) Methane emission from natural wetlands: global distribution, area and environmental characteristics of sources. *Global Biogeochemical Cycles,* **1**(1), 61-86.

Mikaloff Fletcher SE, Tans PP, Bruhwiler LM, Miller JB, Heimann M (2004a) CH_4 source estimated from atmospheric observations of CH_4 and its $^{13}C/^{12}C$ isotopic ratios: 1.Inverse modelling of source processes. *Global Biogeochemical Cycles*, **18**, GB4004.

Mikaloff Fletcher SE, Tans PP, Bruhwiler LM, Miller JB, Heimann M (2004b) CH_4 source estimated from atmospheric observations of CH_4 and its $^{13}C/^{12}C$ isotopic ratios: 2.Inverse modelling of CH4 fluxes from geographic regions. *Global Biogeochemical Cycles*, **18**, GB4004.

Miller, JB (2005) Chapter 16: The carbon isotopic composition of atmospheric methane and its constraint on the global methane budget. In *Stable Isotopes and Biosphere-Atmosphere Interactions: Processes and Biological Controls* (eds. Flanagan LB, Ehleringer JR, Pataki DE), pp. 288-306. Elsevier, Amsterdam.

Miller JB, Tans PP (2003) Calculating isotopic fractionation from atmospheric measurements at various scales. *Tellus B,* **55**(2), 207-214.

Moore TR, Roulet NT, Knowles R (1990) Spatial and temporal variations of methane flux from subarctic/northern boreal fens. *Global Biogeochemical Cycles*, **4**(1), 29-46.

Moore TR, Dalva M (1993) The influence of temperature and water table position on methane and carbon dioxide emissions from laboratory columns of peatland soils. *Journal of Soil Science*, **44**(4), 651-664.

Moore TR, Roulet NT, Waddington JM (1998) Uncertainty in predicting the effect of climatic change on the carbon cycling of Canadian peatlands. *Climatic Change*, **40,** 229-45.

Moore TR (2001) Chapitre 8: Les processus biogéochimiques liés au carbone. In *Écologie des tourbières du Quebec-Labrador* (eds. Payette S, Rochefort L), pp. 183-198. Les Presses de l'Université Laval, Québec.

Moore TR, Dalva M (2001) Some controls on the release of dissolved organic carbon by plant tissues and soils. *Soil Science*, **166**(1), 38-47.

Moore TR, Bubier J, Lafleur P, Frolking S, Roulet N (2002) Plant biomass, production and CO_2 exchange in an ombrotrophic bog. *Journal of Ecology*, **90**, 25-36.

Moore TR, De Young A, Bubier JL, Humphreys ER, Lafleur PM, Roulet NT (2011) A multi-year record of methane flux at the Mer Bleue bog, Southern Canada. *Ecosystems*, **14**, 646-657.

Murphy MT, Moore TR (2010) Linking root production to aboveground plant characteristics and water table in a temperate bog. *Plant and Soil*, **336**, 219-231.

Neef L, van Weele M, van Velthoven P (2010) Optimal estimation of the present-day global methane budget. *Global Biogeochemical Cycles,* **24**, GB4024.

Nilsson M, Sagerfors J, Buffam I *et al.* (2008) Contemporary carbon accumulation in a boreal oligotrophic minerogenic mire- a significant sink after accounting for all C-fluxes. *Global Change Biology*, **14**, 2317-2332.

Nykänen H, Alm J, Silvola J, Tolonen K, Martikainen PJ (1998) Methane fluxes on boreal peatlands of different fertility and the effect of long-term experimental lowering of the water table on flux rates. *Global Biogechemical Cycles,* **12**(1), 53-69.

Nykänen H, Vasander H, Huttunen JT, Martikainen PJ (2002) Effects of experimental nitrogen load on methane and nitrous oxide fluxes on ombrotrophic boreal peatland. *Plant and Soil*, **242**, 147-155.

Oke TR (1987) *Boundary Layer Climates: Second Edition.* Routledge, New York.

Olefeldt D, Roulet NT (2012) Effects of permafrost and hydrology on the composition and transport of dissolved organic carbon in a subarctic peatland complex. *Journal of Geophysical Research*, **117**, G01005.

Öquist M, Sundh I (1998) Effects of a transient oxic period on mineralization of organic matter to CH_4 and CO_2 in anoxic peat incubations. *Geomicrobiology*, **15**, 325-333.

Parmentier FJW, van Huissteden J, van der Molen MK *et al.* (2011) Spatial and temporal dynamics in eddy covariance observations of methane fluxes at a tundra site in northeastern Siberia. *Journal of Geophysical Research,* **116**, G03016.

Pataki DE, Ehleringer JR, Flanagan LB *et al.* (2003) The application and interpretation of Keeling plots in terrestrial carbon cycle research. *Global Biogeochemical Cycles*, **17**(1), 1022.

Petrescu AMR, van Beek LPH, van Huissteden, *et al.* (2010) Modeling regional to global CH_4 emissions of boreal and arctic wetlands. *Global Biogeochemical Cycles*, **24**, GB4009.

Petrescu AMR, Lohila A, Tuovinen J-P *et al.*(2015) The uncertain climate footprint of wetlands under human pressure. *Proceedings of the National Academy of Sciences of the United States of America*, **112**(15), 4594-4599.

Peuravuori J, Pihlaja K (1997) Molecular size distribution and spectroscopic properties of aquatic humic substances. *Analytica Chimica Acta*, **337**, 133-149.

Picarro, Inc. (2015) Data sheet G2201-*i* CRDS analyzer for isotopic carbon in CO_2 and CH_4.

Pihlatie MK, Christiansen JR, Aaltonen H, *et al.* (2013) Comparison of static chambers to measure CH_4 emissions from soils. *Agirucultural and Forest Meteorology*, **171**, 124-136.

Preston MD, Eimers MC, Watmough SA (2011) Effect of moisture and temperature variation on DOC release from a peatland: conflicting results from laboratory, field and historical data analysis. *Science of the Total Environment*, **409**, 1235-1242.

Quay PD, King SL, Stutsman J, *et al.* (1991) Carbon isotopic composition of atmospheric CH_4: fossil and biomass burning source strengths. *Global Biogeochemical Cycles*, **5**(1), 25-47.

Rabenhorst MC, Hively WD, James BR (2009) Measurements of soil redox potential. *Soil Science Society of America Journal*, **73**(2), 668-674.

Rattle J (2006) Dissolved nitrogen dynamics in an ombrotrophic bog. M.Sc. Thesis. McGill University, Montréal, QC.

Reay DS, Davidson EA, Smith KA *et al.* (2012) Global agriculture and nitrous oxide emissions. *Nature Climate Change*, **2**(6), 410-416.

Rinne J, Riutta T, Pihlatie M *et al.* (2007) Annual cycle of methane emission from a boreal fen measured by the eddy covariance technique. *Tellus B*, **59**(3), 449–457.

Rodwell JS (1991) British Plant Communities Volume 2: Mires and Heaths. Cambridge University Press, Cambridge.

Rosenberry DO, Glaser PH, Siegel DI (2006) The hydrology of northern peatlands as affected by biogenic gas: current developments and research needs. *Hydrological Processes*, **20**(17), 3601-3610.

Roslev P, King GM (1994) Survival and recovery of methanotrophic bacteria starved under oxic and anoxic conditions. *Applied and Environmental Microbiology*, **60**, 2602–2608.

Roslev P, King GM (1995) Aerobic and anaerobic starvation metabolism in methanotrophic bacteria. *Applied and Environmental Microbiology*, **61**, 1563–1570.

Roulet NT, Moore TR, Bubier J, Lafleur PM (1992) Northern fens: methane flux and climatic change. *Tellus B*, **44**, 100-105.

Roulet NT, Lafleur PM, Richard PJH, Moore TR, Humphreys ER, Bubier J (2007) Contemporary carbon balance and late Holocene carbon accumulation in a northern peatland. *Global Change Biology*, **13**, 397-411.

Rydin H, Jeglum JK (2013) *The Biology of Peatlands: Second Edition.* Oxford University Press, Oxford.

Saleska S (2009) *Genes, isotopes and ecosystem biogeochemistry: dissecting methane flux at the leading edge of global change*, University of Arizona, Tuscon.

Segers R (1998) Methane production and methane consumption: a review of processes underlying wetland methane fluxes. *Biogeochemistry,* **41**: 23-51

Shotyk W (1988) Review of the inorganic geochemistry of peats and peatland waters. *Earth-Science Reviews*, **25**, 95-176.

SigmaXL (2015) Minimum sample size for robust t-tests and ANOVA. *SigmaXL version 7*.

Soegaard H, Nordstroem C, Friborg T, Hansen BU (2000) Trace gas exchange in a high-arctic valley 3. Integrating and scaling CO2 fluxes from canopy to landscape using flux data, footprint modeling, and remote sensing. *Global Biogeochemical Cycles,* **14**(3), 725-744.

Steinmann P, Shotyk W (1996) Sampling anoxic pore waters in peatlands using "peepers" for in situ-filtration. *Fresenius' Journal of Analytical Chemistry*, **354**, 709-713.

Strack M, Waller MF, Waddington JM (2006) Sedge succession and peatland methane dynamics: a potential feedback to climate change. *Ecosystems,* **9**, 278-287.

Strack M, O'Brien JRP, Waddington JM (2008) Assessing the role of ecological succession for peatland methane dynamics: potential climate change feedback. *Peatlands and climate change*, International Peat Society, Jväskylä, Finland.

Stull RB (1995) *Meteorology Today for Scientists and Engineers.* West Publishing Company, St.Paul.

Stull RB (1988) *An Introduction to Boundary Layer Meteorology*. Kluwer Academic Publishers, Dordrecht.

Suyker AE, Verma SB, Clement RJ, Billesbach DP (1996). Methane flux in a boreal fen: Season-long measurement by eddy correlation. *Journal of Geophysical Research,* **101**, 28,637–28,647.

Syed KH, Flanagan LB, Carlson PJ, Glenn AJ, Van Gaalen KE (2006) Environmental control of net ecosystem CO_2 exchange in a treed, moderately rich fen in northern Alberta. *Agricultural and Forest Meteorology*, **140**, 97-114.

Thomas KL, Benstead J, Davies KL, Lloyd D (1996) Role of wetland plants in the diurnal control of CH_4 and CO_2 fluxes in peat. *Soil Biology and Biochemistry*, **28**(1), 17-23.

Tokida T, Miyazaki T, Mizoguchi M *et al.* (2007) Falling atmospheric pressure as a trigger for methane ebullition from peatland. *Global Biogeochemical Cycles*, **21**, GB2003.

Turetsky MR, Treat CC, Waldrop MP, Waddington JM, Harden JW, McGuire AD (2008) Short-term response of methane fluxes and methanogen activity to water table and soil warming manipulations in an Alaskan peatland. *Journal of Geophysical Research*, **113**, G00A10.

Turetsky MR, Kotowska A, Bubier J *et al.* (2014) A synthesis of methane emissions from 71 northern, temperate, and subtropical wetlands. *Global Change Biology,* **20**, 2183-2197.

Turunen J, Tomppo E, Tolonen K, Reinikainen A (2002) Estimating carbon accumulation rates of undrained mires in Finland- application to boreal and subarctic regions. *The Holocene*, **12**, 69-80.

US EPA (2010) Methane and nitrous oxide emissions from natural sources.

Vasander H, Kettunen A (2006) Chapter 9: Carbon in boreal peatlands. In *Boreal Peatland Ecosystems* (ed. Wieder RK, Vitt DH), pp. 165-194. Springer-Verlag, Berlin Heidelberg.

Valentine DW, Holland EA, Schimel DS (1994). Ecosystem and physiological controls over methane production in northern wetlands. *Journal of Geophysical Research*, **99**(D1), 1563–1571.

Vorenhout M, van der Geest HG, van Marum D, Wattel K, Eijsackers HJP (2004) Automated and continuous redox potential measurements in soil. *Journal of Environmental Quality*, **33**, 1562-1567.

Vorenhout M, van der Geest HG, Hunting ER (2011) An improved datalogger and novel probes for continuous redox measurements in wetlands. *International Journal of Environmental Analytical Chemistry*, **91**(7), 801-810.

Waddington JM, Ketcheson SJ, Kellner E, Strack M, Baird AJ (2009) Evidence that piezometers vent gas from peat soils and implications for pore-water pressure and hydraulic conductivity measurements. *Hydrological Processes,* **23**(8), 1249-1254.

Walker MD, Wahren CH, Hollister RD *et al.* (2006) Plant community responses to experimental warming across the tundra biome. *Proceedings of the National Academy of Sciences of the United States of America*, **103**(5), 1342-1346.

Walter KM, Chanton JP, Chapin FS, Schuur EAG, Zimov SA (2008) Methane production and bubble emissions from arctic lakes: Isotopic implications for source pathways and ages. *Journal of Geophysical Research*, **113**, G00A081342-1346.

Wallace JM, Hobbs PV (1977) *Atmospheric Science: An Introductory Survey.* Academic Press, New York.

Wang M, Moore TR, Talbot J, Riley JL (2015) The stoichiometry of carbon and nutrients in peat formation. *Global Biogeochemical Cycles*, **29**, 113-121.

Wanninkhof R (1992) Relationship between wind speed and gas exchange over the ocean. *Journal of Geophysical Research*, **97**, 7373-7382.

Ward SE, Ostle NJ, Oakley S, Quirk H, Henrys PA, Bardgett RD (2013) Warming effects on greenhouse gas fluxes in peatlands are modulated by vegetation composition. *Ecology Letters*, **16**, 1285-1293.

Weishaar JL, Aiken GR, Bergamaschi BA, Fram MS, Fujii R, Mopper K (2003) Evaluation of specific ultraviolet absorbance as an indicator of the chemical composition and reactivity of dissolved organic carbon. *Environmental Science & Technology*, **37**, 4702-4708.

Weiss RF (1974) Carbon dioxide in water and seawater: the solubility of a non-ideal gas. *Marine Chemistry,* **2**, 2013-215.

Weiss RF, Price BA (1980) Nitrous oxide solubility in water and seawater. *Marine Chemistry*, **8**, 347-359.

Werner C, Schnyder H, Cuntz M *et al.* (2012) Progress and challenges in using stable isotopes to trace plant carbon and water relations across scales. *Biogeosciences*, **9**, 3083-3111.

Whalen SC (2005) Biogeochemistry of methane exchange between natural wetlands and the atmosphere. *Environmental Engineering Science*, **22**(1), 73-94.

Whiticar MJ, Faber E, Schoell M (1986) Biogenic methane formation in marine and freshwater environments: CO_2 reduction vs. acetate fermentation- isotopic evidence. *Geochimica et Cosmochimica Acta*, **50**(5), 693-709.

Whitcar MJ (1999) Carbon and hydrogen isotope systematics of bacterial formation and oxidation of methane. *Chemical Geology*, **161**, 291-314.

Whiticar, MJ (2000) Chapter 5: Can Stable Isotopes and Global Budgets Be Used to Constrain Atmospheric Methane Budgets? In *Atmospheric Methane: Its Role in the Global Environment* (ed. Khalil MAK), pp. 63-85. Springer-Verlag, Berlin Heidelberg.

Wiesenburg DA, Guinasso NL Jr. (1979) Equilibrium solubilities of methane, carbon monoxide, and hydrogen in water and sea water. *Journal of Chemical and Engineering Data,* **24**(4), 356-360.

Wilson KS, Humphreys ER (2010) Carbon dioxide and methane fluxes from Arctic mudboils. *Canadian Journal of Soil Science*, **90**, 441-449.

Wuebbles D, Hayhoe K (2002) Atmospheric methane and global change. *Earth-Science Reviews,* **57**, 177-210.

Yavitt JB, Lang GE (1990) Methane production in contrasting wetland sites: response to organic-chemical components of peat and to sulfate reduction. *Geomicrobiology Journal*, **8**(1), 27-46.

Yavitt JB, Seidman-Zager M (2006) Methanogenic conditions in northern peat soils. *Geomicrobiology Journal*, **23**, 119-127.

Zhi-Guang L (1985) Oxidation-reduction potential. In *Physical Chemistry of Paddy Soils* (ed. Tian-ren Y), pp. 1-26. Springer, Berlin.